

NASW-4066

MECA WORKSHOP ON ATMOSPHERIC H₂O OBSERVATIONS OF EARTH AND MARS



MECA

(NASA-CR-183335) MECA WORKSHOP ON
ATMOSPHERIC H₂O OBSERVATIONS OF EARTH AND
MARS. PHYSICAL PROCESSES, MEASUREMENTS AND
INTERPRETATIONS (Lunar and Planetary Inst.)
95 p

N89-25790
--THRU--
N89-25814
Unclas
CSCL 03B G3/91 0187391



LPI Technical Report Number 88-10

LUNAR AND PLANETARY INSTITUTE 3303 NASA ROAD 1 HOUSTON, TEXAS 77058

MECA WORKSHOP ON ATMOSPHERIC H₂O OBSERVATIONS OF
EARTH AND MARS
Physical Processes, Measurements, and Interpretations

Edited by

Stephen M. Clifford
and
Robert M. Haberle

September 25–27, 1986

Sponsored by
Lunar and Planetary Institute

Lunar and Planetary Institute 3303 NASA Road One Houston, Texas 77058-4399

LPI Technical Report Number 88-10

Compiled in 1988 by the
LUNAR AND PLANETARY INSTITUTE

The Institute is operated by Universities Space Research Association under Contract NASW-4066 with the National Aeronautics and Space Administration.

Material in this document may be copied without restraint for library, abstract service, educational, or personal research purposes; however, republication of any portion requires the written permission of the authors as well as appropriate acknowledgment of this publication.

This report may be cited as:

Clifford S. M. and Haberle R. M. (1988) *MECA Workshop on Atmospheric H₂O Observations of Earth and Mars: Physical Processes, Measurements, and Interpretations*. LPI Tech. Rpt. 88-10. Lunar and Planetary Institute, Houston. 94 pp.

Papers in this report may be cited as:

Author A. A. (1988) Title of paper. In *MECA Workshop on Atmospheric H₂O Observations of Earth and Mars: Physical Processes, Measurements, and Interpretations* (S.M. Clifford and R. M. Haberle), pp. xx-yy. LPI Tech Rpt. 88-10. Lunar and Planetary Institute, Houston.

This report is distributed by:

ORDER DEPARTMENT
Lunar and Planetary Institute
3303 NASA Road One
Houston, TX 77058-4399

Mail order requestors will be invoiced for the cost of shipping and handling.

Contents

Introduction	1
Program	3
Workshop Summary	7
Abstracts	11
Water in the Martian Regolith <i>D. M. Anderson</i>	13
Transport of Mars Atmospheric Water Into High Northern Latitudes During a Polar Warming <i>J. R. Barnes and J. L. Hollingsworth</i>	19
The Effect of Global-scale Divergent Circulation on the Atmospheric Water Vapor Transport and Maintenance <i>T.-C. Chen</i>	22
Seasonal and Diurnal Variability of Mars Water-Ice Clouds <i>P. R. Christensen, R. W. Zurek, and L. L. Jaramillo</i>	29
The Interpretation of Data from the Viking Mars Atmospheric Water Detectors (MAWD): Some Points for Discussion <i>S. M. Clifford</i>	31
Regolith Water Vapor Sources on Mars: A Historical Bibliography <i>S. M. Clifford and R. L. Huguenin</i>	33
Factors Governing Water Condensation in the Martian Atmosphere <i>D. S. Colburn, J. B. Pollack, and R. M. Haberle</i>	37
Cumulus Convection and the Terrestrial Water-Vapor Distribution <i>L. J. Donner</i>	41
Possible Significance of Cubic Water-Ice, H ₂ O-Ic, in the Atmospheric Water Cycle of Mars <i>J. L. Gooding</i>	46
On the Vertical Distribution of Water Vapor in the Martian Tropics <i>R. M. Haberle</i>	50
The Behavior of Water Vapor in the Mars Atmosphere <i>B. M. Jakosky</i>	53
Solar Mesosphere Explorer Observations of Stratospheric and Mesospheric Water Vapor <i>B. M. Jakosky, G. E. Thomas, D. W. Rusch, C. A. Barth, G. M. Lawrence, J. J. Olivero, R. T. Clancy, R. W. Sanders, and B. G. Knapp</i>	54
Circumpolar Hoods and Clouds and their Relation to the Martian H ₂ O Cycle <i>P. B. James and L. J. Martin</i>	56
Very High Elevation Water Ice Clouds on Mars: Their Morphology and Temporal Behavior <i>F. Jaquin</i>	58
Observations of Atmospheric Water Vapor with the SAGE II Instrument <i>J. C. Larsen, M. P. McCormick, L. R. McMaster, and W. P. Chu</i>	62

Flux of Water Vapor in the Terrestrial Stratosphere and in the Martian Atmosphere <i>C. Leovy, M. Hitchman, and D. McCleese</i>	67
Regelation and Ice Segregation <i>R. D. Miller</i>	70
Measurements of H ₂ O in the Terrestrial Mesosphere and Implications for Extra- Terrestrial Sources <i>J. J. Olivero</i>	71
Diurnal and Annual Cycles of H ₂ O in the Martian Regolith <i>J. R. Philip</i>	75
The Nimbus 7 LIMS Water Vapor Measurements <i>E. E. Remsberg and J. M. Russell, III</i>	80
Measurements of the Vertical Profile of Water Vapor Abundance in the Martian Atmosphere from Mars Observer <i>J. T. Schofield and D. J. McCleese</i>	82
Atmospheric H ₂ O and the Search for Martian Brines <i>A. P. Zent, F. P. Fanale, and S. E. Postawko</i>	87
The Interannual Variability of Atmospheric Water Vapor on Mars <i>R. W. Zurek</i>	91
The Martian Atmospheric Water Cycle as Viewed from a Terrestrial Perspective <i>R. W. Zurek</i>	92
List of Workshop Participants	93

Introduction

On September 25–27, 1986, a three-day MECA workshop on “Atmospheric H₂O Observations of Earth and Mars: Physical Processes, Measurements, and Interpretation” was held at the Lunar and Planetary Institute. The purpose of the workshop was to discuss a variety of questions related to the detection and cycling of atmospheric H₂O. Among the questions addressed were: What factors govern the storage and exchange of H₂O between planetary surfaces and atmospheres? What instruments are best suited for the measurement and mapping of atmospheric H₂O? Do regolith sources and sinks of H₂O have uniquely identifiable column abundance signatures? What degree of time and spatial resolution in column abundance data is necessary to determine dynamic behavior? Finally, does our understanding of how atmospheric H₂O is cycled on Earth provide any insights for the interpretation of Mars atmospheric data?

These questions were addressed by researchers from fields as diverse as soil physics, atmospheric dynamics, atmospheric H₂O instrumentation, and martian volatiles. This interdisciplinary approach gave scientists from traditionally isolated disciplines a unique opportunity to meet and discuss issues of common interest. Of particular importance was the participation of scientists from the terrestrial community, whose fresh perspectives contributed to an improved understanding of the Mars water cycle. This technical report is the final product of that discussion.

Stephen M. Clifford
Houston, Texas

Program

Thursday Morning, September 25, 1986

8:00 am Registration

8:30 am Welcome — Kevin Burke, Director of LPI

8:35 am Opening Remarks — Stephen Clifford, Workshop Convener

8:45 am **SESSION I: BACKGROUND**
Chairman: Stephen Clifford

The behavior of water vapor in the Mars atmosphere
B. M. Jakosky

The Earth atmospheric water cycle as viewed from a planetary perspective
R. W. Zurek

11:00 am **SESSION II: MARS ATMOSPHERIC H₂O**
Chairmen: Robert Haberle and Bruce Jakosky

The interpretation of data from the Viking Mars Atmospheric Water Detectors (MAWD): Some points for discussion
S. M. Clifford

The inter-annual variability of atmospheric water vapor on Mars
R. Zurek

Thursday Afternoon, September 25, 1986

1:30 pm **SESSION II: MARS ATMOSPHERIC H₂O (CONTINUED)**

The vertical distribution of water vapor in the martian tropics
R. M. Haberle

Factors governing water condensation in the martian atmosphere
D. S. Colburn, J. B. Pollack, and R. M. Haberle

Seasonal and diurnal variability of Mars water-ice clouds
P. Christensen and R. W. Zurek

Seasonal dependence of very high water ice clouds on Mars
F. Jaquin

Discussion

Transport of Mars atmospheric water into high northern latitudes during a polar warming
J. R. Barnes and J. L. Hollingsworth

Circumpolar hoods and clouds and their relation to the martian H₂O cycle
P. B. James and L. J. Martin

Measurements of the vertical profile of water vapor abundance in the martian atmosphere from Mars Observer
D. McCleese and J. T. Schofield

Discussion

PRECEDING PAGE BLANK NOT FILMED

8:00 pm - 9:45 pm

THURSDAY EVENING DISCUSSION SESSION

Chairmen: Robert Haberle and Conway Leovy

Topic: Determining the dynamic behavior of atmospheric H₂O from orbital observations alone - is it possible?

Friday Morning, September 26, 1986

8:30 am

SESSION III: EARTH ATMOSPHERIC H₂O

Chairmen: Conway Leovy and John Olivero

The effect of global-scale divergent circulation on the atmospheric water vapor transport and maintenance
T. C. Chen

Cumulus convection and the terrestrial water vapor distribution

L. J. Donner

Measurements of lower stratospheric/upper tropospheric water vapor by the Sage II instrument

J. Larsen

The Nimbus 7 LIMS water vapor measurements

E. E. Remsberg and J. M. Russell III

Discussion

Solar Mesosphere Explorer observations of stratospheric and mesospheric water vapor

B. M. Jakosky, G. E. Thomas, D. W. Rusch, C. A. Barth, G. M. Lawrence, J. J. Olivero, R. T. Clancy, R. W. Sanders, and B. G. Knapp

Flux of water vapor in the terrestrial stratosphere and in the martian atmosphere

C. B. Leovy, M. H. Hitchman, and D. J. McCleese

Measurements of H₂O vapor in the terrestrial mesosphere and implications for extraterrestrial sources

J. J. Olivero

Discussion

Friday Afternoon, September 26, 1986

1:45 pm

SESSION IV: THE REGOLITH AS A SOURCE AND SINK OF ATMOSPHERIC H₂O

Chairmen: Duwayne Anderson and Stephen Clifford

Evidence for regolith water vapor sources on Mars

S. M. Clifford and R. L. Huguenin

Atmospheric H₂O and the search for martian brines

A. P. Zent, F. P. Fanale, and S. E. Postawko

Atmospheric heat engines, and H₂O in the martian regolith

J. R. Philip

Diurnal fluctuations in simultaneous transport of water and heat through the surface as affected by soil properties

D. Hillel

Discussion

Crystalization and exchange of atmospheric water with Mars regolith

D. Anderson

Regelation and ice segregation

R. D. Miller

Possible significance of H₂O-Ic ice in the martian atmospheric water cycle

J. L. Gooding

Discussion

8:00 pm - 9:45 pm

FRIDAY EVENING DISCUSSION SESSION
Chairmen: Stephen Clifford and Philip Christensen

Topic: Detecting regolith sources and sinks of atmospheric H₂O from orbit

Saturday Morning, September 27, 1986

9:00 am

SESSION V: DISCUSSION AND SUMMARY
Chairmen: Bruce Jakosky and Richard Zurek

Atmospheric H₂O studies of Earth and Mars: Where do we stand?

The importance of ground-based and endoatmospheric studies

Unresolved problems

Opportunities for cooperative and interdisciplinary research

Future investigations

Mars Observer

WORKSHOP ADJOURNS

2/11/77
P.13
7

Workshop Summary

The workshop began with reviews of the atmospheric water cycles of the Earth and Mars. Our understanding of the martian water cycle is based on over six Mars years of water vapor column abundance measurements compiled by Earth-based telescopes and the Viking Orbiter Mars Atmospheric Water Detectors (MAWD). B. Jakosky discussed the current interpretation of this data, which suggests that the observed seasonal variation results from a combination of advective transport, local saturation, and exchange between the atmosphere, polar caps, and regolith. Still unknown, however, is the relative extent to which each of these factors contributes to the observed distribution.

In the second review, R. Zurek noted that the conditions of temperature and pressure that characterize the atmosphere of Mars are similar to those found in the Earth's stratosphere. Of particular significance is the fact that liquid water is unstable in both environments. Thus, it is expected that terrestrial studies of the dynamical behavior of stratospheric water should benefit our understanding of H₂O transport on Mars as well.

The observed seasonal and latitudinal variability of atmospheric water vapor on Mars provides important clues about the nature of the martian hydrologic cycle. For example, on an annual and zonally averaged basis, there is a gradient in atmospheric water vapor abundance from north to south. Jakosky has argued that this gradient implies a net north-to-south transport. However, asymmetries in the global circulation pattern due to dust storms, or the seasonal mass flux of carbon dioxide to and from the caps, could conceivably counter the gradient-induced flux, resulting in a situation of no net transport.

The uncertain vertical distribution of water vapor further complicates this analysis. S. Clifford argued that if a significant fraction of the total atmospheric vapor content is concentrated within the lowermost scale height, then the hemispheric asymmetry in zonally averaged topography/air-mass might itself explain the observed gradient in the annual and zonally averaged vapor abundance. In a later talk, however, R. Haberle presented dynamical arguments that favor a uniform distribution of water throughout the first several scale heights, at least in the tropics. Measurement of the actual vertical distribution of water vapor is one of the goals of the Pressure Modulated Infrared Radiometer (PMIRR) experiment onboard the Mars Observer. J. T. Schofield presented an

analysis of the instrument's capabilities and discussed how the vertical profiles will be obtained.

Another important issue is the extent of interannual variability. To address this question, R. Zurek compared Viking MAWD data obtained during and after the mission's first year. He found that in some areas the behavior of water appeared to repeat in the zonal mean. However, this interpretation is complicated by both poor coverage and the variability of dust and clouds. As a result, the extent and nature of interannual variability remains unclear.

One of the least understood aspects of the martian water cycle is the role of clouds. Four papers were given in the afternoon that dealt with their temporal and spatial variability. On theoretical grounds, D. Colburn presented modeling results suggesting a diurnal condensation cycle at high altitudes at some seasons and latitudes. On observational grounds, P. Christensen presented his efforts to map the seasonal and diurnal occurrence of clouds from Viking Infrared Thermal Mapper (IRTM) data. Interestingly, he finds a seasonal variability in cloudiness (haziness is probably a more accurate term) that is consistent with theoretical expectations of Hadley cell variability. Very high and extremely thin water ice clouds were also detected in limb scans by F. Jaquin, and these also show a seasonal behavior that may be correlated with lower atmosphere dynamics. Finally, P. James reviewed the hemispheric asymmetries in the so-called "polar hood" clouds and discussed their significance to the seasonal water cycle.

Later that evening, after a leisurely dinner break, the conference participants reconvened to discuss whether the magnitude and direction of atmospheric water transport could be determined from satellite observations alone. The conferees noted that transport can only be determined with accurate and simultaneous measurements of the wind and water vapor fields. For Mars Observer, the absence of a wind-sensing instrument means that wind speed and direction must be inferred from the temperature field. Although difficult to assess, this approach is unlikely to provide data of the required accuracy. On a zonal and time-averaged basis, however, the data anticipated from Mars Observer may be adequate to determine meridional transport—information that alone would be of considerable value.

The Friday morning session concentrated on the detection, distribution, and dynamics of atmospheric H₂O

PRECEDING PAGE BLANK NOT FILMED

PAGE 6 INTENTIONALLY BLANK

on Earth. T. C. Chen discussed how the high levels of water vapor and precipitation that occur over the tropics during the monsoon season result from the development of a strong divergent atmospheric circulation. L. Donner elaborated on one aspect of this circulation by discussing the role of cumulus convection, which "dries" the atmospheric column through condensation and precipitation and redistributes vapor through cumulus-induced eddy circulation. An improved understanding of these processes has greatly aided the ability of researchers to interpret the seasonal and spatial distribution of atmospheric water vapor, providing information on the nature of sources and sinks and the global circulation.

Earth-orbital instruments, designed to measure the vertical and spatial distribution of atmospheric water vapor, were the focus of the next three talks. E. Remsberg discussed the operation of the Limb Infrared Monitor of the Stratosphere (LIMS) experiment, a six-channel limb-scanning radiometer that was launched aboard Nimbus 7 in 1978. Profiles of stratospheric and mesospheric temperature, water vapor, and various other constituents were obtained by inverting the LIMS radiance measurements. This same technique was used in 1981 to analyze the data returned from another limb-scanning radiometer aboard the Solar Mesosphere Explorer (SME). B. Jakosky noted that while the SME data was consistent with the earlier LIMS results, its interpretation was complicated by significant aerosol contamination, particularly at altitudes below 35 km. This contamination arose from several volcanic eruptions, including that of El Chichon on April 4, 1982.

Jack Larsen concluded the review of terrestrial instruments with a discussion of the Stratospheric Aerosol and Gas Experiment II (SAGE II), which was launched in 1984. The SAGE II instrument was a multichannel spectrometer that inferred the vertical distribution of water vapor, aerosols, nitrogen dioxide, and ozone by measuring the extinction of solar radiation at spacecraft sunrise/sunset. At altitudes above 20 km, the SAGE II and LIMS data are in close agreement. The discrepancies below this altitude may be attributable to differences in the instruments' field-of-view and time of data acquisition.

One advantage that terrestrial investigators have over their planetary counterparts is the ability to ground-truth their instruments. In at least two of the examples cited above, this was done with balloon-borne devices that provided *in situ* water vapor measurements coincident with those made from orbit. Such techniques vastly heighten the confidence that terrestrial scientists have in the

accuracy of their interpretations, a confidence that planetary investigators will be unable to match for many years to come.

A summary of the terrestrial satellite data was presented by C. Leovy. The observations indicate that at equatorial latitudes relatively dry air is introduced at the tropopause and carried to the upper stratosphere. At that altitude, any methane present in the ascending air mass is photochemically oxidized into water vapor. This vapor is eventually transported to high latitudes, where it is carried to the lower stratosphere by the descending leg of the diabatic circulation. Leovy noted that the PMIRR instrument aboard the Mars Observer should provide a comparable picture of vapor transport in the martian atmosphere.

The final talk of the morning session was by J. Olivero, who discussed recent measurements of mesospheric water vapor and their implications for the existence of extraterrestrial sources of H₂O. This study was prompted by the work of L. Frank and his coworkers who, based on their interpretation of transient dark spots visible in ultraviolet images of the Earth's dayglow emission, have proposed that a large flux ($\sim 3 \times 10^4$) of small (~ 100 -ton) comets enters the Earth's upper atmosphere each day. To date, however, Olivero's analysis does not conclusively refute or support the idea of an external source.

The Friday afternoon session centered on the regolith as a potential source and sink of atmospheric H₂O. Clifford began the discussion by reviewing the controversy surrounding Solis Lacus, a region on Mars first identified by R. Hugenin as a possible regolith source of atmospheric water vapor. In a related talk, A. Zent examined the feasibility of detecting regolith vapor sources with the Viking MAWD data. Zent concluded that any plausible near-surface source, smaller than several hundred kilometers in diameter, would have gone undetected by the MAWD instrument.

Terrestrial scientists offered their own insights into regolith-atmosphere interactions during the next four talks. J. Philip led off the discussion with a comparison of the atmospheric heat engines of Earth and Mars. Although H₂O latent heat transfer drives the circulation of the Earth's atmosphere, particularly in the tropics, its contribution to the circulation of the martian atmosphere is negligible. The "working fluid" on Mars is CO₂, which exerts its greatest influence on atmospheric circulation at the poles.

Philip also examined the diurnal and seasonal flux of H₂O within the martian regolith. His calculations indicate that, for a mean annual temperature of 200 K, a diurnal

and annual temperature variation of 30 K will drive a maximum exchange of 1.2 pr μm and 120 pr μm of H_2O , respectively. D. Hillel's discussion of the factors that influence mass and energy transport in soil complemented Philip's analysis. Hillel described how such variables as atmospheric relative humidity, soil temperature, and the soil's physical properties interact to determine the magnitude and direction of atmosphere-regolith exchange.

The state of water in the regolith was also addressed by D. Anderson. Experiments have shown that, for temperatures below freezing and relative humidities less than 100%, adsorbed water and vapor are the only stable phases in the regolith. When the relative humidity reaches 100%, ice may form and coexist with the adsorbed liquid phase. The adsorbed water content declines with decreasing temperature; however, the presence of dissolved solutes can result in an appreciable (>1% dry weight of soil) adsorbed liquid phase at temperatures as low as 210 K. Such properties may have a profound influence on martian geomorphology, physical and chemical weathering, and the exchange of H_2O between the atmosphere and regolith.

However, macroscopic processes can also have an important effect on the state of regolith H_2O . R. Miller reviewed the two primary mechanisms responsible for the formation of segregated ice on Earth, thermally-induced regelation and hydraulic fracturing, and examined their potential importance on Mars. While regelation is the dominant terrestrial process, it requires a warmer and wetter environment than currently exists on Mars. In this respect, the conditions required for hydraulic fracturing are less demanding. In assessing its potential importance on Mars, Miller noted that hydraulic fracturing can produce a localized zone of high-pressure water that could readily disrupt an overburden of frozen ground. Such a process, he concluded, may have triggered the release of groundwater that led to the formation of the major outflow channels.

The final talk of the workshop was presented by J. Gooding, who discussed the possible formation and potential significance of the cubic ice polymorph Ice-Ic on Mars. When water ice crystalizes on Earth, the ambient conditions of temperature and pressure result in the formation of the hexagonal ice polymorph Ice-Ih; however, on Mars, the much lower temperatures and pressures may permit the crystallization of the cubic polymorph Ice-Ic. Ice-Ic has two properties of possible importance on Mars: (1) it is an excellent nucleator of other volatiles (such as CO_2), and (2) it undergoes an exothermic transition to Ice-Ih at temperatures above 170 K. These properties may have

significant implications for both martian cloud formation and the development of the seasonal polar caps.

On Friday evening the group discussion returned to the topic of regolith water vapor sources on Mars. Following two hours of often spirited debate, the conferees reached a consensus on several issues. The majority opinion held that although the Viking observations did not preclude the possibility of localized regolith sources, neither did they provide any persuasive evidence for the existence of such sources. The published terrestrial remote-sensing evidence was deemed equally ambiguous. However, neither the

TABLE 1. Principal conclusions.

I.	<i>Annual Behavior of Mars Atmospheric Water Vapor: General Observations</i>
	<ul style="list-style-type: none"> a. There is little global-scale interannual variability. b. Most observed variability can be attributed to interference by dust and condensate clouds. c. There are strong similarities with the state of water vapor in the Earth's stratosphere.
II.	<i>Vertical Distribution of Water Vapor</i>
	<ul style="list-style-type: none"> a. Arguments exist for both low-altitude concentration and uniform mixing to several scale heights. b. Actual distribution of vapor is vital to understanding net annual transport. c. The Viking MAWD experiment was not designed to address this question. d. However, the Mars Observer PMIRR was.
III.	<i>Net Annual Transport of H_2O to and from the Poles</i>
	<ul style="list-style-type: none"> a. Interpretation of the Viking MAWD data is complicated by several uncertainties: <ul style="list-style-type: none"> 1. Quantity of atmospheric water present as condensate and adsorbed on dust. 2. Speed and direction of winds at time of observations. 3. Vertical distribution of H_2O. 4. Effect of global dust storms. 5. Extent of exchange with regolith. b. Mars Observer PMIRR should resolve vertical profile. c. Answers to many of the remaining questions will require deployment of multiple meteorological stations over the planet's surface.
IV.	<i>Regolith Sources and Sinks of H_2O</i>
	<ul style="list-style-type: none"> a. Existence of regolith vapor sources appears geologically reasonable. b. However, no unambiguous evidence for such sources has yet been reported. c. Sources as large as several hundred kilometers in diameter are probably not detectable with the MAWD data. d. The performance capabilities of the Mars Observer radar altimeter appear inadequate for the direct detection of soil moisture. e. The Mars Observer gamma-ray spectrometer may have more success in this regard.

seasonal melting of water ice nor any other simple scenario can as yet explain the apparent seasonal variability of radar reflectivity observed in Solis Lacus. The debate over regolith sources may finally be resolved by the Mars Observer gamma-ray spectrometer, an instrument that is capable of detecting soil moisture within ~10 cm of the surface over regions >300 km in diameter.

At the conclusion of the workshop on Saturday, a final summary of the conclusions reached by the participants was prepared (Table 1). They also considered what type of investigation would best follow the Mars Observer PMIRR. The deployment of a global meteorological network

was identified as the most logical next step to understanding the hydrologic cycle of Mars. The individual stations making up such a network need not be complex; a simple collection of sensors to monitor air temperature, pressure, relative humidity, wind speed and direction is all that is required. Ten or more such stations, distributed over the planet, should permit researchers to develop a detailed model of the planet's general circulation. Such a model, when combined with the data provided by the Viking MAWD and Mars Observer PMIRR instruments, should provide scientists with an accurate picture of the current diurnal and seasonal cycling of water on Mars.

ABSTRACTS

WATER IN THE MARTIAN REGOLITH

187392

Duwayne M. Anderson
Associate Provost for Research
Texas A&M University

In earlier papers, we have considered the occurrence of water and permafrost on Mars (1, 2, 3, 4), some important questions relating to the phases and physical states of water and ice on Mars (5, 6), and their terrestrial analogues (7, 8), and some of their possible consequences in forming Martian landscapes (9, 10, 11). This paper focuses on the water-ice phase composition, adsorption-desorption and evaporation phenomena, and brine compositions of six antarctic soils that are considered to be good terrestrial analogues of the Martian surface materials.

The water-ice phase composition diagram is shown in schematic form in Figure 1. Water-ice phase composition data for a very large number of frozen terrestrial soils can be adequately represented in this manner, although important, second order, deviations have been recognized in certain special cases (6). The diagram in Figure 1 represents the general equilibrium that is established between ice formed within a particulate matrix and the water remaining unfrozen when temperature, solute concentration, etc. are fixed. All evidence available to date indicates that the ice formed is normal, hexagonal ice I, although differential scanning calorimetry has revealed certain complexities in the release of latent heat on freezing that have been ascribed to the presence of complex phases in the unfrozen, interfacial water. Similarly, anomalous melting behavior also has been observed (11).

Figures 2 and 3 show the water-ice phase composition for one of the six Antarctic soils from the lower Wright Valley (Site 1, Figure 4) Antarctica studied in this investigation. Values of the quantity of water remaining in the unfrozen state as a function of temperature are given when this equilibrium is approached in both cooling and warming cycles. As is evident from these data, the agreement is extremely good, indicating that the transfer of water from one phase to another is nearly reversible. Small discrepancies, when they occur, are attributed to capillary and interfacial effects that cannot be easily controlled.

That equilibrium exists between the vapor phase, also, can be demonstrated. Figure 5 shows the desorption isotherm of water in montmorillonite clay at -5 degrees C. The isotherm cuts the ordinate sharply at a relative humidity of 100% precisely at the value of the unfrozen water content of an ice containing frozen sample of the same montmorillonite clay at -5 degrees C. The results of many experiments have

verified that as water vapor is pumped away from the frozen ice containing clay, the unfrozen water content remains constant until the solid phase is removed. Only after all the ice is gone, does subsequent removal of water vapor deplete the unfrozen interfacial water phase.

Figure 6 shows the evolution of adsorbed water vapor (mass 18) on heating one of the six Antarctic soils in this investigation. Similar curves were obtained for each of the six samples investigated. The detector in this case was a scanning mass spectrometer functioning as an effluent gas analyzer. In addition to measuring the water vapor release, it also measured the release of other volatiles. Release curves were obtained for NO, SO, O, N and CO₂, the most abundant volatile component species of the natural brines present in these soils. The curves for NO (mass 30) and CO₂ with N₂O (mass 44) are included in Figure 6.

The water-ice phase composition curves in Figures 2 and 3 reflect the presence of the natural brines that decompose on heating to yield the mass 30 and mass 44 curves in Figure 5. The values of the water remaining unfrozen at a given temperature are larger in the case of the natural soils than those observed when they are washed free of the brines and again subjected to a determination of the water-ice phase composition curve. The effect of the presence of these brines can be predicted from theory as was done in an earlier paper by Banin and Anderson (12). The difference between the two curves shown in Figures 2 and 3 are consistent with the prediction of their equation 9.

Atmospheric exchange of water vapor with the Martian regolith involves a number of dynamic processes. Some of these involve changes of phase as illustrated in the data shown above. Whenever a change of phase occurs, there is an accompanying latent heat effect. As these data show, latent heat effects in terrestrial soils are not isothermal; they are involved at nearly all stages when ground temperatures fluctuate. This has been graphically shown in diagrams such as those in Figures 7 and 8. Calculations done for temperature fluctuations in Arctic permafrost have shown that these effects are not negligible, but they are relatively easy to include in theoretical calculations (13).

In addition to correlating a number of experimental measurements, all relating to the composition and behavior of permafrost and frozen ground, this discussion illustrates the general utility of a Differential Scanning Calorimetry / Effluent Gas Analysis (DSC/EGA) instrument such as was proposed earlier for the Viking Lander Mission and more recently, for the Comet Rendez-vous and Asteroid Flyby (CRAF) mission (14). Data obtainable from a properly designed and operated DSC/EGA instrument can provide the

means of deducing the answers to many of the questions that have been posed in the papers presented in this workshop.

References:

1. Anderson, D.M., 1978. Water in the Martian Regolith. Comparative Planetology, pp. 219-224, Academic Press, Inc.
2. Anderson, Duwayne M., 1976. NASA SP-417, A Geological Basis for the Exploration of the Planets. Editors, R. Greeley, University of Santa Clara, and M.H. Carr, U.S. Geological Survey.
3. Anderson, Duwayne M., and Amos Banin, 1975. Soil and Water and its Relationship to the Origin of Life. Presented at the 4th International Congress on the Origin of Life, Barcelona, Spain, 25-29 June, 1973. Origins of Life, Vol. 6, pp. 23-26.
4. Anderson, Duwayne M., Lawrence W. Gatto, and Fiorenzo Ugolini, 1973. An Examination of Mariner 6 and 7 Imagery for Evidence of Permafrost Terrain on Mars. PERMAFROST: The North American Contribution to the Second International Conference, Yakutsk, Siberia. National Academy of Sciences, pp. 499-508.
5. Anderson, Duwayne M., 1981. Some Thermodynamic Relationships Governing the Behavior of Permafrost and Frozen Ground. Proceedings NATO-Advanced Study Institute, "Comparative Study of the Planets," Vulcano, Italy. Mem. S.A. It., pp. 327-331.
6. Anderson, Duwayne M., 1985. Subsurface Ice and Permafrost on Mars. Ices in the Solar System, J. Klinger et al., (eds.), pp. 565-581. D. Reidel Publishing Company.
7. Gatto, L.W., and D.M. Anderson, 1975. Alaskan Thermokarst Terrain and Possible Martian Analog. Science, Vol. 188, No. 4185, pp. 255-257.
8. Anderson, Duwayne M., Lawrence W. Gatto, and Fiorenzo C. Ugolini, 1972. An Antarctic Analog of Martian Permafrost Terrain. Antarctic Journal of the United States, Vol. VII, No. 4, pp. 114-116.
9. Lucchitta, B.K., and D.M. Anderson, 1979-80. Martian Outflow Channels Sculptured by Glaciers. NASA Technical Memorandum 81776, Reports of Planetary Geology Program, pp. 271-273.

10. Anderson, D.M., and L.W. Gatto, 1978. Thermokarst Topography of Yakutsk, and Analog of Martian Chaotic Terrain. Third International Conference on Permafrost, Edmonton, Alberta, Canada. National Academy of Sciences publication.
11. Anderson, Duwayne M., and A.R. Tice, 1985. Thawing of Frozen Clays. Freezing and Thawing of Soil-Water Systems. Technical Council of Cold Regions Engineering Monograph, pp. 1-9.
12. Banin, Amos, and Duwayne M. Anderson, 1974. Effects of Salt Concentration Changes During Freezing on the Unfrozen Water Content of Porous Materials. Water Resources Research, Vol. 10, No. 1, pp. 124-128.
13. Andersland, O.B., and D.M. Anderson (eds.), 1978. Geotechnical Engineering for Cold Regions. McGraw-Hill.
14. Boynton, W.V., 1985. Comet Penetrator-Nucleus Analyzer; a proposal submitted to the National Aeronautics and Space Administration for the Comet Rendez-vous and Asteroid Flyby Mission (unpublished).

WATER IN THE MARTIAN REGOLITH
D. M. Anderson

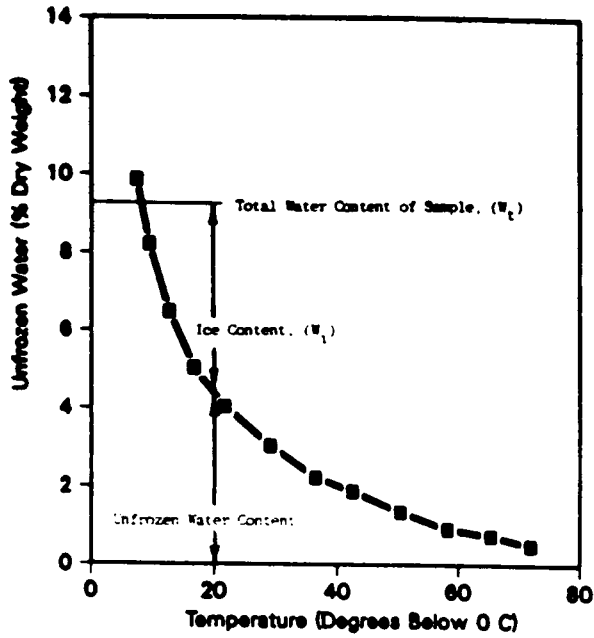


Figure 1. The generalized water-ice phase diagram for frozen soil and permafrost. Note that the total sample water content is the sum of the ice content and the unfrozen water content at any given temperature.

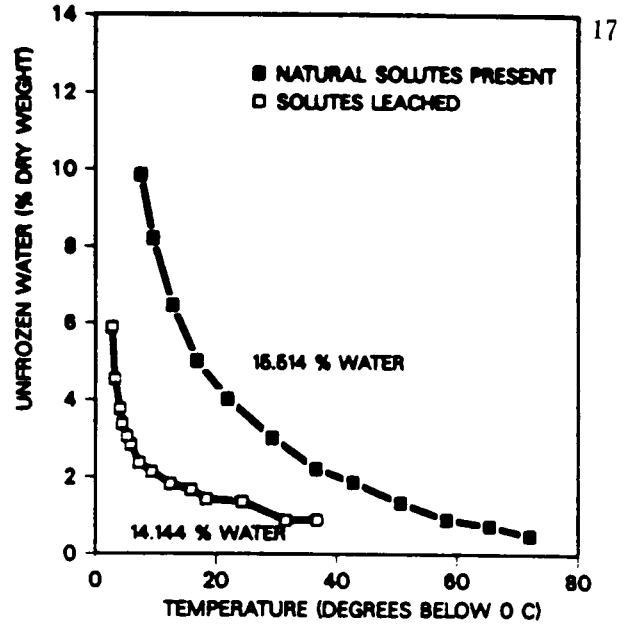


Figure 2. Water-ice phase composition data for Antarctic soil No. 1 obtained during a cooling cycle.

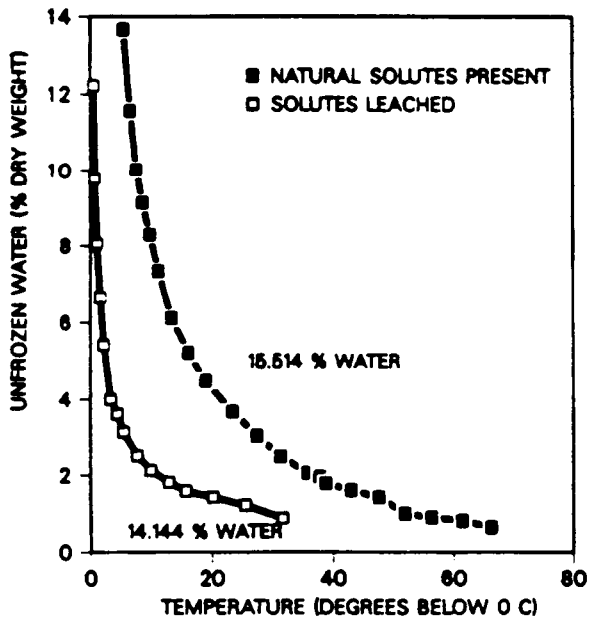


Figure 3. Water-ice phase composition data for Antarctic soil No. 1 obtained during a warming cycle.

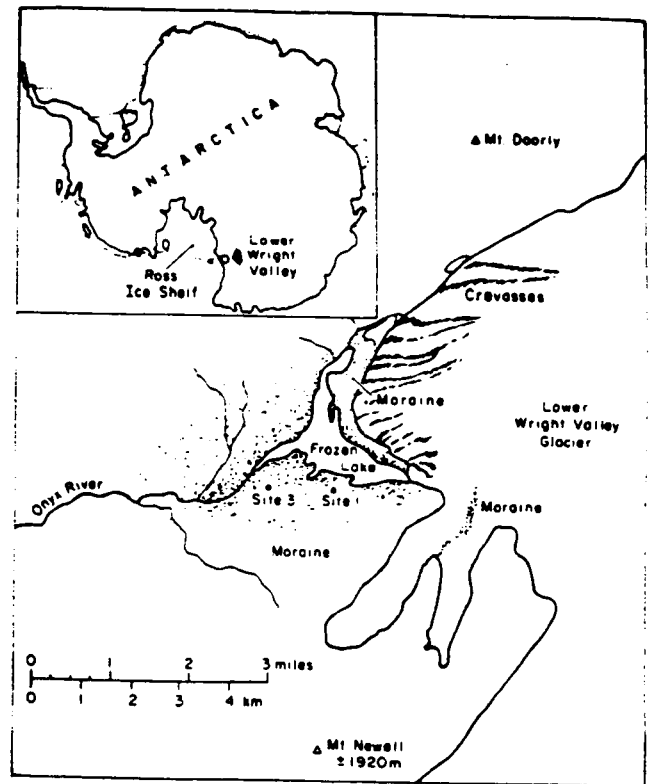


Figure 4. Location map; sample No. 1 was obtained at site 1.

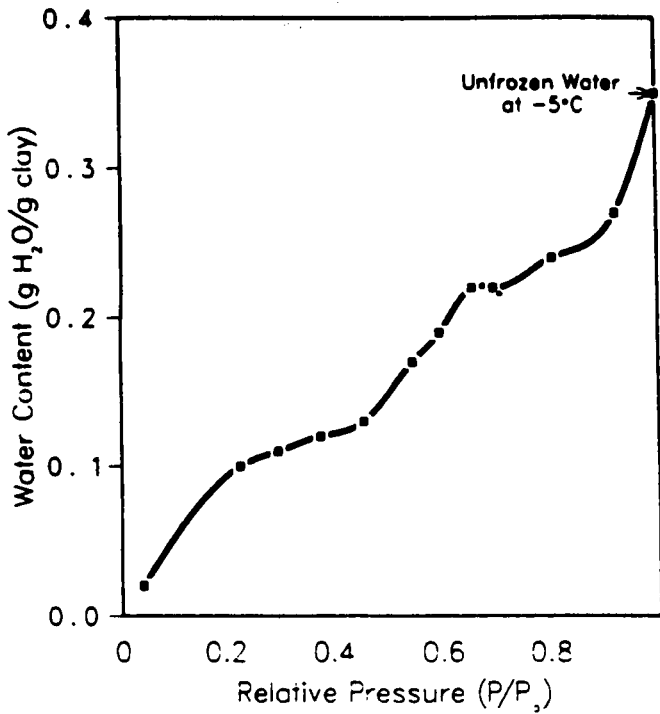


Figure 5. Water vapor desorption isotherm for sodium saturated montmorillonite illustrating the maximum amount of unfrozen water that can exist at -5°C .

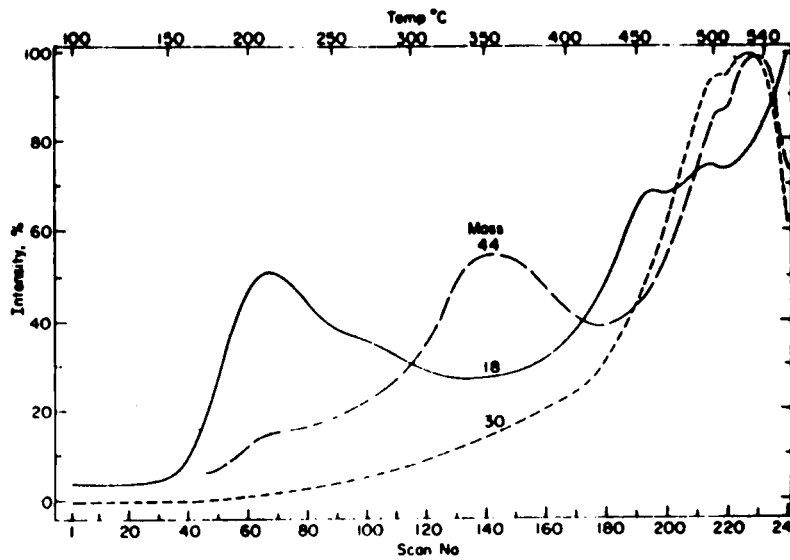


Figure 6. The evolution of H_2O , CO_2 , N_2O and NO on heating Antarctic soil No. 1 from 100° to 550°C .

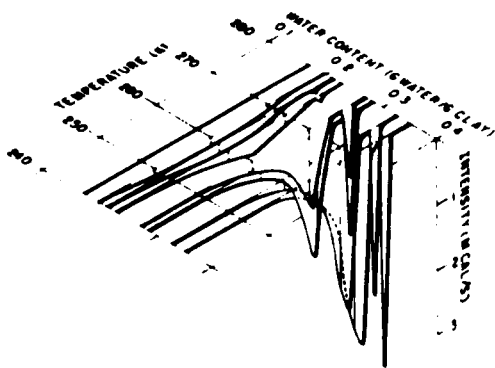


Figure 7. Scanning calorimeter traces for montmorillonite No. 26 containing no salt (warming curves).

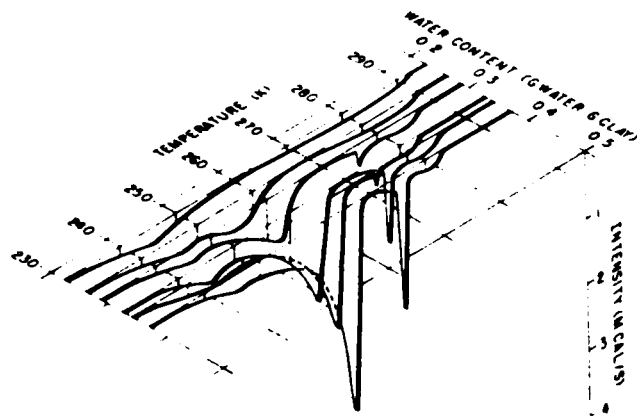


Figure 8. Scanning calorimeter traces for montmorillonite No. 26 containing salt (warming curves).

TRANSPORT OF MARS ATMOSPHERIC WATER INTO HIGH NORTHERN LATITUDES
DURING A POLAR WARMING; J.R. Barnes and J.L. Hollingsworth, Department of
Atmospheric Sciences, Oregon State University, Corvallis, OR 97331

187323

Several numerical experiments have been conducted with a simplified tracer transport model in order to attempt to examine the poleward transport of Mars atmospheric water during a polar warming like that which occurred during the winter solstice dust storm of 1977. Such transport is of considerable potential significance, both for the formation of the layered terrains as discussed by Pollack *et al.*, (1,2), and for the overall Mars water cycle as suggested by Davies (3). The transport model is identical to that previously employed to examine the transport of dust during a polar warming (4); it is beta-plane and essentially like that developed by Garcia and Hartmann (5). It represents tracer transport by a single planetary-scale wave and the zonal-mean flow, with a severely spectrally truncated latitudinal tracer distribution. This latter aspect of the model constitutes probably its greatest limitation.

The flow for the transport experiments has been taken from numerical simulations with a nonlinear beta-plane dynamical model. Previous studies with this model have demonstrated that a polar warming having essential characteristics like those observed during the 1977 dust storm can be produced by a planetary wave mechanism analogous to that responsible for terrestrial sudden stratospheric warmings (6,7). As discussed by Barnes and Hollingsworth, the residual mean circulation for such a model warming is strongly poleward and downward throughout a deep region at high latitudes (4). To the extent that the residual mean circulation represents a good first approximation to the Lagrangian mean circulation, then poleward and downward tracer transport is implied.

Several numerical experiments intended to simulate water transport in the absence of any condensation have been carried out. Observations and modeling indicate that atmospheric temperatures are sufficiently high during a dust storm that condensation would be restricted to high latitudes and altitudes (8,9). The initial water distribution in these experiments is sinusoidal in latitude, with column abundances ranging from 30 pr μm at 30° latitude to 0.1 pr μm at the north pole (or any constant multiple of these values). Cases with the water uniformly mixed to 40 and 20 km, and falling off rapidly above, have been examined. For some of the experiments an atmospheric source of water has been incorporated, intended to crudely simulate transport of water into the model domain by the cross-equatorial Hadley circulation (which is not explicitly represented in the dynamical model). The source has essentially the same structure as the initial distribution, and a rate such as to largely "replace" the initial water within the period of the simulations (40 sols).

The numerical experiments indicate that the flow during a polar warming can transport very substantial amounts of water to high northern latitudes, given that the water does not condense and fall out before reaching the polar region. For an initial water abundance of 30 pr μm at 30°N, abundances of ~7-15 pr μm are obtained at the pole after ~20 sols (the lower values for no source, the higher with a source). The total water transported north of 60° ranges from $1-2 \times 10^{14}$ g (not including the implicit transport by the source). Such amounts would be very significant for the water cycle: net southward transports of this magnitude have been inferred from the annually averaged water distribution (10).

The water and dust transport experiments together appear to lend support to the type of scenario proposed by Pollack et al. (1,2) as playing a key role in the formation of the layered terrains. The mass of water obtained at very high latitudes is roughly comparable to (perhaps slightly smaller than) the mass of dust deposited on the surface in dust transport experiments incorporating sedimentation. Condensation of the water onto dust grains would thus imply slightly larger composite particles; production of very large particles would need to then be by CO₂ condensation or possibly particle aggregation. The dust transport experiments with sedimentation indicate that a composite (water and dust) layer ~10 μm thick can easily be deposited at the north pole during a polar warming event. This is close to the magnitude required for formation of an individual polar layer over the time scale of the Martian orbital variations.

References:

- (1) Pollack, J.B., D.S. Colburn, R. Kahn, J. Hunter, W. Van Camp, C. Carlston, and M. Wolfe (1977) Properties of aerosols in the Martian atmosphere, as inferred from Viking Lander imaging data. J. Geophys. Res., 82, 4479-4496.
- (2) Pollack, J.B., D.S. Colburn, F.M. Flasar, R. Kahn, C.E. Carlston, and D.C. Pidek (1979) Properties and effects of dust particles suspended in the Martian atmosphere. J. Geophys. Res., 84, 2929-2945.
- (3) Davies, D.W. (1981) The Mars water cycle. Icarus, 45, 398-414.
- (4) Barnes, J.R. and J.L. Hollingsworth (1986) Numerical simulations of dust transport into northern high latitudes during a Martian polar warming. In MECA Workshop on Mars: Evolution of its Climate and Atmosphere. Lunar and Planetary Institute, Houston, in press.
- (5) Garcia, R.R. and D.L. Hartmann (1980) The role of planetary waves in the maintenance of the zonally averaged ozone distribution of the upper stratosphere. J. Atmos. Sci., 37, 2248-2264.
- (6) Barnes, J.R. and J.L. Hollingsworth (1985) Dynamical modeling of a Martian polar warming. Bull. Amer. Astron. Soc., 17, 3:733.
- (7) Barnes, J.R. and J.L. Hollingsworth (1986) Dynamical modeling of a planetary wave mechanism for a Martian polar warming. Submitted to Icarus.
- (8) Haberle, R.M., C.B. Leovy, and J.B. Pollack (1982) Some effects of global dust storms on the atmospheric circulation of Mars. Icarus, 50, 322-367.

- (9) Jakosky, B.M. and T.Z. Martin (1984) Mars: Polar atmospheric temperatures and the net transport of water and dust. Unpublished manuscript.
- (10) Jakosky, B.M. (1983) The Seasonal Behavior of Water Vapor in the Mars Atmosphere. Ph.D. Thesis, California Institute of Technology, Pasadena.

THE EFFECT OF GLOBAL-SCALE DIVERGENT CIRCULATION ON THE ATMOSPHERIC WATER VAPOR TRANSPORT AND MAINTENANCE, Tsing-Chang Chen, Department of Earth Sciences, Iowa State University, Ames, IA 50011

1. Introduction

Many efforts have been made by meteorologists in the past three decades to examine the local maintenance of water vapor by the moisture transport. It was pointed out by Starr and Peixoto (1) that it is difficult to explain the relationship between regions of high water vapor content and total moisture. As it is well known, the precipitation caused by condensation is often associated with the vertical motion of atmospheric divergent circulation. Based upon this practice, we would like to show how the high water vapor content over certain regions is attributed to the convergence by divergent circulations. Two aspects will be presented. One aspect is how the high water vapor content in the tropics during winter and summer seasons is maintained. The other is how the sudden intensification of the tropical divergent circulations associated with the monsoon onset enhances the water vapor content over monsoon regions. The data used in this study were generated by the FGGE III-b analyses of the European Center for Medium Range Weather Forecasts. The specific humidity is computed from temperature and relative humidity in Chen et al. (2).

2. Theoretical Background

The hydrological cycle of the atmosphere can be illustrated with the water balance equation,

$$\frac{\partial W}{\partial t} + \nabla \cdot \mathbf{Q} = E - P, \quad (1)$$

where W is precipitable water in an air column, \mathbf{Q} is water vapor transport, ∇q , and q is specific humidity. E and P are evaporation and precipitation. The long-term, say a season or a month, average of Eq. (1) can be approximated as

$$\nabla \cdot \bar{\mathbf{Q}} = \bar{E} - \bar{P}, \quad (2)$$

($\bar{\quad}$) = time average. Note that the water vapor transport vector can be separated into the rotational and divergent component, i.e. $\nabla q = (\nabla q)_\psi + (\nabla q)_\chi$ or $Q = Q_\psi + Q_\chi$. These two components can be expressed in terms of streamfunction (ψ) and potential function (χ). Therefore, Eq. (2) can be written as

$$\nabla \cdot \bar{\mathbf{Q}}_\chi = \nabla^2 \bar{\chi} = \bar{E} - \bar{P}. \quad (3)$$

Based upon Eq. (3), we can relate \mathbf{Q} to the source and sink of water vapor. This approach was proposed by Chen ⁽³⁾. ψ and χ are obtained from Poisson equation by specifying boundary conditions at the northern and southern boundaries. Our analysis covers the entire globe.

3. Global Water Vapor Flux and Maintenance

The largest water vapor content exists in the tropics. The zonal asymmetry in the geographic distribution of this quantity occurs essentially over three tropical continents. They are the northern part of South America,

Chen, T.-C.

equatorial Africa, and the equatorial western Pacific during the northern winter (December-February), and Central America and the northern part of South America, equatorial west Africa, and monsoon areas during the northern summer (June-August). The water vapor transport is mainly carried out by Q_{ψ} (not shown) and follows the low-level atmospheric circulations because the major part of the water vapor is located there. According to Eq. (2), Q_{ψ} is not related to the difference between evaporation (E) and precipitation (P), while Q_{χ} is. The latter component of water vapor transport is displayed in Fig. 1 for both northern summer and winter. Observations reveal that the water vapor converges toward three tropical areas of high water vapor content. This indicates that the local Hadley circulation and the longitudinal Walker circulation perform the water vapor transport to maintain the high water vapor content over three preferable tropical regions. The converged water vapor would be transported upward by the two types of divergent circulations to increase the moisture content of the atmosphere and, in turn, to enhance the condensation. Therefore, the large rainfall in the tropics is consistently distributed with the significant convergence of water vapor flux.

4. Divergent Water Vapor Flux Associated with Monsoon Onset

The onset of both Australian and Indian monsoon is always characterized by the deepening of the low-level monsoon trough and the intensification of the upper-level high center over monsoon regions, and sudden heavy rainfall (Chen and Yen (4)). This implies the abrupt development of divergent circulations over monsoon regions when the monsoon onset occurs. The strong upward motions associated with divergent circulations converge and pump upward water vapor. Intensive cumulus convective activities are induced and heavy rainfall follows. The moisture transported by the divergent mode before and after monsoon onset for both Australian and Indian monsoon is exhibited in Figs. 2 and 4, respectively. The onset of the former monsoon occurs between December 21-26 of 1978 and that of the latter monsoon occurs between June 10-16, 1979. It is very obvious from these two figures that a tremendous enhancement of water vapor flux converged toward monsoon regions by the divergent mode after monsoon onset occurs. To demonstrate the abrupt increase of water vapor with divergent circulations when the monsoon onset occurs, averages of the 200-mb divergent kinetic energy (k_D), water vapor content, and root mean square of divergent water vapor flux over key monsoon areas, which are encircled in Figs. 2 and 4, are displayed in Figs. 3 and 5. These figures confirm our above argument.

5. Concluding Remarks

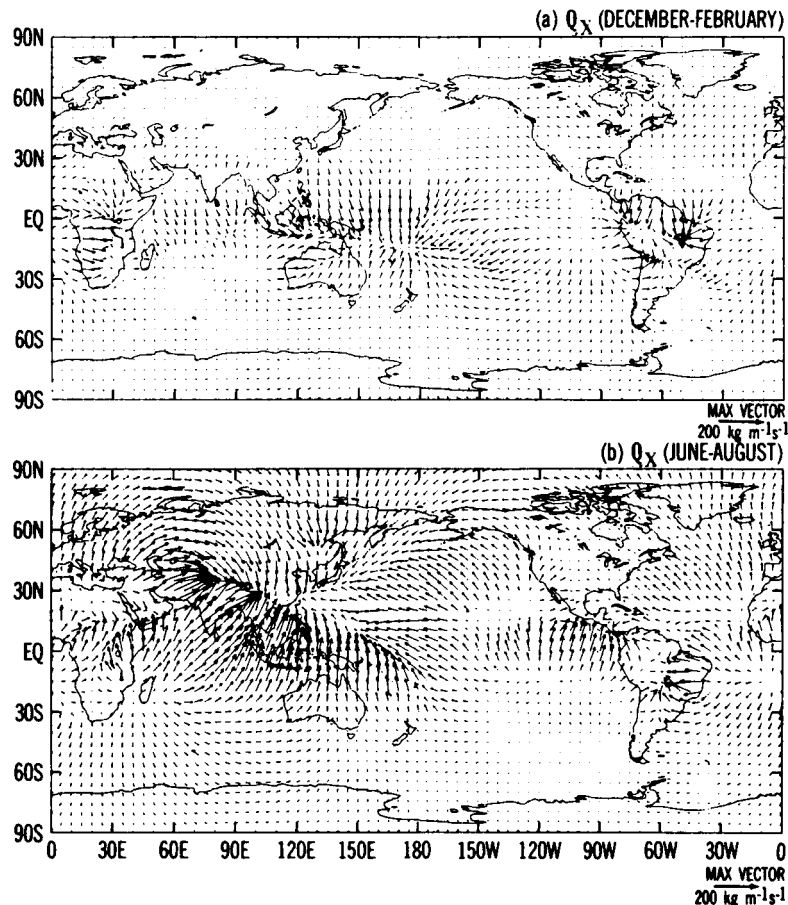
It was shown by our past studies (Chen and Wiin-Nielsen (5); Chen (6)) that the atmospheric circulation is dominated by the rotational component. However, it is the divergent component of motion which releases the available potential energy to drive atmospheric motions. The water vapor transport by atmospheric motions works in a same manner. Although the water vapor is essentially transported by rotational component, this study demonstrates that only the water vapor transported by divergent component is linked to the source and sink, and maintenance of atmospheric water vapor content.

6. Acknowledgements

This study is supported by the NSF Grant ATM-8611476. Figs. 2-5 were prepared by Mr. M.-C. Yen, whose help is highly appreciated. The computations were performed with the NCAR CRAY computer which is sponsored by the National Science Foundation. Thanks also go to Ms. Linda Claussen for her typing.

7. References

- Starr, V. P. and Peixoto, J. P. (1964), Arch. Meteor. Geoph. Biokl., Ser. A, 14, p. 111-130.
- Chen, T.-C., Chang, C. B., and Perkey, D. J. (1985), Monthly Weather Review 113, p. 349-361.
- Chen, T.-C. (1985), Monthly Weather Review, 113, p. 1801-1819.
- Chen, T.-C. and Yen, M.-C. (1986), The Second International Conference on Southern Hemisphere Meteorology, 1-5 December 1986, Wellington, New Zealand.
- Chen, T.-C. and Wiin-Nielsen, A. (1976), Tellus, 28, 486-498.
- Chen, T.-C. (1980), Monthly Weather Review, 108, p. 896-912.

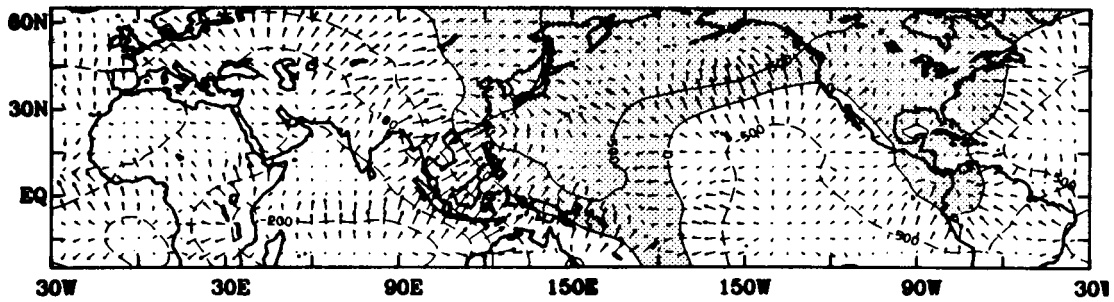


ORIGINAL PAGE IS
OF POOR QUALITY

Fig. 1. Divergent component of the vertically integrated water vapor transport vector field. Vector units: $\text{kg m}^{-1}\text{s}^{-1}$.

Q_D and χ

(a) 5/20-6/2 (1979) before onset of Indian monsoon



(b) 6/17-6/30 (1979) after onset of Indian monsoon

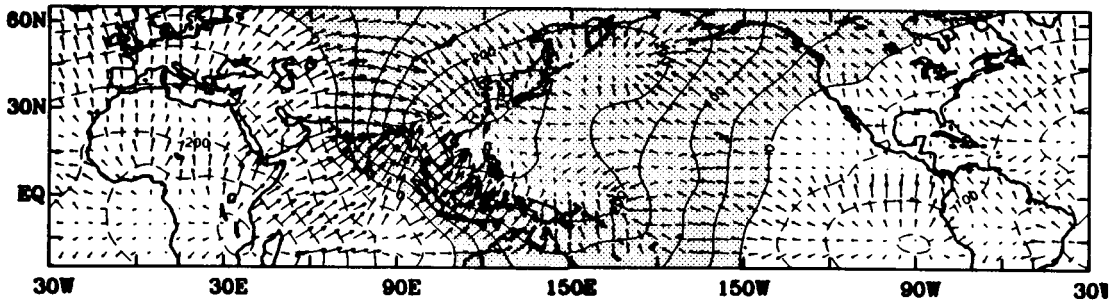


Fig. 2. Global distribution of potential for the vertically integrated water vapor flux superimposed with divergent component of water vapor transport vector field. Contour intervals of potential are 5×10^5 kg s^{-1} and vector units are $\text{kg m}^{-1} \text{s}^{-1}$.

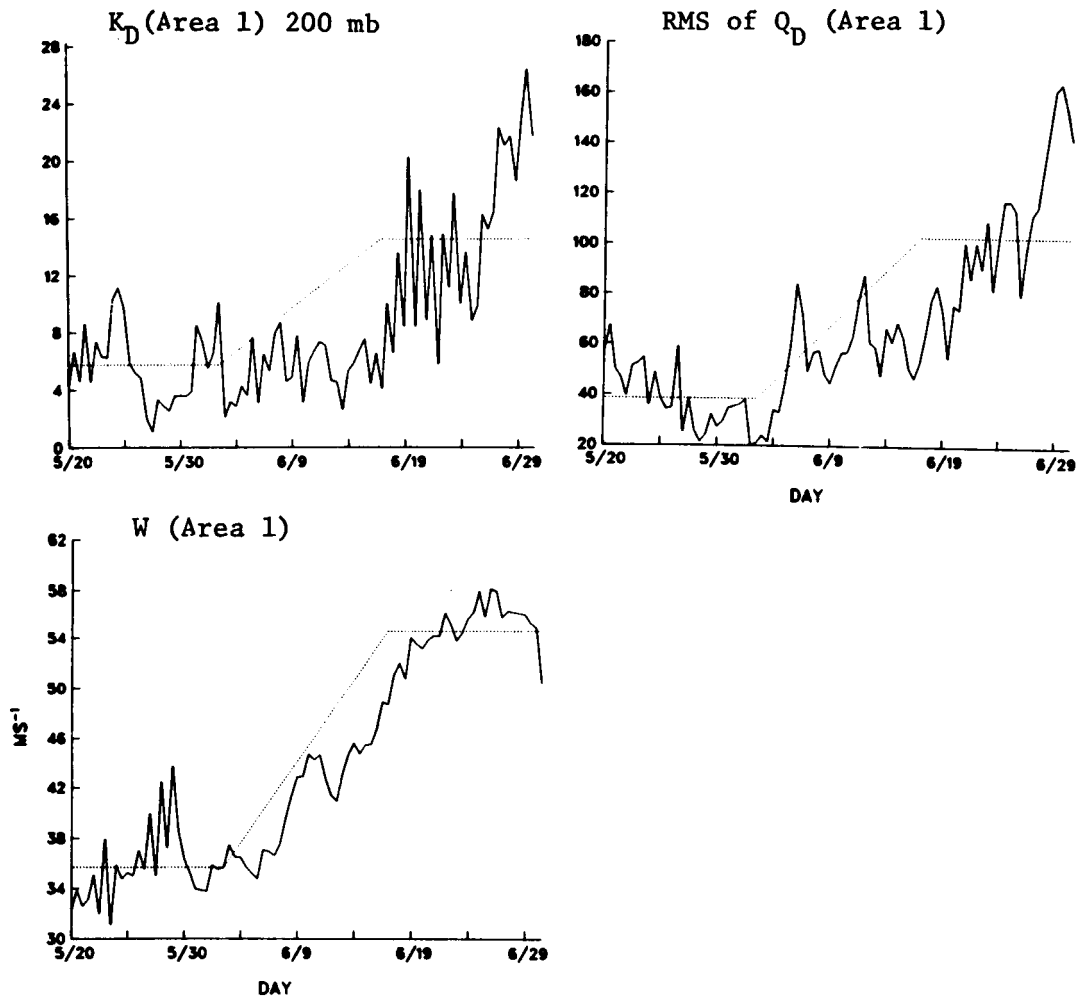
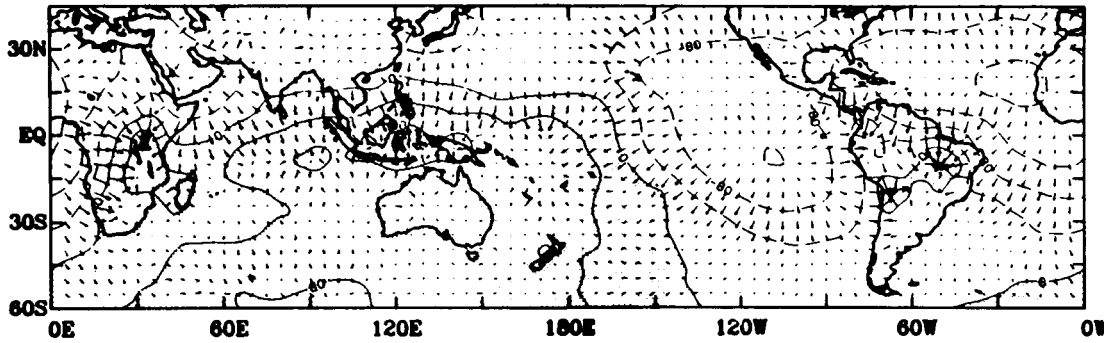


Fig. 3. Time series of K_D , root mean square (RMS) of Q_D and precipitable water (W). Area 1: (60°E-90°E, 15°N-25°N)
 Units: K_D m^2s^{-2} , RMS of Q_D $ms^{-1}g\ kg^{-1}$,
 W mm.

Q and χ

(a) 12/1-12/21 (1978) before onset of Australian monsoon



(b) 1/1-1/31 (1979) after onset of Australian monsoon

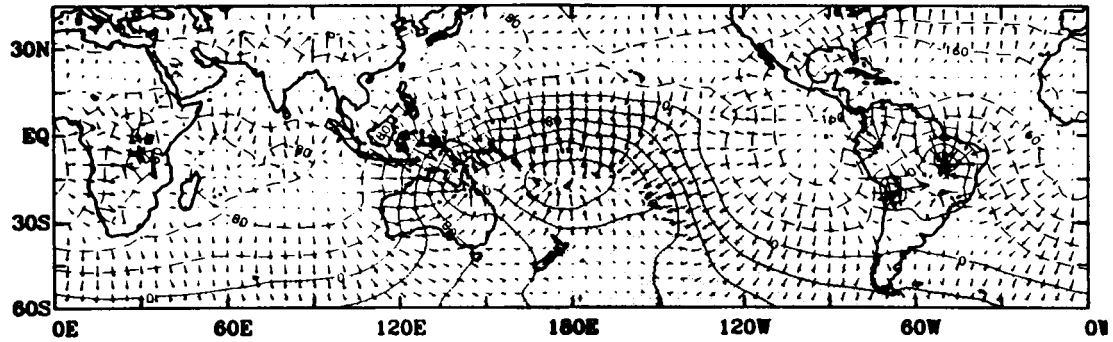


Fig. 4. The same as Fig. 2, except for the onset of Australian monsoon. Contour intervals of potential are 4×10^5 .

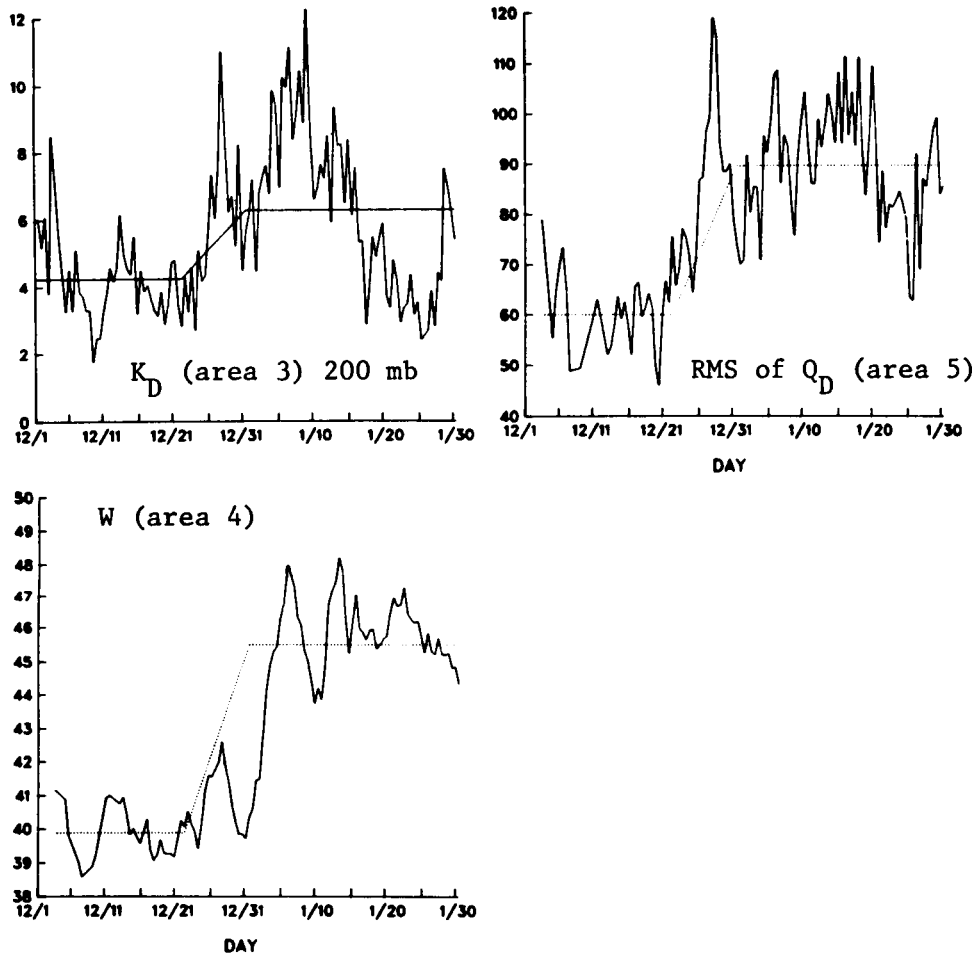


Fig. 5. Time series of K_D , root mean square (RMS) of Q_D and precipitable water (W).

Area 3: (112.5°E-120°W, 45°S-10°S)

Area 4: (150°E-140°W, 20°S-5°S)

Area 5: (112.5°E-150°W, 30°S-0°)

N89-25794

54-91

187395 ABS JILLY
28

29

SEASONAL AND DIURNAL VARIABILITY OF MARS WATER-ICE CLOUDS

P.R. Christensen ⁽¹⁾, R.W. Zurek, ⁽²⁾ and L.L. Jaramillo ⁽¹⁾, ⁽¹⁾, Department of Geology, Arizona State University, Tempe, AZ 85287, ⁽²⁾, Jet Propulsion Laboratory, Pasadena, CA 91103.

Water-ice clouds have been observed on Mars both visually (e.g. 2) and using Viking IRTM spectral observations (5). Visual observations show the presence of discrete clouds, hazes, and detached limb hazes. The more complete IRTM coverage shows that clouds are consistently present over specific northern hemisphere regions, including Tharsis, Arabia, and Elysium, and are less common in the south. In addition, Viking Lander measurements of atmospheric opacity have shown the presence of atmospheric hazes that vary with season and time of day (4,5). These diurnal variations suggest that there is a contribution to these hazes due to condensates which vary in thickness from morning to afternoon (4). The purpose of this project is to study the diurnal and season behavior of cloud opacity and frequency of occurrence using an atlas of cloud occurrence compiled from the IRTM data set.

The results of cloud occurrence can be determined as a function of L_s for different regions on the planet. The data can be separated into morning, midday, and afternoon cloud occurrences to show the diurnal as well as seasonal variability. The cloud occurrence is presented as a percentage of the IRTM observations over a given period that had a cloud in the field of view.

Clouds are most common over the Tharsis region (0 to 10N°, 120 to 140W°) during northern spring and summer (L_s 0 to 150°), with all clouds present in up to 40% of all observations. However, some clouds occur at all times throughout the year. During spring and early summer clouds are most abundant during midday, and are more common in the morning than in the evening. This diurnal variation is consistent with the presence of morning fogs, with clouds building up during the day due to orographic uplift and dissipating somewhat in the late afternoon. Other IRTM observations suggest that clouds are also present at night, with fogs already present before dawn.

From late summer through winter, clouds are again most common near midday, but during this period, afternoon clouds occur more frequently than do morning clouds. This behavior suggests that fogs may not be forming predawn during fall and winter, with the early morning hours being the least cloudy.

Morning-afternoon differences in atmospheric opacity were also observed at the Viking Lander sites (3). However, the Lander observations, which were made using reflected energy, could not distinguish between dust and condensate hazes, although morning condensate fogs have been proposed to explain the observed diurnal differences. The IRTM thermal observations can distinguish dust from condensate, and support the suggestion that variations in water cloud abundance or opacity produce the observed effects. Lander observations indicated that low-level fogs began forming at approximately 2 AM (3), again consistent with the IRTM observations in Tharsis.

Other areas show similar patterns of seasonal variation in cloud abundance, although the data are insufficient to accurately determine diurnal variability in many cases. For example, Lunae Planum (10 to 20°N, 60 to 70°W)

MARS WATER-ICE CLOUDS

Christensen, P.R. et al.

30

has a very pronounced increase in cloud abundance during early summer, with clouds occurring up to 40% of the time at L_s 130° compared to 1 to 5% during fall and winter. Cloud occurrence at the Lander 1 site varies from 9% in early summer to 1% in fall and winter.

References: 1) Kahn, R., 1984, J. Geophys. Res., 89, 6671-6688. 2) Briggs, G., K. Klaasen, T. Thorpe, J. Wellman, and W. Baun, 1977, J. Geophys. Res., 82, 4121-4149. 3) Christensen, P.R. and R.W. Zurek, 1984 J. Geophys. Res., 89, 4587-4596. 4) Pollack, J.B. et al., 1977, J. Geophys. Res., 82, 4479-4496. 5) Pollack, J.B. et al., 1984, J. Geophys. Res., 84, 2929-2945.

THE INTERPRETATION OF DATA FROM THE VIKING MARS ATMOSPHERIC WATER DETECTORS (MAWD): SOME POINTS FOR DISCUSSION; Stephen M. Clifford, Lunar and Planetary Institute, 3303 NASA Road One, Houston, TX 77058.

Properly interpreted, water vapor column abundance measurements can provide important insights into many of the processes that govern the diurnal, seasonal, and climatic cycles of atmospheric water on Mars. Presently, the largest body of such data comes from the Viking Orbiter Mars Atmospheric Water Detectors (MAWD). These instruments were operational from 1976 to 1979; their mode of operation and preliminary results have been discussed in detail by Farmer et al. (1977), Jakosky and Farmer (1982) and Jakosky (these abstracts).

Unfortunately, some uncertainty exists over the correct interpretation of the MAWD data — particularly with regard to estimates of the magnitude and direction of atmospheric H₂O transport (e.g., James, 1985) and the identification of possible regolith sources and sinks (i.e., Huguenin and Clifford, 1982). This uncertainty stems from our almost complete inability to 'ground-truth' the interpretations made from orbital data. Indeed, there are only two locations on the martian surface for which we have any quantitative meteorological information. This consists of limited measurements of windspeed, direction, atmospheric pressure, temperature, and opacity, at the landing sites of VL 1 (22.4°N, 47.5°W) and VL 2 (44°N, 226°W).

While direct tests of the various interpretations of the MAWD data are not possible, an alternative approach may exist. Since the mid 1950's, a number of detailed studies have been made of the diurnal and seasonal behavior of atmospheric water vapor on Earth. Over the past decade many of these studies have included atmospheric H₂O column abundance measurements made from Earth orbit. The functional similarities between these Earth orbital instruments and the MAWD experiment are striking. In terrestrial studies, the existence of numerous concurrent surface and airborne meteorological observations greatly aids the task of interpreting the dynamic behavior of H₂O from orbital measurements. This experience may provide an important observational foundation from which to analyze and interpret any similar Mars data - whether it be measurements already obtained by the Viking MAWD, or those anticipated from Mars Observer.

Among the questions that might benefit from a comparative analysis of Earth and Mars water vapor observations are:

What factors and processes govern the storage and exchange of H₂O between planetary surfaces and atmosphere on diurnal and seasonal time scales?

Do regolith sources and sinks of H₂O have uniquely identifiable water vapor column abundance signatures?

How much can be learned about the diurnal and seasonal cycles of H₂O from an analysis of water vapor data alone?

What levels of time and spatial resolution are necessary for determining dynamic behavior?

Can the direction of vapor transport be accurately inferred from the magnitude and direction of atmospheric column abundance gradients, or do processes exist that can drive vapor transport counter to the observed gradient?

What specific design and operational similarities exist between the various Earth and Mars orbital instruments?

Finally, how might our experience with Earth orbital instruments and the Viking MAWD benefit our understanding of the data we hope to receive from Mars Observer?

References:

Farmer, C. B., D. W. Davies, A. L. Holland, D. D. LaPorte, and P. E. Doms (1977) J. Geophys. Res. 82, 4225-4248.

Huguenin, R. L. and S. M. Clifford (1982) J. Geophys. Res. 87, 10227-10251.

Jakosky, B. M. and C. B. Farmer (1982) J. Geophys. Res. 87, 2999-3019.

James, P. B. (1985) Icarus 64, 249-264.

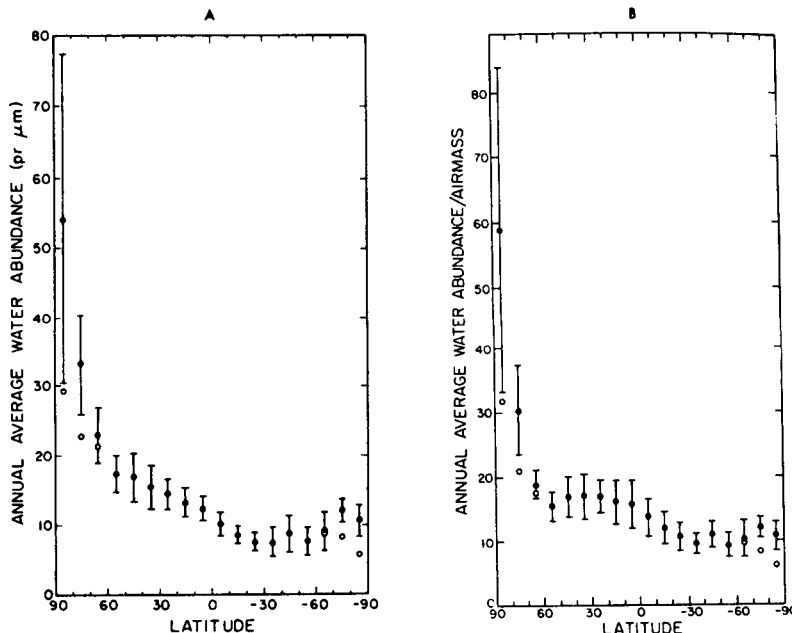


Fig. 1 . (a) Latitudinal behavior of the annual average vapor abundance. One-sigma bars show the variation at each latitude rather than errors. The near-polar data have been corrected (open circles) for lack of observations during the polar night by assuming zero abundance at that time. (b) Latitudinal behavior of the annual average vapor abundance/airmass. [Jakosky and Farmer, 1982].

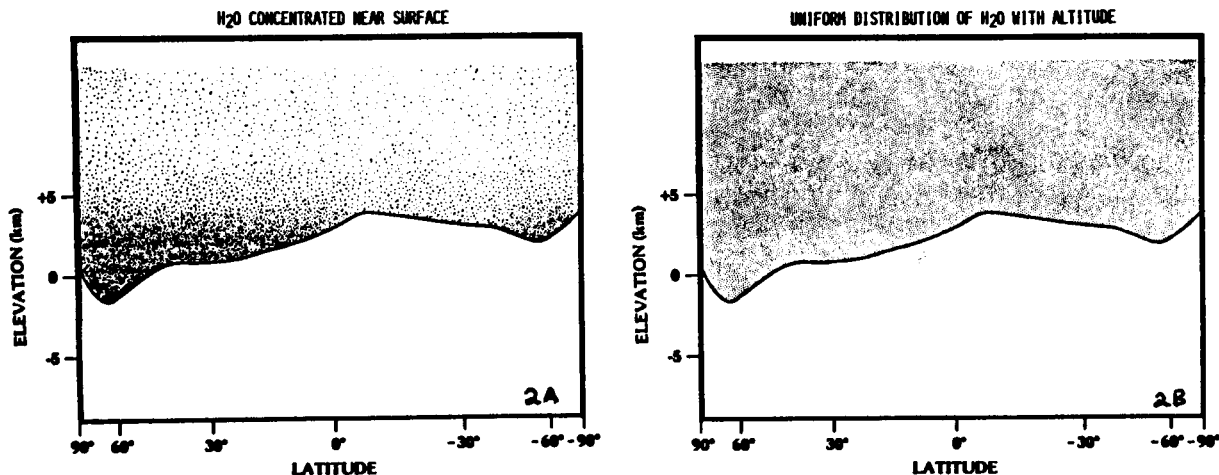


Figure 2. The apparent north to south gradient in zonally averaged vapor abundance seen in Figure 1, may result from an inadequate correction for airmass. Figures 2a and 2b depict the relationship between zonally averaged airmass and topography. Although the horizontal latitude scale for these figures is projected from a sphere (in contrast to the linear scale in Figure 1), a distinct inverse correlation is readily identified between the zonally averaged topography and the zonally averaged vapor abundance. The magnitude of the vapor gradient should reflect the vertical distribution of H₂O in the atmosphere. Clearly, the gradient will be strengthened by vapor concentrated within the lowermost scale height (Figure 2a) and weakened by uniform mixing to several scale heights (Figure 2b). Since the concentration of vapor in either case is constant for a given geopotential, no net hemispheric exchange of vapor is implied.

REGOLITH WATER VAPOR SOURCES ON MARS: A HISTORICAL BIBLIOGRAPHY, S.M. Clifford and R.L. Huguenin, Lunar and Planetary Institute, 3303, NASA Rd 1, Houston, TX 77058.

The existence of regolith water vapor sources on Mars was first considered by several investigators during the early 1970s. They speculated on the possible existence of a down slope source for the vapor that condensed to form the prominent Tharsis 'W' cloud. These discussions appeared in the following papers:

Leovy et al., Mariner Mars 1969: Atmospheric results, J. Geophys. Res. 76, 297-312, 1971.

Leovy et al., Mars atmosphere during the Mariner 9 extended mission: Television results, J. Geophys. Res. 78, 4252-4266, 1973.

Peale, S. J., Water and the Martian W cloud, Icarus 18, 497-501, 1973.

Fanale, F. P. and W. A. Cannon, Exchange of adsorbed H₂O and CO₂ between the regolith and atmosphere of Mars caused by changes in surface insolation, J. Geophys. Res. 79, 3397-3402, 1974.

During the 1973 Mars opposition, a major dust storm was observed in the Solis Lacus (-25°S, 85°W) region. Earth-based vidicon images revealed that the initial dust cloud was bright at both blue and red wavelengths. McCord et al. (1977) interpreted this observation as an indication that the cloud contained a significant amount of condensate. Blue filter brightenings were also observed in an apparent ring around the central plume. The radius of the ring was estimated to be 600-1000 km. The relationship of these features led McCord et al. (1977) and Huguenin et al. (1978; 1979) to conclude that the ring was the result of vapor transport from the central plume. Based on this assumption, they argued that a major source of atmospheric water vapor existed in Solis Lacus. The case for a regolith source is detailed in the following publications:

McCord et al., Photometric imaging of Mars during the 1973 opposition, Icarus 31, 293-314, 1977.

Huguenin et al., Mars: Remote spectral identification of H₂O frost and mineral hydrate, Proc. 2nd Colloq. Planetary Water and Polar Processes, 100-108, 1978.

Huguenin, R.L., Mars: possible occurrence of near-surface liquid H₂O brines in the Solis Lacus region (-25°S, 85°W), LPSC X, 596-597, 1979.

Clifford, S.M. and R.L. Huguenin

34

Huguenin et al., Mars: An oasis in Solis Lacus (-25°S , 85°W)?
Eos: Trans. AGU 60, 306, 1979.

Huguenin et al., Remote sensing evidence for oases on Mars, NASA TM-80339, 208-214, 1979.

Huguenin, R.L. and S.M. Clifford, Additional remote sensing evidence for oases on Mars, NASA TM-81776, 153-155, 1980.

Huguenin, R.L. and S.M. Clifford, Remote sensing evidence for regolith water vapor sources on Mars, J. Geophys. Res. 87, 10227-10251, 1982.

Huguenin et al., Freeze/thaw injection of dust into the Martian atmosphere, LPSC XVI, 376-377, 1985.

Huguenin et al., Injection of dust into the Martian atmosphere: Evidence from the Viking gas exchange experiment, Icarus 68, 99-119, 1986.

The suggestion that Solis Lacus was a significant source of atmospheric vapor was vigorously contested by a number of investigators associated with the Viking mission, most notably the team members of the Mars Atmospheric Water Detector (MAWD) experiment. They argued that the water vapor column abundances measured over Solis Lacus did not differ appreciable from those measured over any other location at the same latitude. Their arguments are best summarized in the following two papers:

Jakosky, B.M. and C.B. Farmer, The seasonal and global behavior of water vapor in the Mars atmosphere: Complete global results of the Viking Atmospheric Water Detector experiment, J. Geophys. Res. 87, 2999-3019, 1982.

Jakosky, B.M., The seasonal cycle of water on Mars, Space Sci. Rev. 41, 131-200, 1985.

The proposal that a near-surface reservoir of H_2O might exist in Solis Lacus led Zisk and Mougins-Mark (1980) to analyze radar data from this region for any anomalous behavior indicative of a seasonal freeze-thaw cycle in the upper few centimeters of regolith. Surprisingly, their preliminary analysis revealed evidence that indicated this kind of activity. Considerable controversy ensued regarding the validity of this interpretation. This led Zisk and Mougins-Mark (1981) and Roth et al. (1984; 1985) to reconsider the radar data. The results of this reanalysis are not conclusive, but tend to favor the original interpretation. However, because a number of questions remain, analysis of the radar data is still ongoing. Readers are therefore advised to consult the current literature for reports

of the most recent results. The following publications provide an overview of the initial stages of the radar debate:

Zisk, S.H. and P.J. Mouginis-Mark, Confirmation of anomalous areas ("oases") on Mars from Earth-based radar data, LPSC XI, 1297-1299, 1980.

Zisk, S.H. and P.J. Mouginis-mark, Anomalous region on Mars: Implications for near-surface liquid water, Nature 288, 126-129, 1980.

Mouginis-Mark et al., Characterization of Martian surface materials from Earth-based radar: The Memnonia Fossae region, Proc. 11th Lunar and Planet. Sci. Conf., vol. 1, 823-837, 1980.

Zisk, S.H. and P.J. Mouginis-Mark, Oases revisited: Further analysis of the Solis Lacus radar anomaly on Mars, LPSC XII, 1239-1241, 1981.

Downs et al., New radar-derived topography for the equatorial belt of Mars, LPSC XIII, 182-183, 1982.

Roth, L.E. and R.S. Saunders, Microwave reflectivity of the multi-layer models of the Martian surface, LPSC XV, 693-694, 1984.

Roth et al., Mars: Seasonally variable radar reflectivity, LPSC XVI, 712-713, 1985.

Roth et al., Radar and the detection of liquid water on Mars, LPI TR 85-03, 71-73, 1985.

Two other publications relevant to the Solis Lacus controversy are:

Lee, S.W., Seasonal and secular variation of the Solis Lacus albedo feature: Relation to the martian dust-transport cycle, LPSC XVI, 483-484, 1985.

Zent, A.P., and F.P. Fanale, Solis Lacus brines: Possible chemistry and kinetics, LPSC XVI, 930-931, 1985.

The publications listed in this bibliography describe the initial debate over the existence of a regolith source of atmospheric water vapor in Solis Lacus. New approaches to the analysis of old data, and the acquisition of new data from Earth-based radar and the Mars Observer spacecraft, may resolve this issue in the near future. If nothing else, the debate over Solis Lacus has motivated a rigorous examination of several important data sets, and helped define the limits of their interpretation.

REGOLITH WATER VAPOR SOURCES ON MARS

Clifford, S.M. and R.L. Huguenin

36

It has also provided at least a partial stimulus for the development of spacecraft sensors capable of detecting near surface reservoirs of H₂O. For these reasons alone, it has been a worthwhile exercise.

Acknowledgment: This research was supported by NASA grants NSG 7405, NSG 7397, and NAGW 40.

FACTORS GOVERNING WATER CONDENSATION IN THE MARTIAN ATMOSPHERE: D. S. Colburn, J. B. Pollack and R. M. Haberle, NASA Ames Research Center, Moffett Field CA 94035

In a previous paper (1) we described the use of atmospheric optical depth measurements at the Viking lander sites to show diurnal variability of water condensation at different seasons of the Mars year. Factors influencing the amount of condensation include latitude, season, atmospheric dust content and water vapor content at the observation site. A one-dimensional radiative-convective model is used here based on the diabatic heating routines under development for the Mars GCM (General Circulation Model). The model predicts atmospheric temperature profiles at any latitude, season, time of day and dust load. From these profiles and an estimate of the water vapor one can estimate the maximum and minimum condensation in the diurnal cycle, the maximum occurring at an early morning hour (AM) and the minimum in the late afternoon (PM). Measured variations in atmospheric optical density between AM and PM measurements have been interpreted as differences in AM and PM water condensation.

A parametric study has been undertaken to investigate further the condensation process. Figures shown here represent model predictions of AM and PM condensation at the two lander sites (Figure 1 for VL1 and Figure 2 for VL2) at various times of the Mars year, as represented by L_s , the solar longitude ($L_s = 0$ is northern vernal equinox). The water vapor content of the atmosphere is fixed for these computations at 11 precipitable microns ($\text{pr-}\mu$), which appears to be a typical value in data supplied by the MAWD experiment (B. Jakosky, private communication). While the amount of water vapor normally changes during the year, it was fixed for this study in order to identify the effects of other parameters. Calculations not shown here indicate that condensation increases with larger water vapor content. Both water vapor and dust are assumed to be uniformly mixed with the atmosphere. Each figure shows the AM and PM condensation predicted for two values of dust content, i.e. with the atmospheric optical depth τ equal to 0.3 and 2.0. The value $\tau=0.3$ is approximately the lowest measured at the lander sites, and can be considered to be background level in the absence of global dust storms. The higher value represents a typical value during the two global dust storms encountered at the lander sites.

Figure 1 shows the maximum AM condensation to occur near $L_s=270$, the northern winter solstice, when atmospheric temperatures are lowest. The lack of symmetry for L_s values less than and greater than 270 is attributed to the eccentricity of the orbit, which places Mars closest to the sun at $L_s=251$. The PM condensation at the latitude of VL1 (22.4 N) is nearly negligible over the whole year, and the AM-PM difference is nearly equal to the AM value. For low dust content, the AM value is appreciable over the whole year, with a maximum of 2.2 $\text{pr-}\mu$.

The effect of the higher dust content ($\tau=2.0$) varies according to the season. Over most of the year it warms the atmosphere sufficient to keep the AM condensation much lower than for lower dust content. However, at $L_s=270$, the AM condensation for $\tau=2.0$ is higher than for lower dust content values. The explanation is believed to lie in the variation in temperature profiles with season, which is being explored using the

model, but not shown here.

Figure 2 shows predicted condensation at the latitude of VL2 (47.9 N). At $L_s=270$ condensation for AM and PM for both dust levels is nearly 11 pr- μ , i.e. the temperature is cold enough over the whole day to condense nearly all of the available water vapor. (For this simplified condensation model, the value 11 pr- μ represents the total of vaporous and liquid H₂O rather than vapor alone.) On either side of $L_s=270$, i.e. $180^\circ \leq L_s \leq 360$, an increase of dust content increases the AM condensation and decreases the PM condensation, thereby increasing the AM-PM difference in two ways. However, at $45^\circ \leq L_s \leq 135$ an increase in dust decreases the AM and PM condensation and their difference.

Consequently, because of the saturation effect at the latitude of VL2, the AM-PM difference is small at $L_s=270$, and there are two peaks during the year, one near $L_s=225$ and the other near $L_s=360$.

In conclusion, it is seen that the diurnal variation in condensation is a complicated function of the latitude, the season, the water vapor content and the dust content of the atmosphere.

REFERENCES

Colburn, D. S., Pollack, J. B. and Haberle, R. M. (1986). Influence of dust on water vapor content at Mars. In MECA Workshop, Tempe Arizona (In press).

Figure 1

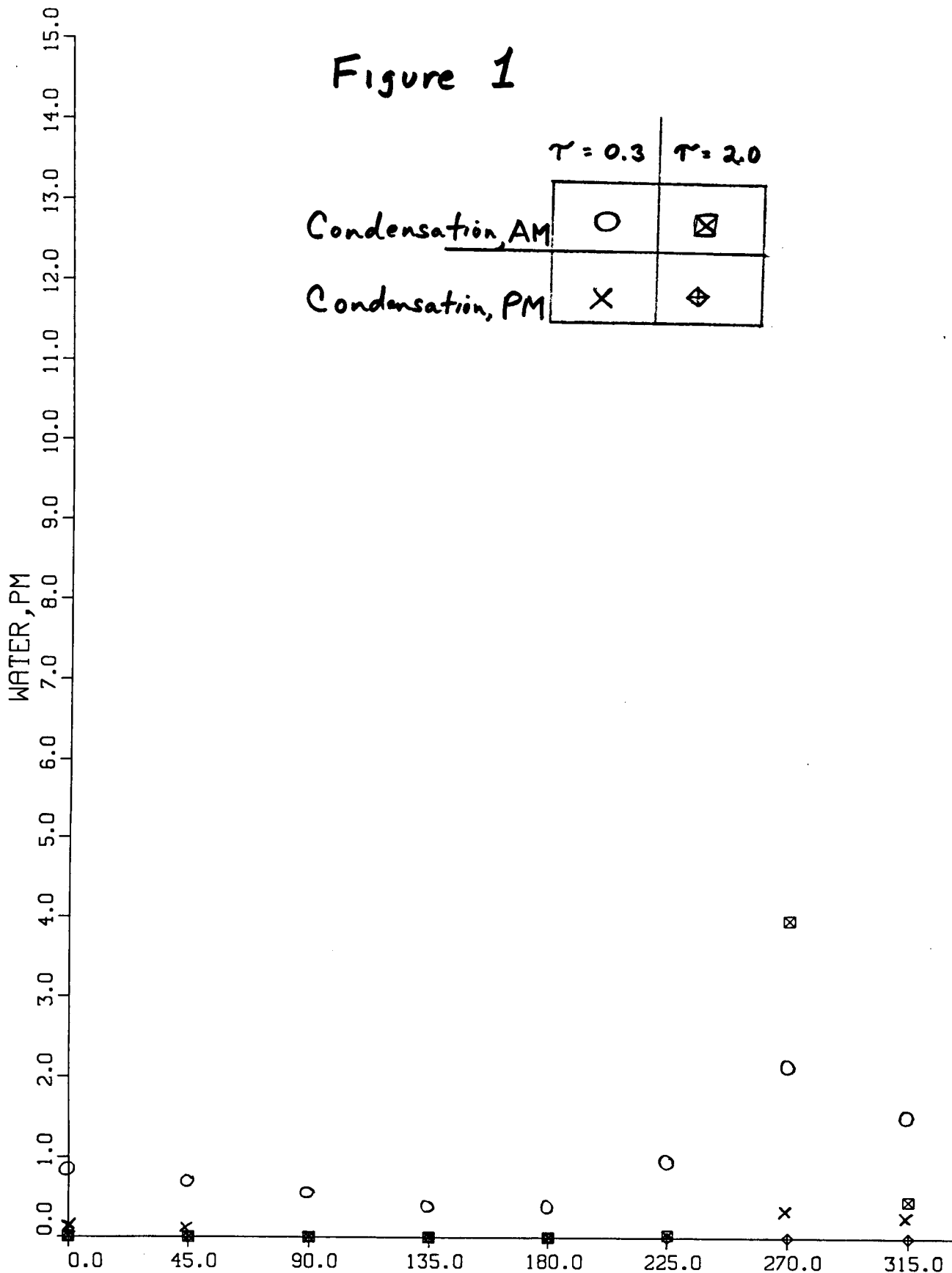
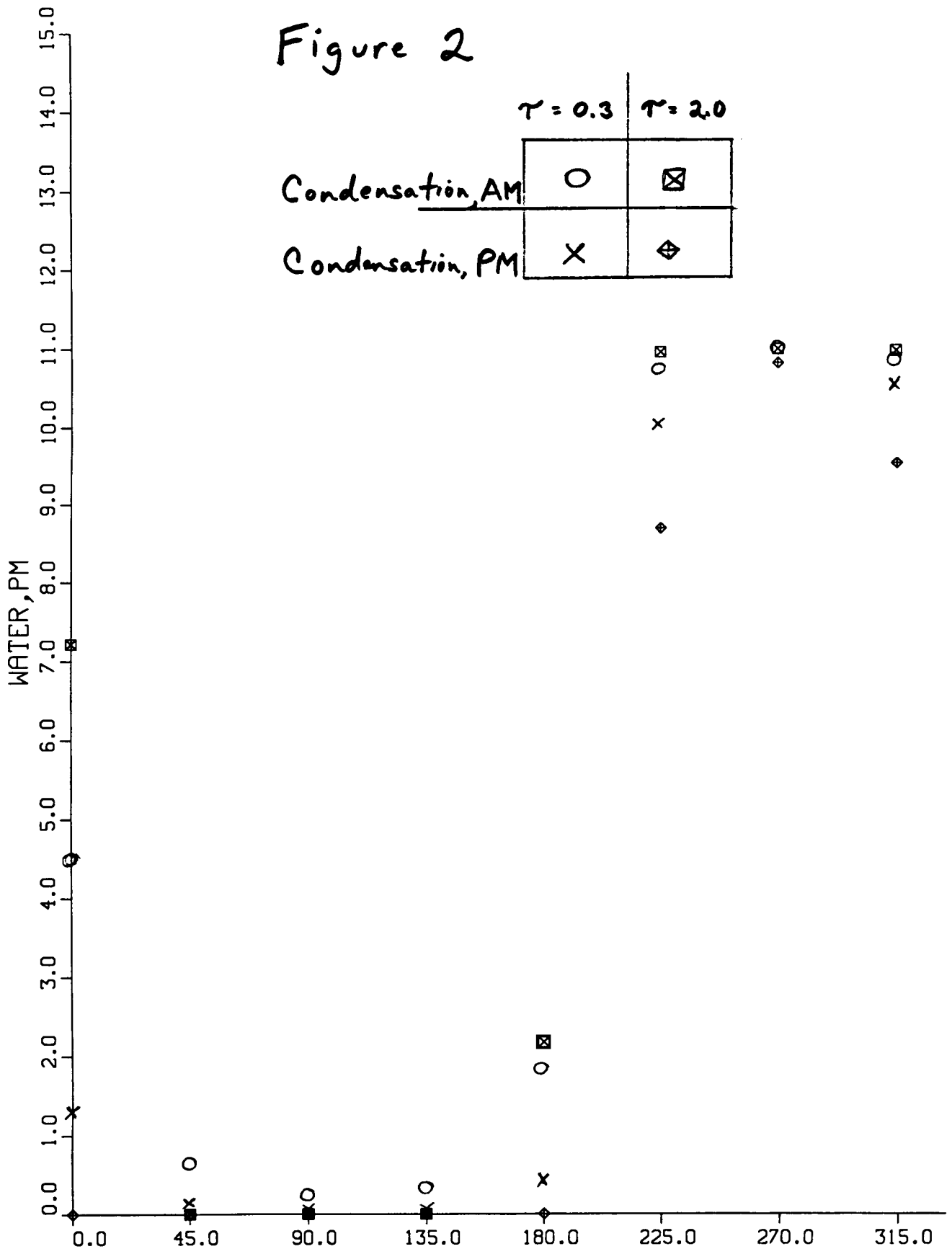


Figure 2



CUMULUS CONVECTION AND THE TERRESTRIAL WATER-VAPOR DISTRIBUTION; L. J. Donner, National Center for Atmospheric Research, * Boulder, Colorado 80307

1. Introduction

Cumulus convection plays a significant role in determining the structure of the terrestrial water-vapor field. (It also contributes substantially to the momentum and thermal fields.) Cumulus convection acts directly on the moisture field by condensing and precipitating water vapor and by redistributing water vapor through cumulus-induced eddy circulations. Additionally, through its radiative and direct interactions with the thermal field, cumulus convection partially establishes the condensation threshold for water vapor.

The purpose of this paper is to outline the mechanisms by which cumulus convection influences the terrestrial water-vapor distribution. As will readily become apparent, this is a problem of enormous complexity, and several theories for its partial resolution exist. In this paper, calculations using a theory due to Kuo (1) will be used to illustrate the mechanisms by which cumulus convection influences the terrestrial water-vapor distribution.

2. Governing Equations and Closures

Relative to scales resolved by the synoptic meteorological network, cumulus convection occupies a small area. Its effects are represented as a turbulent fluctuation on the large-scale field. The large-scale (spatially averaged) water-vapor mixing ratio (\bar{q}) changes locally due to large-scale advection of water vapor, condensation on the large scale (\bar{c}), condensation on the scale of cumulus convection (\bar{c}^*), and convergence of water-vapor fluxes induced by cumulus convection:

$$\frac{\partial \bar{q}}{\partial t} = -\bar{\mathbf{v}} \cdot \nabla \bar{q} - \bar{w} \frac{\partial \bar{q}}{\partial p} - \bar{c} - \bar{c}^* - \frac{\partial \overline{w'q'}}{\partial p} - \nabla \cdot \overline{\mathbf{v}'q'}. \quad (1)$$

An overbar refers to the large scale, and a prime, to a cumulus deviation from the large scale. The vertical coordinate is pressure p and $w = \frac{dp}{dt}$. The goal of cumulus parameterization is to find a closure for (1) in terms of the large-scale variables. Three major theories of cumulus parameterization are:

- (a) Moist adiabatic adjustment (2). The \bar{q} and temperature profiles are constrained so as not to become supersaturated and moist adiabatically unstable.
- (b) Arakawa-Schubert parameterization (3). The role of condensation \bar{c}^* in (1) is taken as the maintenance of the vertical mass flux in the cumulus elements and, by continuity, subsidence outside the cumulus elements. The local change in \bar{q} then is due to

* The National Center for Atmospheric Research is sponsored by the National Science Foundation.

detrainment from cumulus elements and cumulus-induced drying due to subsidence outside the cumulus elements. An ensemble of clouds with varying vertical structures is assumed to exist, and the distribution of mass flux among the members of the ensemble is obtained by assuming buoyancy generated in the cumulus ensemble equilibrates changes in the large scale.

- (c) Kuo parameterization (1). The condensation rate \bar{c}^* is assumed to be proportional to large-scale moisture convergence. A cumulus model and an estimate for cumulus fractional area using the large-scale moisture convergence provide closures for the flux-convergence terms in (1).

The validity of the assumptions in all of these cumulus parameterizations is at least restricted in spatial scale, although such limitations have not yet been studied. For the most part, the parameterizations all assume that the forcing of the large scale by cumulus convection depends on the instantaneous large-scale state; the limitations of this approximation are also largely unexplored.

3. Forcing of the Water-Vapor Field by Cumulus Convection

Donner *et al.* (4) and Donner (5) used a Kuo cumulus parameterization in an atmospheric general circulation model to assess the role of cumulus convection in determining the water-vapor distribution and other circulation characteristics. Figure 1 illustrates the time-mean, zonally averaged forcing of the water-vapor field by cumulus convection (July) from the simulation described in (5). Condensation acts as a drying tendency with a maximum of about $1.0 \text{ g kg}^{-1} \text{ day}^{-1}$ in the tropics. The one-dimensional cloud model used in the cumulus parameterization in (5) is characterized by vertical velocities which increase with height in the lower portion of the cloud, while decreasing in the upper portion. This cloud velocity distribution leads to a divergence of moisture flux in the lower troposphere (maximum drying about $2.6 \text{ g kg}^{-1} \text{ day}^{-1}$) and a convergence in the upper troposphere (maximum moistening about $1.5 \text{ g kg}^{-1} \text{ day}^{-1}$). The net moisture forcing is the sum of the condensation and eddy-flux processes. The time-mean, zonally averaged water-vapor tendency due to cumulus convection also exhibits a maximum drying in the stormy baroclinic zone of Southern Hemisphere winter.

4. The effect of cumulus convection on the mean water-vapor field

The simulation of atmospheric water-vapor fields is fairly sensitive to the parameterization for cumulus convection. Figure 2 shows changes in the humidity field achieved by adding a Kuo cumulus parameterization to the National Center for Atmospheric Research Community Climate Model, which in its control version included a moist adiabatic adjustment. (As discussed in (5), these changes can perhaps plausibly be interpreted as qualitative indications of the effect of cumulus convection on the atmospheric water-vapor distribution.) The specific humidity is reduced significantly, consistent with the moisture tendencies shown in Fig. 1. As discussed in (4) and (5), the Kuo cumulus parameterization cools the atmosphere; as a consequence, changes in relative humidity are less obvious. Still, in the convectively most active areas, significant reductions in relative

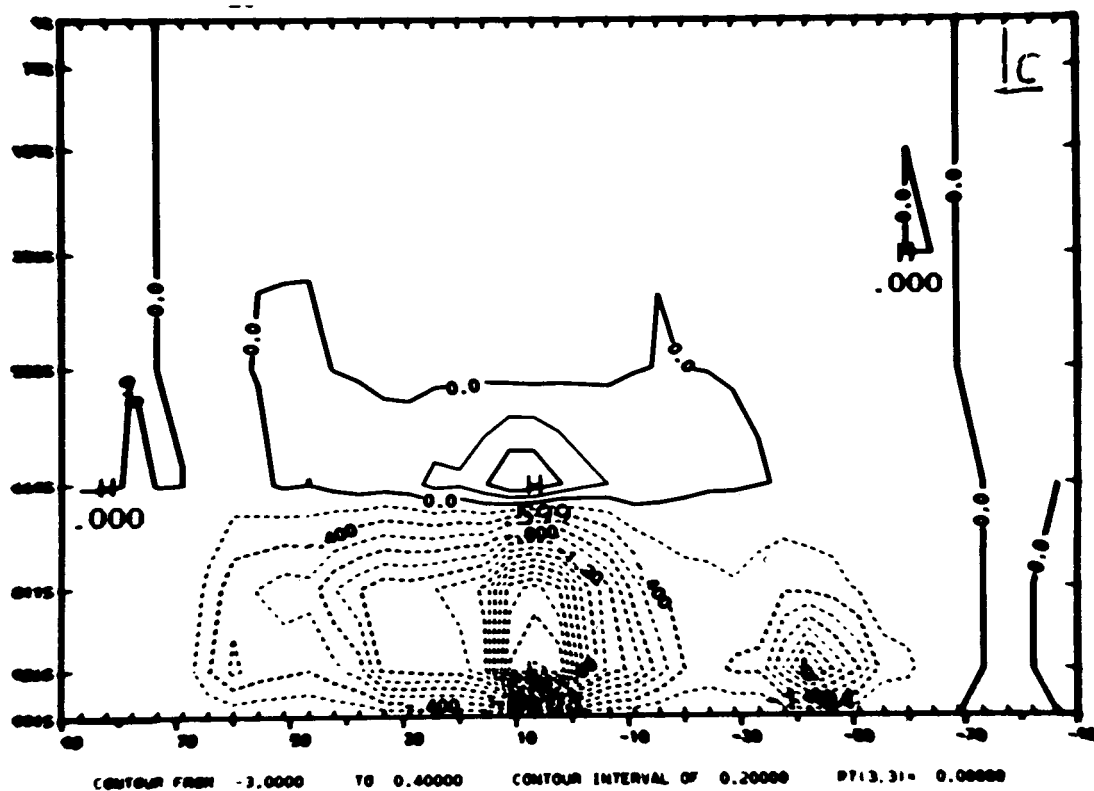
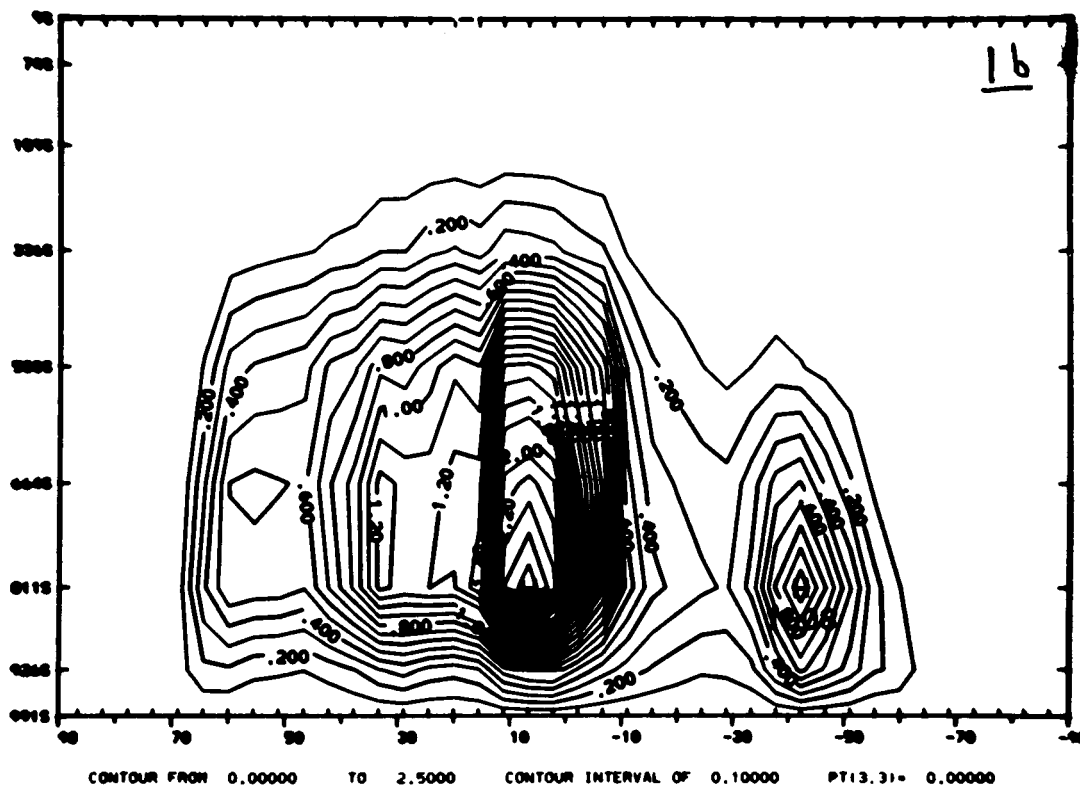


Fig. 1 Simulated forcing of the water-vapor field for mean July conditions (a) cumulus-induced flux convergence ($\text{g kg}^{-1} \text{ day}^{-1}$) (b) latent heat release (to convert to a water-vapor tendency in $\text{g kg}^{-1} \text{ day}^{-1}$, multiply by -4), (c) net forcing by cumulus convection ($\text{g kg}^{-1} \text{ day}^{-1}$). Ordinate gives (pressure/surface pressure) X1000.

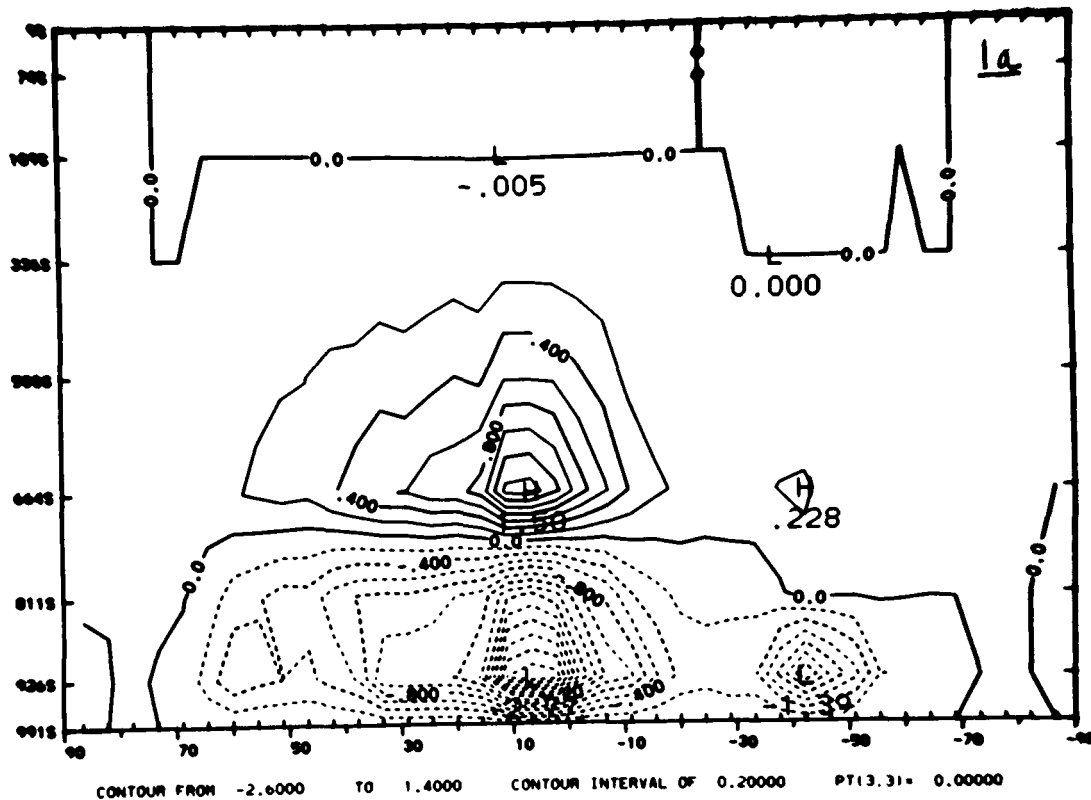
humidity also occur. These changes in water-vapor distribution interact strongly with the cloud formation and radiative transfer.

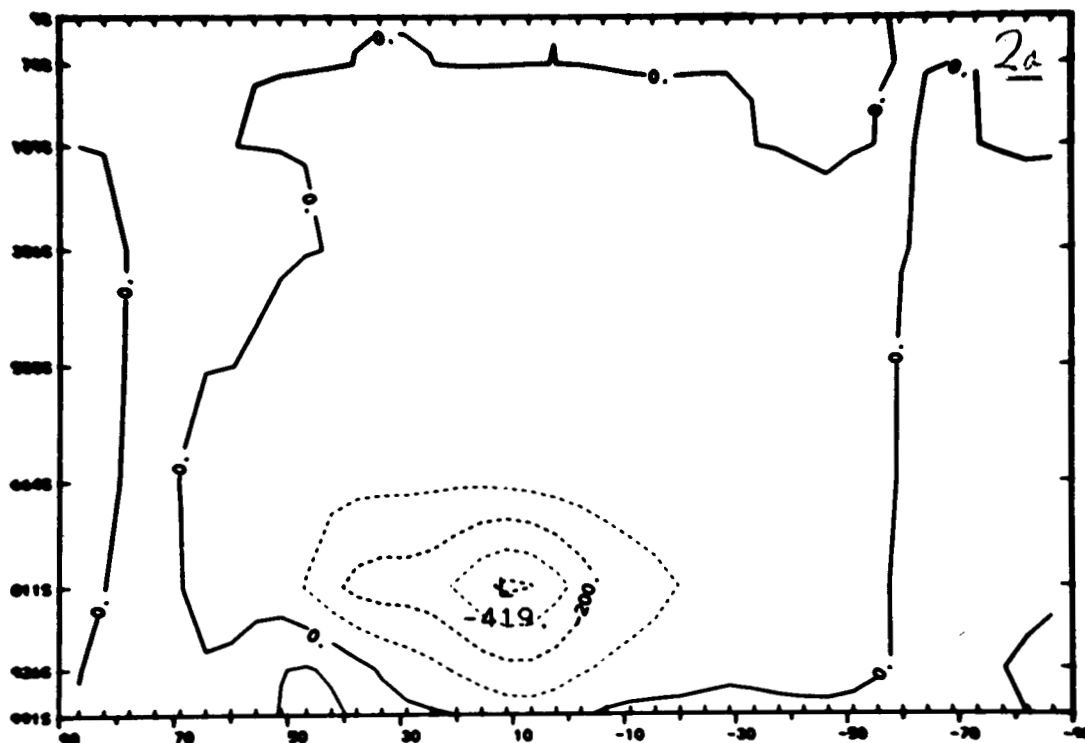
5. Summary

Cumulus convection is a dominant mechanism in the transport and removal of atmospheric water vapor in the terrestrial atmosphere. Cumulus parameterizations seek to link the effects of small-scale cumulus convection to the properties of large, synoptic-scale atmospheric flows. Several families of cumulus parameterization exist, differing fundamentally in their basic assumptions. The effects of cumulus convection are most evident in the tropics and baroclinic zones of the middle latitudes and consist primarily of a mean drying.

REFERENCES

- (1) Kuo, H.-L., (1974) *J. Atmos. Sci.*, **31**, 1232-1240.
- (2) Manabe, L., Smagorinsky, J., and Strickler, J. T. (1965) *Mon. Wea. Rev.*, **93**, 769-798.
- (3) Arakawa, A., and Schubert, W. H. (1974) *J. Atmos. Sci.*, **31**, 674-701.
- (4) Donner, L. J., Kuo, H.-L., and E. J. Pitcher (1982) *J. Atmos. Sci.*, **39**, 2159-2181.
- (5) Donner, L. J. (1986) *J. Atmos. Sci.*, in press.





CONTOUR FROM -0.40000E-02 TO 0.10000E-02 CONTOUR INTERVAL OF 0.10000E-02 PT(3.31) 0.1767E-03 LABELS SCALED BY 0.10000E-06

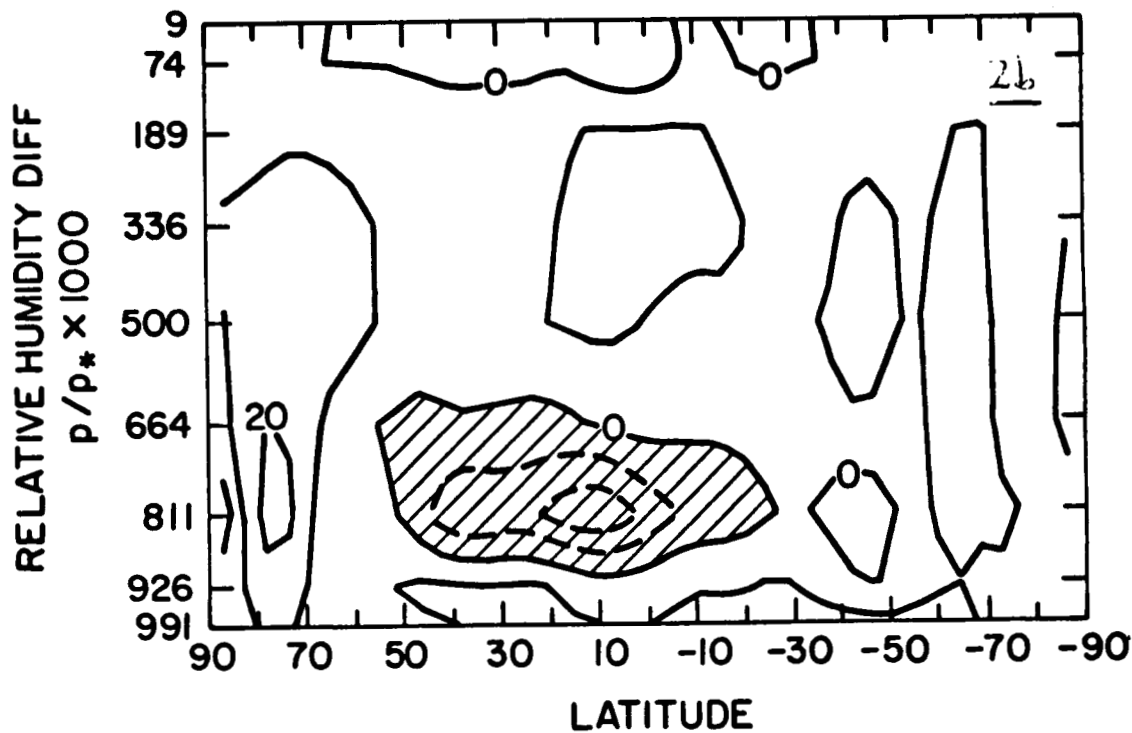


Fig. 2 Changes in (a) specific humidity and (b) relative humidity due to the Kuo cumulus parameterization. Units: (a) $\text{g kg}^{-1} \times 10^5$ (b) %.

59-91
46 48
187400

POSSIBLE SIGNIFICANCE OF CUBIC WATER-ICE, H₂O-Ic, IN THE ATMOSPHERIC WATER CYCLE OF MARS. J. L. Gooding, SN2/Planetary Materials Branch, NASA/Johnson Space Center, Houston, Texas 77058.

Introduction. Most discussions of water ice on Mars tacitly assume that common hexagonal ice, H₂O-Ih, is the appropriate phase. Although ice-Ih is the dominant polymorph of water-ice on Earth, a second low-pressure polymorph which crystallizes in the isometric (cubic) system, H₂O-Ic, can form in special ultracold environments. Indeed, the conditions that are known to favor formation of ice-Ic might be more prevalent on Mars than on Earth.

Occurrence of ice-Ic in the Mars water cycle would be significant for two reasons. First, the Ic/Ih phase transition might comprise a significant but previously unrecognized term in heat-balance equations that have been applied to evaporation or condensation in the water cycle in models for atmosphere/polar-cap or atmosphere/regolith interactions. Second, ice-Ic might possess distinctive properties as a nucleator of other condensates that could substantially affect the processing and distribution of volatiles in both the water and carbon dioxide cycles. Accordingly, it is important to assess prospects for the occurrence and probable behavior of ice-Ic on Mars.

Formation and Stability of Ice-Ic. As summarized by Hobbs [1], ice-Ic is known to form in at least three ways (Fig. 1). First, Ic can form by crystallization of noncrystalline ("amorphous") ice that was initially deposited onto an ultracold substrate (heterogeneous nucleation) from vapor but which subsequently experienced warming. Second, Ic can form directly by vapor deposition under similar (though slightly warmer) ultracold conditions. Third, Ic can form during heating of initially ultracold high-pressure polymorphs of ice (principally ices II, III, V, and IX; Fig. 2) from which confining pressure has been unloaded. A fourth, but still unconfirmed mechanism for production of ice-Ic, involves rapid "quench" solidification of liquid water containing dissolved ferrous or ferric ions. From all indications, it seems that the Ic/Ih transition is sluggish and irreversible. No experiments have succeeded in producing ice-Ic by cooling ice-Ih.

Thermodynamic and kinetic factors that govern ice-Ic are still imperfectly known. Stability of ice-Ic (relative to evaporation or transformation to ice-Ih) is influenced by various factors including nature of the substrate (for vapor-deposited ices), composition and pressure of surrounding gas, and heating rate [1]. Experiments that produced vapor-deposited ice under vacuum, followed by calorimetric measurements under 27 mbar of helium gave enthalpies of key transitions as follows: -1.64 kJ/mol ("amorphous" to Ic) and -0.16 kJ/mol (Ic to Ih) [2]. (For comparison, the enthalpy of the familiar transition of liquid water to ice-Ih is -6.0 kJ/mol).

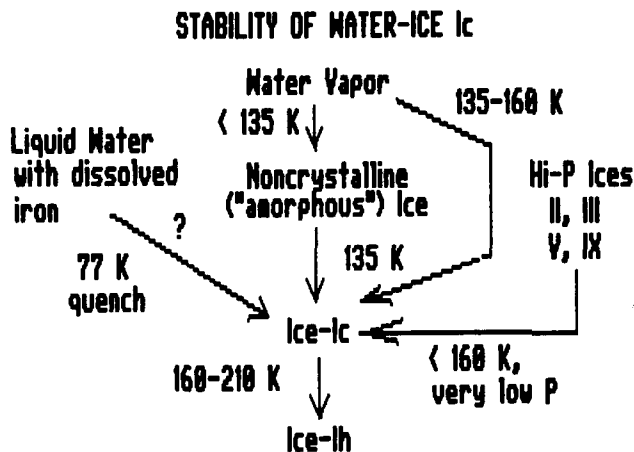


Figure 1.

Schematic summary of processes that form ice-Ic under laboratory conditions. Transition temperatures vary with experimental conditions, including nature of the substrate in vapor-deposition modes. Temperatures suggested here are those derived from the calorimetric study by Sugisaki et al. [2]. Production of ice-Ic by the "77 K quench mode" was reported in one study but has not been confirmed [1].

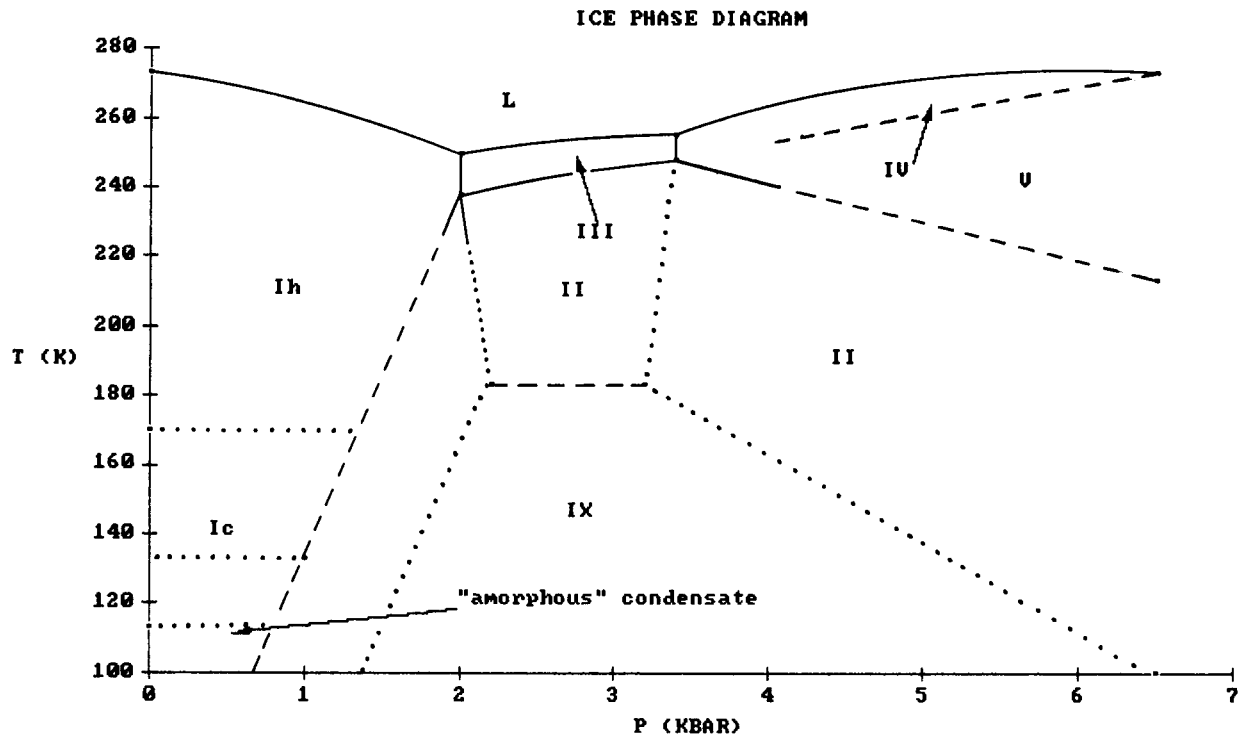


Figure 2.

Phase diagram for water (neglecting vapor) in the pressure and temperature domains that support formation of ice-Ic. Phase demarcations include known equilibrium boundaries (solid lines), approximate metastable boundaries (dashed lines), and suspected metastable boundaries (dotted lines). The "amorphous condensate" field refers simply to the temperature fence below which noncrystalline ice is formed by vapor deposition (no reaction relationship between "amorphous" ice and ice-IX is implied). Below 113 K, vapor condensates tend to be noncrystalline whereas condensation at 113-135 K can produce mixtures of noncrystalline and Ic ices. The 170 K fence between Ic and Ih represents the extrapolated-onset of the Ic/Ih transition as determined by calorimetry [2]. Compiled from data summarized by Hobbs [1].

Prospects for Ice-Ic on Mars. On Mars, conditions that favor formation of ice-Ic might occur naturally whereas the necessary conditions on Earth are almost entirely restricted to laboratory experiments. Water vapor on Mars occurs mostly in the lower 20 km of the atmosphere where prevailing temperatures and pressures typically vary from 150 K/1 mbar at altitude to 250 K/10 mbar near the surface [3,4]. Condensate clouds near and above the summits of the Tharsis volcanoes (20-27 km elevation) have been interpreted as high-altitude water-ice clouds [5], indicating that atmospheric condensation on Mars does, in fact, occur under the ultracold, low-pressure conditions that should favor formation of ice-Ic by the vapor-deposition mode.

The Martian polar caps might be regarded as possible environments for formation of ice-Ic by the pressure-unloading mechanism. However, the conditions required to produce the high-pressure polymorphic precursors of ice-Ic might be unachievable in the Martian polar caps. A pressure of 1 kbar, which might represent a minimum value for producing ice-IX from ice-Ih (Fig. 2), would require on Mars a column of ice-Ih that was ≥ 30 -km thick (11 km on

Earth). Although thicknesses of the Martian ice caps are not known, it is doubtful that they could ever have exceeded a few km. For example, transfer of a Martian global water budget of 10 m [6] to the north pole, with uniform deposition poleward of 80 N latitude, would produce a cap only 1.2-km thick. Of course, greater ice thicknesses could be invoked by appealing to much greater Martian water budgets.

Further pursuit of natural Martian conditions for achieving the ice-Ih/IX transformation at 1 kbar could invoke overburdens of either ≥ 17 -km of solid carbon dioxide or ≥ 14 km of rocky regolith materials. However, seasonal accumulations of carbon dioxide frost at the Martian poles are probably < 1 -m thick [7] and complete transfer of a Martian global carbon dioxide budget of 1060 g/sq cm [6] to the north pole would translate to a frost cap of only 0.8 km thickness. Therefore, overburdens of carbon dioxide appear inadequate whereas overburdens of rocky material are at least plausible. Ice-Ih deeply buried in the Martian regolith might transform to one or more high-pressure polymorphs although subsequent transformation to ice-Ic would still require a mechanism for pressure (overburden) unloading. Deep exhumations might be accomplished by impact cratering although such catastrophic events could tend to favor melting or vaporization instead of solid-state phase changes of ice. It is at least conceivable, though, that unmelted blocks of ice excavated from great depth might transform to ice-Ic by the pressure-unloading mechanism.

Probable Behavior of Ice-Ic on Mars. Ice-Ic exposed at the Martian surface should tend to either evaporate or to transform to ice-Ih. However, if the ambient temperature was < 170 K, ice-Ic might persist metastably for extended periods of time. Regardless of the kinetics, though, transformation of ice-Ic to ice-Ih would be a modest but real heat source (i.e., transformation is exothermic). The vapor/solid transformation of carbon dioxide is the dominant phase transition in the Martian polar-cap heat balance and transitions involving water are considered negligible [7]. However, the ice-Ic/Ih transformation might be important to heat balance at the microphysical scale of processes that govern cloud and fog formation.

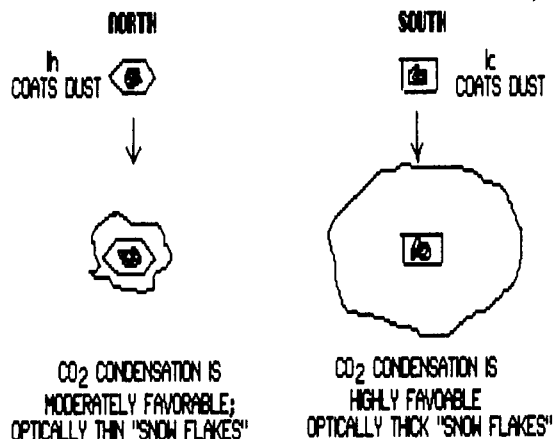
In a previous paper [8], calorimetric measurements of ice-Ih nucleation were combined with computations that relate to epitaxial overgrowth of water ice on foreign nuclei to emphasize the possible role of heterogeneous nucleation in the formation of condensates on Mars. One of the major results of that study was recognition of the potentially excellent properties of ice-Ic as a nucleator of other condensates. In theory, ice-Ic should be an outstanding nucleator of solid carbon dioxide and possibly carbon dioxide hydrate (clathrate) [8].

Paige and Ingersoll [7] ascribed the preferential accumulation of carbon dioxide frost at the Martian south pole to higher reflectivity (hence, lower heat absorption) of the southern cap relative to the northern cap. Lower reflectivities of the north polar cap were attributed to contamination of the frost deposits by admixed dust. Indeed, competing hypotheses involving ice-Ic and nucleation of frosts on dust particles are possible (Fig. 3). First, if ice-Ic was the earliest condensate to nucleate above the south polar cap, then carbon dioxide frost might have preferentially condensed on those nuclei. The net effect might have been to bury dust particles (as nuclei of ice-Ic) in optically thick layers of condensate that would have favored high reflectivity in the bulk deposits. If dust above the north pole favored a phase other than ice-Ic as the earliest condensate (e.g., ice-Ih), then overgrowth by carbon dioxide frost might have been much less favorable and subsequent growth might have led to particles with optically thin condensate layers. Alternatively, condensation of carbon dioxide, aided by ice-Ic, might have occurred equally at both poles but conditions at the north pole might have favored the exothermic transformation of ice-Ic to ice-Ih, thereby evaporating some of the condensed carbon dioxide. In that case, lower reflectivities would have

NORTH/SOUTH DICOTOMY OF SEASONAL CO₂ CAP

HYPOTHESIS 1 FOR POSSIBLE ROLE OF ICE-Ic

SOUTH FAVORS Ic AS FIRST CONDENSATE,
NORTH FAVORS Ih



HYPOTHESIS 2 FOR POSSIBLE ROLE OF ICE-Ic

Ic IS FIRST CONDENSATE AT BOTH POLES,
BUT Ic/Ih TRANSITION IS IMPORTANT IN NORTH

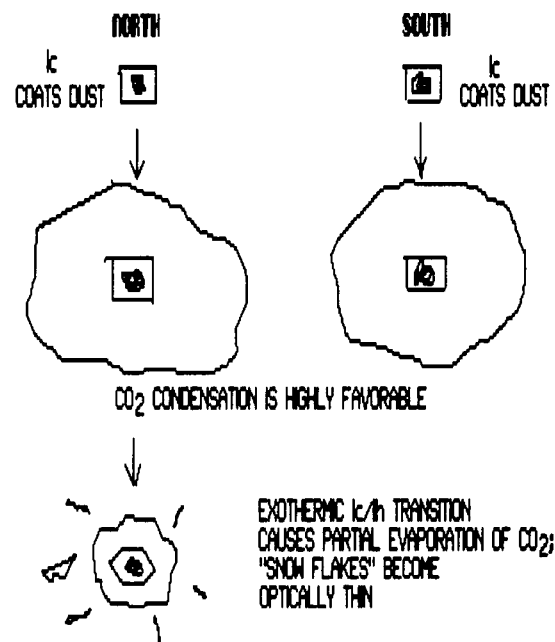


Figure 3.

Schematic summaries of alternative hypotheses for possible role of ice-Ic in condensation of CO₂ at the Martian poles.

followed from partial loss of the carbon dioxide mantles on the ice particles. With the loss of favorable condensation nuclei, recondensation of the carbon dioxide might have been inhibited.

At present, existence of ice-Ic on Mars has not been demonstrated so that the possible role of ice-Ic on the atmospheric water and carbon dioxide cycles is only speculative. However, potential implications of ice-Ic on Mars are sufficiently meaningful that further work on the problem is warranted.

Experimental Tests for Ice-Ic on Mars. The infrared spectra of ice-Ih and ice-Ic are identical [1] so that it is doubtful that remote sensing will be able to either confirm or refute the existence of ice-Ic on Mars. Although near- and mid-infrared spectrophotometry might not be able to address the problem, there is a small chance that sufficiently sensitive thermal-infrared measurements of ice clouds and polar caps might provide some evidence for exothermic events that would be correlatable with the ice-Ic/Ih transformation. However, a preferred method of detecting ice-Ic would be by means of soft-landed spacecraft equipped with instrumentation for differential scanning calorimetry (DSC). The best detection strategy would probably rely on extended missions to the Martian poles to sample and analyze condensates as a function of location and season.

References:

- [1] Hobbs P. V. (1974) Ice Physics, Oxford.
- [2] Sugisaki M., Suga H., and Seki S. (1969) In Physics of Ice, N. Riehl, B. Bullemer, and H. Engelhardt (Eds.), 329-343, Plenum.
- [3] Seiff A. and Kirk D. B. (1977) J. Geophys. Res., **82**, 4364-4378.
- [4] Davies D. W. (1979) J. Geophys. Res., **84**, 8335-8340.
- [5] Hunt G. E. and James P. B. (1985) Adv. Space Res., **5**, 93-99.
- [6] Anders E. and Owen T. (1977) Science, **198**, 453-465.
- [7] Paige D. A. and Ingersoll A. P. (1985) Science, **228**, 1160-1168.
- [8] Gooding J. L. (1986) Icarus, **66**, 56-74.

ON THE VERTICAL DISTRIBUTION OF WATER VAPOR IN THE MARTIAN TROPICS. Robert M. Haberle, NASA/Ames Research Center, Moffett Field, CA 94035.

Although measurements of the column abundance of atmospheric water vapor on Mars have been made (1,2), measurements of its vertical distribution have not. How water is distributed in the vertical is fundamental to atmosphere-surface exchange processes, and especially to transport within the atmosphere. Several lines of evidence suggest that in the lowest several scale heights of the atmosphere, water vapor is nearly-uniformly distributed (3). However, most of these arguments are suggestive rather than conclusive since they only demonstrate that the altitude to saturation is very high if the observed amount of water vapor is distributed uniformly. The purpose of this paper is to present a simple yet compelling argument, independent of the saturation constraint, which suggests that in tropical regions, water vapor on Mars should be very nearly uniformly mixed on an annual and zonally averaged basis.

To begin the discussion consider the situation for Earth. On Earth, the average annual precipitation at any given latitude does not necessarily balance the average annual evaporation. Near the equator for example, precipitation exceeds evaporation (4). From the point of view of the atmosphere, therefore, this region is a moisture sink, and water vapor must be transported in to maintain the long-term balance. At these latitudes the transport is accomplished mainly by the thermally driven mean meridional circulation (Hadley Cell). To accomplish this transport, however, the water vapor mixing ratio (specific humidity) must decrease with height in the mean. This is, of course, the situation for Earth: the concentration of water vapor is a strong function of height.

For Mars, however, the situation is different since it has no oceans to redistribute water meridionally. As a consequence, any difference between the average annual precipitation and evaporation at a given latitude must result in a change in the size of surface ice deposits. The only regions on the planet where ice can exist all year long are the polar regions, but it is not known if these reservoirs are changing or not. On the one hand, Davies (1980) has suggested that there is no net annual change in the size of polar reservoirs (5), in

which case precipitation and evaporation are balanced at all latitudes and there is no net meridional transport. This implies, in turn, that water vapor must be uniformly mixed in the tropics where transport by the mean meridional circulation dominates. On the other hand, Jakosky (1983) has argued that the existence of a north-south gradient in column water vapor implies a net southward transport of water from the north cap to the south cap (6). An upper limit for this transport is 5×10^{11} Kg per Mars year. Based on model estimates of the Martian Hadley cell mass flux (7), it can be shown that this transport can be achieved with a tropical mixing ratio that decreases by less than 10% of its near surface value.

There is yet another possibility. Water could be redistributed globally in subpermafrost aquifers (8). According to Clifford (1981), water thermally diffuses to the surface from this aquifer in equatorial regions, is transported to the poles where it precipitates, and then passes back into the groundwater system when melting occurs at the base of the polar caps. He estimates that as much a 1 km^3 of water may be introduced into the crust each Martian year in this manner. This amount, however, is only a factor of two larger than Jakosky's north-south transport and we still expect, therefore, water vapor to be nearly uniformly mixed in the tropics.

It should be emphasized that this conclusion is for annual mean conditions. Given the expected large seasonal variations in the structure and intensity of the Martian circulation, departures from uniform mixing are certainly possible. However in the annual mean, it appears that water must be nearly uniformly distributed in height on Mars, at least in the tropics. If future observations by the Mars Observer spacecraft find otherwise, then significant sources and sinks for water must exist at the surface.

REFERENCES

1. Farmer, C.B., Davies, D.W., Holland, A.L., LaPorte, D.D., and Doms, P.E. (1977) *J. Geophys. Res.*, **82**, 4225.
2. Jakosky, B.M. and Farmer, C.B. (1982) *J. Geophys. Res.*, **87**, 2999.

3. Jakosky, B.M. (1985) *Space Sci. Rev.*, **41**, 131.
4. Lorentz, E.N. (1967) World Meteorological Organization WMO - no. 218 TP. 115, 161 pp.
5. Davies, D.W. (1981) *Icarus*, **45**, 398.
6. Jakosky, B.M. (1983) *Icarus*, **55**, 19.
7. Haberle, R.M., Leovy, C.B., and Pollack, J.B. (1982) *Icarus*, **50**, 322.
8. Clifford, S.M. (1981) *Third International Colloquium on Mars*, Lunar and Planetary Institute, Houston, Texas.

N89-25801

511-91
HES JULY 53

THE BEHAVIOR OF WATER VAPOR IN THE MARS ATMOSPHERE. Bruce M. Jakosky,
Laboratory for Atmospheric and Space Physics, University of Colorado, Boulder,
CO 80309.

187402

The behavior of water vapor in the atmosphere of Mars is important to understanding the Mars climate and its evolution as well as the nature of ongoing seasonal processes of exchange and transport. On the seasonal timescales, exchange of water between the atmosphere, regolith, and polar caps combine with advection of water and the possible saturation at some locations and seasons in order to produce the observed distribution of water. Chemical effects (such as the oxidation of methane) are of much less significance; water also affects the behavior of other constituents such as ozone or carbon monoxide. On longer timescales, the behavior of water reflects the larger variability of climate on Mars. Forcing at the polar caps via the Milankovitch cycles of changing orbital obliquity causes a dramatic redistribution of water between polar caps, atmosphere, and regolith; layering of dust and ice within the polar regions is probably indicative of such long-term climate variations.

Observations of water on Mars have been made since the early 1960's, using Earth-based measurements as well as observations from the Mariner and Viking spacecraft. These measurements have been used to define the seasonal cycle of water vapor column abundance at each location on Mars. Models of the various exchange and transport processes have been used to help determine the efficacy of each process. There are still major uncertainties, however, in terms of the relative importance of each non-atmospheric reservoir of water and the trade-off between transport and vertical exchange as a means of regulating the atmospheric water content. A summary of the observations and analyses of the seasonal cycle of water will be presented, along with a brief discussion of the implications for the long-term variability of water. The upcoming Mars Observer mission will also be briefly discussed.

SOLAR MESOSPHERE EXPLORER OBSERVATIONS OF STRATOSPHERIC AND MESOSPHERIC WATER VAPOR. Bruce M. Jakosky (1, 2), Gary E. Thomas (1, 2), David W. Rusch (1, 2), Charles A. Barth (1, 2), George M. Lawrence (1, 2), John J. Olivero (3), R. Todd Clancy (1, 2), Ryan W. Sanders (1, 4), and Barry G. Knapp (1). (1) Laboratory for Atmospheric and Space Physics, University of Colorado, (2) Department of Astrophysical, Planetary, and Atmospheric Sciences, University of Colorado, (3) Department of Meteorology, Pennsylvania State University, (4) Aeronomy Laboratory, National Oceanic and Atmospheric Administration.

The Solar Mesosphere Explorer satellite was launched in late 1981, and returned thermal-infrared limb-scanning emission measurements at two wavelengths for the period 1982-1985. Measurements centered at $6.8 \mu\text{m}$, in the wings of the $6.3\text{-}\mu\text{m}$ water vapor band, were designed to determine vertical profiles of the water vapor mixing ratio throughout the stratosphere and mesosphere. We report here analyses of a subset of this data, concentrating primarily on the period January-March 1982 so as to avoid contamination from the El Chichon volcanic aerosol.

Inversion of radiance measurements is accomplished using an iterative technique based on the forward calculation of radiance followed by successive perturbations to the water vapor mixing ratio profile. The forward calculation uses a look-up table of pre-calculated emissivities as a function of temperature, pressure, and water vapor path length, and uses the emissivity-growth approximation of Gordley and Russell. Emission from O_2 , which becomes important below about 30 km, is included by an approximate correction term. Atmospheric temperatures are obtained from nadir-sounding measurements compiled by the National Meteorological Center, and provide adequate accuracy between 20 and 40 km; above 40 km, a climatological model is used, and accuracy drops significantly. Data are inverted between 20 and 60 km, but only the results below 50 km are retained.

Contamination due to aerosol loading is a significant problem in the analysis. The eruption of El Chichon had a major impact on the observations, with the largest fraction of the observed emission below about 30 km being due to aerosol emission. Even prior to this eruption, however, significant emission occurs that appears to be due to aerosol. Assuming no aerosol results in unreasonably high water vapor mixing ratios of up to 10 ppmv at mid and high latitudes between 20 and 30 km. This same pattern of increased emission also shows up in the analysis of the $9.6\text{-}\mu\text{m}$ ozone observations, and increased scattering of sunlight is seen in the visible light data to as high as ~ 45 km. During the several years preceding the SME observations, there were a number of volcanic eruptions into the stratosphere, including that which produced the so-called "mystery cloud" just prior to the initial observations; given the 1- to 2-year timescale for the removal of volcanic debris from the stratosphere, it is not surprising that the data are contaminated. Observations by LIMS in 1978-1979 do not appear to show significant contamination by aerosol, but one must go back to 1974 to find a significant low-latitude volcanic eruption into the stratosphere. Based on the observed record of volcanic eruptions, we estimate that observations of the stratosphere would be significantly affected approximately 1/3 to 1/2 of the time.

Observations by SME above 30-35 km appear to not be significantly contaminated by aerosol during the January-March 1982 time period. Water vapor mixing ratios there are in the range of 4-6 ppmv. The minimum appears near the equator, and values increase toward both poles. These results are consistent with the earlier LIMS measurements to within the uncertainties in the data inversions. They are also consistent with the previously-suggested processes of oxidation of methane to water in the stratosphere and the poleward transport of water. Water vapor mixing ratios also increase with altitude above 35 km, but not as markedly as was seen in the LIMS analysis; uncertainties in the SME inversion above 40 km prevent us from making a stronger statement than this.

In summary, we have inverted the SME observations of water vapor between 20 and 60 km for the first three months of 1982 as well as for selected additional periods. Reasonable results are obtained at locations where no contamination by aerosol is suspected; the analyses are consistent with prior observations from the LIMS experiment. Significant contamination by aerosol emission is seen below 35 km, even prior to the eruption of the El Chichon volcano; future observations of the stratosphere should be designed to simultaneously measure aerosol properties so that its effects can be removed from temperature or minor species observations.

CIRCUMPOLAR HOODS AND CLOUDS AND THEIR RELATION TO THE MARTIAN H₂O CYCLE; P. B. James, University of Missouri-St. Louis, St. Louis, MO 63121 and L. J. Martin, Lowell Observatory, Flagstaff, AZ. 86002

Water exists in both vapor and solid phases in the martian atmosphere. Ice particles are revealed in clouds when their concentration becomes on the order of 1 pr. μm . Cloud observations are therefore relevant to the distribution, sources and sinks, and transport of water on Mars as well as to the atmospheric dynamics on the planet. Earth based visible wavelength astronomy has been one of the most successful tools used to study the synoptic behavior of martian clouds. Most of our knowledge of the polar hoods, global duststorms, volcano clouds, etc. has come from terrestrial observations. We believe that these observations can continue to be of value, particularly when combined with other data bases.

The polar hoods are shrouds of condensate clouds which obscure both polar regions at times during their respective fall and winter seasons. They are dynamic atmospheric phenomena which are undoubtedly involved in both the CO₂ and H₂O cycles; but neither their exact origin nor their feedback effects in the cycles are well understood. Most information on the seasonal and spatial extents of the hoods has come from earth based astronomy although relevant observations were made by both Mariner 9 and Viking. The hoods are quite variable seasonally and spatially, and there seem to be distinct differences between the behaviors in the north and the south. In the martian antarctic the hood seems to form at about $L_S = 140^\circ$, when models predict that conditions at the edge of the south polar surface cap are changing from net CO₂ condensation to net sublimation. Water trapped near the edge of the cap near the solstice would, as it sublimates, be transported poleward by the CO₂ mass flux, which is still directed to the south; it could condense into clouds or haze upon encountering the much colder atmosphere nearer the pole and ultimately be trapped on the surface cap, where it could account for the bright annulus observed in the cap's recession.⁽¹⁾ In the north, the hood is a much more permanent fixture during fall, winter, and early spring suggesting sustained transport of water from outside sources into the arctic region, more efficient atmospheric condensation processes, significant differences in atmospheric dynamics in the hemispheres, or a combination of such processes.

Careful study of telescopic data can, despite limited resolution, also provide more detailed insights into the hydrologic cycle on Mars. Comparisons of images acquired using short wavelength filters, which provide maximum cloud contrast, and long wavelength filters, which are sensitive to surface features including the surface cap, provide correlations between cloud formation and large scale planetary dynamics. An example is provided by the 1978 north polar cap recession which was observed by the International Planetary Patrol as well as by Viking orbiters. The following figure shows regression curves determined from red/green filter pictures compared to those using a blue filter. Between $L_S=20$ and $L_S=40$ the curves both show a stationary surface cap, quite consistent with Viking results.⁽²⁾ The two curves diverge between $L_S=40$ and $L_S=50$; the receding cap edge in red/green is consistent with the observed surface cap regression, while the cap appears to grow in blue. These results suggest that clouds are formed in an annulus surrounding the edge of the surface cap as the CO₂ cover begins to disappear around latitude 65 N.

This correlates with an increase in water vapor observed by MAWD at the same space-time point in 1978.⁽³⁾ Taken together, these results indicate that significant amounts of water ice are incorporated in the portion of the north polar cap between 65 and 70 N.

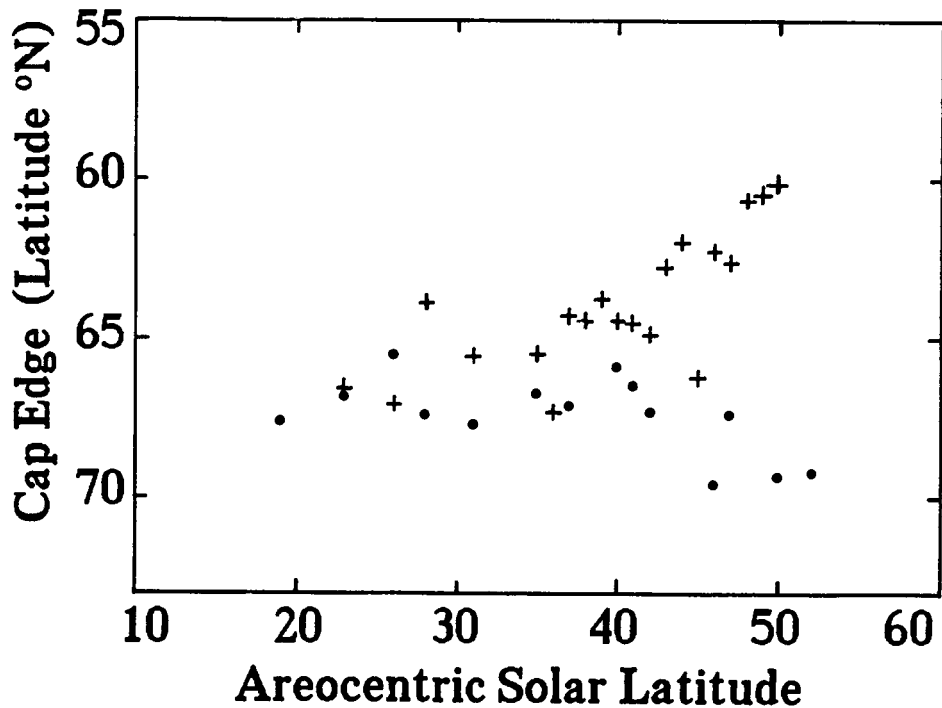


Figure 1. 1978 north polar regression curves are shown for red and green (dots) and blue (crosses) filter data. Generally, the cap edge was measured for seven longitudes for each picture; each data point represents the average of several pictures.

This result supports the usefulness and accuracy of earth based observations in the study of Mars dynamical phenomena, particularly when they can be studied in concert with less synoptic snapshots of phenomena from spacecraft and observations in other spectral regions.

The authors acknowledge support from NASA Grants NAGW-742 and NAGW-638 for various phases of this work.

REFERENCES

1. P. B. James, G. Briggs, J. Barnes, and A. Spruck. J. Geophys. Res. 84, 2889-2922 (1979).
2. P. B. James, J. Geophys. Res. 84, 8332-8334 (1979).
3. B. M. Jakosky and C. B. Farmer, J. Geophys. Res. 87, 2994-3019 (1982).

514-91
187435
VB

VERY HIGH ELEVATION WATER ICE CLOUDS ON MARS: THEIR MORPHOLOGY AND TEMPORAL BEHAVIOR; F. Jaquin, Cornell University

Quantitative analysis of Viking Orbiter images of the martian planetary limb has uncovered the existence and temporal behavior of water ice clouds that form between 50 and 90 km elevation. These clouds form a thin haze layer over most of the planet during southern spring and summer when Mars is near perihelion. At other times of year this high elevation haze is absent. As well as seasonal control, the cloud has a strong diurnal dependence, being observed in the early morning, but not in the afternoon. A radiometric inversion indicates that the optical depth of this high elevation haze is less than 0.05 and may contain a few hundredths of a precipitable micron of water. Enhanced vertical mixing of the atmosphere as Mars nears perihelion is hypothesized as the cause of the seasonal dependence, and the diurnal dependence is most easily explained by the temporal behavior of the martian diurnal thermal tide. The small water content of this high elevation haze indicates that the haze layer is unimportant with regard to volatile storage or transport. However, the seasonal dependence of the haze provides preferential protection from sunlight to the southern polar cap during southern summer. This may be important in maintaining the cap through the summer.

Viking Orbiter images of the martian limb provide a seasonally and latitudinally complete data set regarding the vertical distribution of aerosols in the martian atmosphere. Sunlight reflected from aerosols above the planetary limb can be measured with a radiometric uncertainty of about 7%, and elevations above the 6.1 millibar pressure surface can be calculated to an accuracy of a few kilometers. Thus, the temporal and spatial distribution of aerosols can be characterized.

The geometric nature of limb viewing introduces a multiplicative constant of about 46 between the vertical optical depth to any level in the atmosphere and the corresponding line-of-sight optical depth. This large factor limits the depth to which information regarding the vertical distribution of aerosols can be measured to those levels above a vertical optical depth of about 0.1. Below this level no information can be retrieved concerning the vertical distribution of aerosols. During periods of very low atmospheric opacity, the aerosol distribution of the entire atmospheric column can be measured. However, in practice, atmospheric opacities are large enough that the line-of-sight optical depth limit is reached at about 30 km elevation. This limit is only a weak function of wavelength, because of the large multiplicative constant. Therefore, these and future orbital observations of the aerosol distribution are limited to elevations above three scale heights. Above this limit a radiometric inversion has been used to retrieve the true vertical aerosol distribution. The inversion assumes spherical symmetry, the aerosol single scattering albedo, asymmetry factor, and surface reflectance properties. Figure 1 illustrates the limb-viewing geometry.

Morning limb profiles from southern spring and summer display a characteristic morphology of an extended detached haze near 60 to 70 km, above a continuous haze that extends to the surface. Afternoon profiles show the detached haze to be absent or diminished in prominence. The

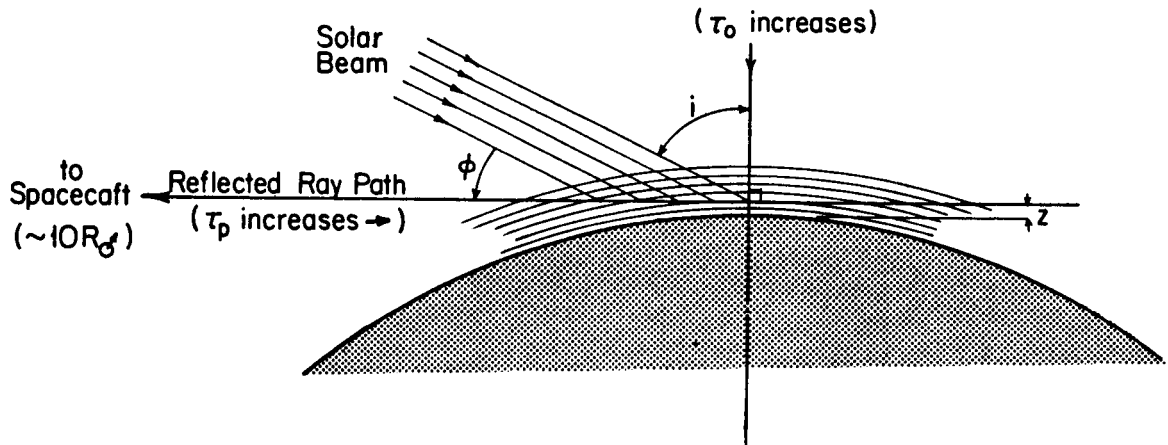


Figure 1. Geometry of limb reflectance measurements. Line-of-sight optical depth τ_p is approximately 46 times larger than the vertical optical depth τ_0 to the same level z .

detached haze often has a layered structure with roughly 5 to 10 km wavelength. Figure 2 illustrates a typical limb profile of the type discussed.

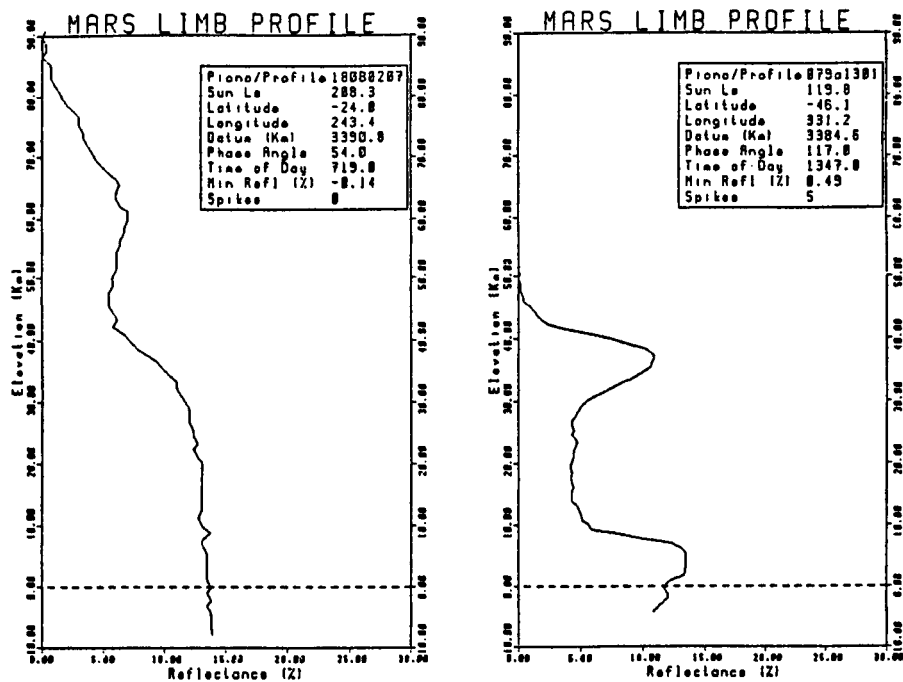


Figure 2. Typical limb reflectance profiles in the Mars atmosphere: (a) illustrating high elevation condensate haze between 85 and 60 km discussed in text, and (b) a lower elevation condensate haze typical of southern mid-latitudes during winter and fall.

The detached haze is inferred to be a water ice condensate based on morphology and atmospheric thermal structure. The detached morphology of the high elevation hazes is most easily explained as a natural result of a condensate haze that forms at some level in the atmosphere. The detached morphology is very difficult to explain if the aerosol is a non-volatile material (i.e., dust particles) that is being transported through the atmosphere in some narrow layer. The diurnal behavior of the detached haze supports the condensate origin of the aerosol. That the condensate is water rather than CO_2 is inferred from the prohibitively high temperatures for CO_2 condensation observed in the martian atmosphere. Temperature profiles from the Viking Landers during entry into the atmosphere, as well as derived temperature profiles from the ϵ Geminorum stellar occultation, indicate atmospheric temperatures in excess of the required 102 K required for CO_2 condensation at these levels.^{2,3} These measurements were made during a different time of the year, but indications are that the upper atmosphere of Mars is warmer during southern spring and summer than during the rest of the year.^{4,5} Measured water vapor abundance of near 10 precipitable microns, if uniformly mixed throughout the atmospheric column, is more than adequate to allow condensation at high elevation.⁶

As indicated in Figure 3, high elevation clouds are observed at most latitudes during southern spring and summer. The coincidence of the appearance of this haze around perihelion suggests that the increased insolation drives a more vigorous vertical mixing, that lifts water vapor to high elevations. Further analysis indicates that the detached haze is more often observed in morning profiles rather than afternoon profiles. This is most readily attributed to the action of the diurnal thermal tide that has a maximum amplitude near 60 km early in the morning.⁷

Results of the radiometric inversion indicate that the vertical optical depth of the high-elevation detached hazes is less than or equal to 0.05. Derived extinction coefficients are on the order of 1×10^{-3} inverse kilometers, similar to terrestrial stratospheric aerosols. Assuming a reasonable average radius of 0.1 μm and a reasonable number density of 100 per cubic centimeter, the detached haze contains about 0.01 precipitable microns of water.⁸ It is clear that this order of magnitude estimate implies that these high-elevation hazes are unimportant in volatile storage and transport.

The seasonal dependence of this haze preferentially shields the south polar cap from sunlight during the southern summer, and provides no such shielding for the northern cap during its summer. Sunlight traversing the haze layer near normal incidence will suffer no appreciable attenuation due to the low optical depth of the haze. However, at high incidence angles, when a large air mass is traversed, the haze layer may provide significant extinction. The southern polar cap is illuminated by sunlight during southern summer at an incidence angle of near 65° . This high elevation haze layer alone attenuates incident solar flux by $\text{EXP}(-\tau/\mu_0) = 0.89$, reducing the surface flux by 11%. This shielding occurs during the peak heating of the south polar cap, and surely influences its final dimensions.

This research was supported by NASA Grant NGL 33-010-186.

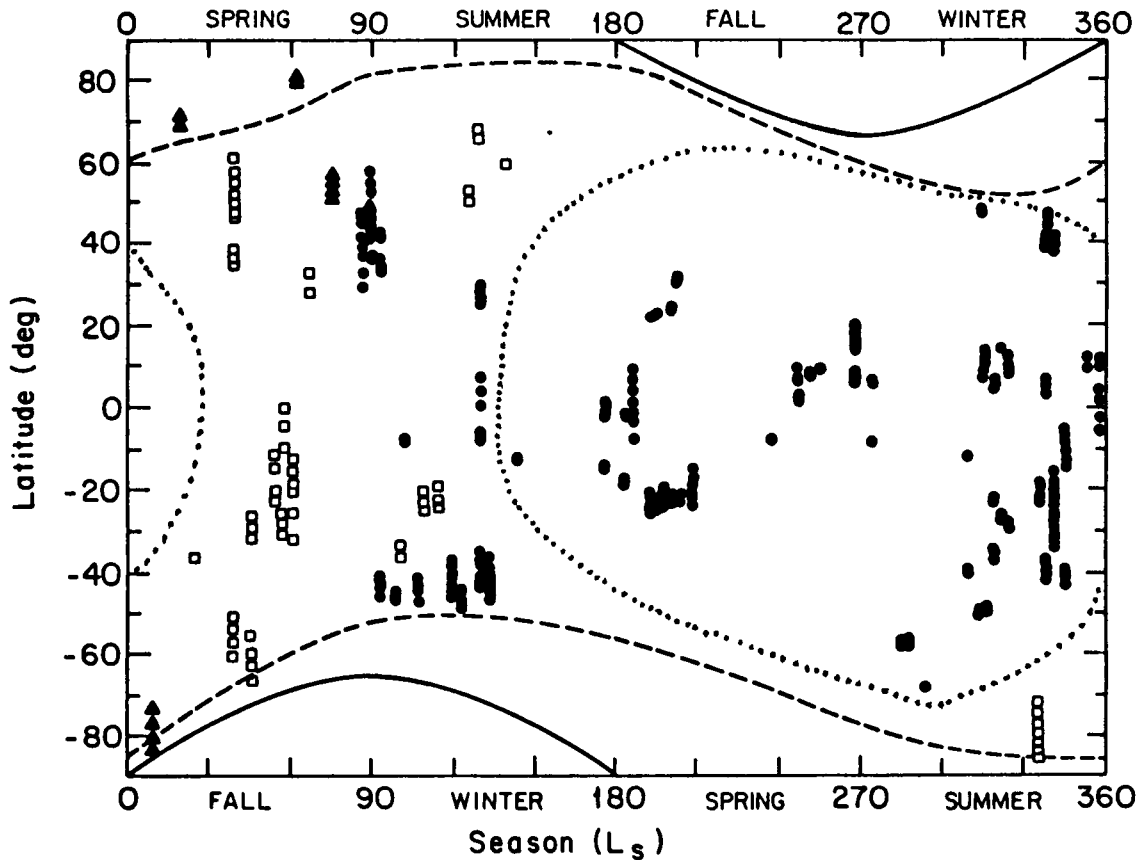


Figure 3. Seasonal and latitudinal distribution of limb profiles. The solid lines bound the area of seasonal night. The dashed line indicates the approximate polar cap edges. Limb profiles with aerosols above 50 km are enclosed by the dotted line.

References

- Jaquin, F., Gierasch, P. J., and Kahn, R. (1986, in press) in *Icarus*.
Seiff, A., and Kirk, D. B. (1977) in *J. Geophys. Res.*, 82, p. 4364-4378.
Elliot, J. L., French, R. G., Dunham, E., Gierasch, P. J., Veverka, J., Church, C., and Sagan, C. (1977) in *Astrophysical J.*, 217, p. 661-679.
McElroy, M. B., Kong, T. Y., and Yung, Y. L. (1977), in *J. Geophys. Res.* 82, p. 4379-4388.
Martin, T. Z., and Kieffer, H. H. (1979) in *J. Geophys. Res.* 84, p. 2843-2852.
Jakosky, B. M., and Farmer, C. B. (1982) in *J. Geophys. Res.* 87, p. 2999-3019.
Zurek, R. W. (1976) in *J. Atmos. Sci.* 33, p. 321-337.
Toon, O. B., and Farlow, N. H. (1981) in *Ann. Rev. Earth Planet. Sci.*, 9, p. 15-58.

OBSERVATIONS OF ATMOSPHERIC WATER VAPOR WITH THE SAGE II INSTRUMENT

J. C. Larsen, SASC Technologies, Inc., Hampton, VA, 23666

M. P. McCormick, L. R. McMaster, W. P. Chu, Atmospheric Sciences Division,
NASA Langley Research Center, Hampton, VA, 23665

1. Introduction

The Stratospheric Aerosol and Gas Experiment II (SAGE II) is a multiwavelength spectrometer which infers the vertical distribution of stratospheric aerosols, ozone, nitrogen dioxide and water vapor from the extinction of solar radiation measured during spacecraft sunrise/sunset. The water vapor channel is centered at 935.5 nm with a bandwidth of 20 nm. The instantaneous field-of-view is rectangular in shape, 0.5 arc minutes in elevation by 2.5 arc minutes in azimuth which corresponds to 0.5 km by 2.5 km at the tangent layer. Each day, 15 sunrise and 15 sunset profiles are obtained with successive measurements separated by 24° in longitude at similar latitudes. Global coverage ranges from 80°N to 80°S at altitudes from 45 km down to cloud tops or 2 km in cloud free regions. SAGE II was launched in October, 1984 and remains operational today. Further details of the instrument and measurement technique may be found in (1, 2). The procedure for converting the solar radiance data to atmospheric slant path transmission and inversion to gas concentration may be found in (3). Since this is the first measurement of water vapor with the SAGE observational technique and the first use of the ρ water vapor band to infer H_2O from space, an extensive validation program has been undertaken that incorporates correlative measurements and comparisons to other global data sets. In this paper, we will present preliminary zonal means for November 1985 and compare them to tropospheric water vapor (4) and the LIMS stratospheric water vapor (5, 6). Correlative measurements from a frost-point hygrometer will also be compared to individual SAGE II profiles.

2. Correlative Measurements

To validate the SAGE II water vapor measurements a balloon-borne frost-point hygrometer (7) was flown several times in the northern hemisphere at low, middle and high latitudes. The flights were planned to coincide as close as possible in space and time with the SAGE II overpasses. Results from two mid-latitude flights are shown in Figure 1 along with the corresponding SAGE II profiles for comparison. The error bars indicate the estimated one standard deviation uncertainties in the SAGE II water vapor retrievals. The time separation between the frost-point hygrometer and SAGE II is less than an hour for the November 30 measurements and less than 2 hours on May 18. The November 30 measurement location is also closer to the SAGE II observations than for May 18. On both days, excellent agreement is apparent above 15 km, below this altitude some discrepancies are evident. Some of the differences at these altitudes are likely a result of comparing point measurements (the hygrometer) to long path occultation measurements (SAGE II) of an atmospheric species with rapid vertical and horizontal variations. Of some interest is the enhancement in water vapor at 10 km measured by the frost-point hygrometer on November 30. Inspection of the SAGE II slant path transmission (not shown) and the $1.0 \mu\text{m}$ aerosol extinction profile indicates a layer of clouds at the tropopause which the balloonsonde passed through and which terminated the aerosol and water vapor inversion. A hint of cloud also appears in the May 18

data at 11 and 12 km in the aerosol extinction and hygrometer profiles.

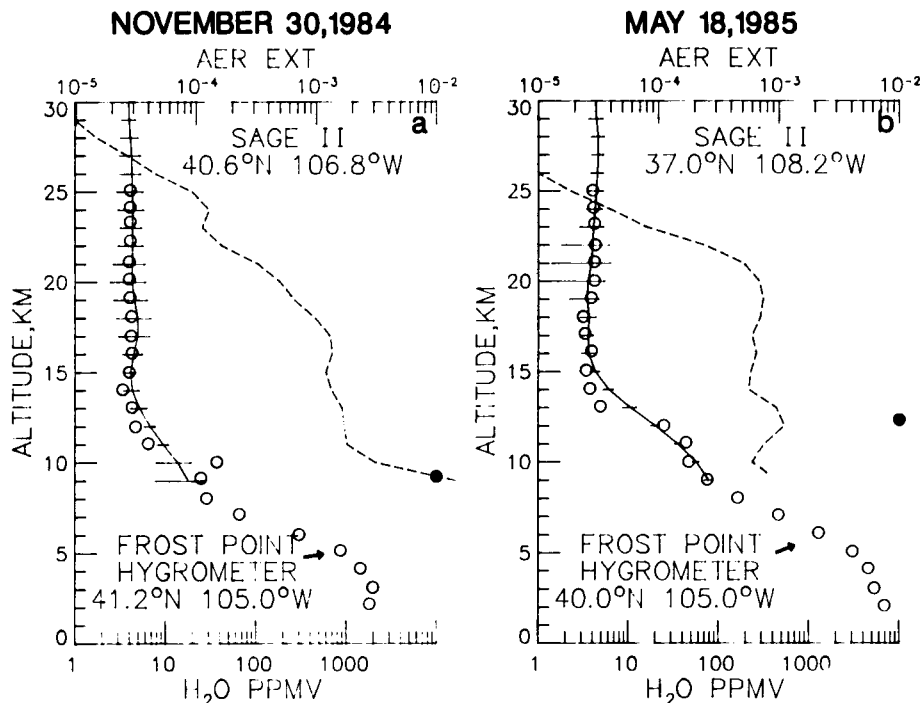


Figure 1. Water vapor correlative measurements for November 30, 1984(a) and May 18, 1985(b). Open circles correspond to frost-point hygrometer measurements, solid curve SAGE II. Error bars indicate estimated one standard deviation uncertainty in SAGE II retrieved H₂O. Dashed line gives the simultaneous SAGE II 1.0 μ m aerosol extinction profile. Solid circle indicates altitude of NMC defined tropopause.

3. Global Water Vapor Compilations

Another approach one can take to validate a large body of data, such as the SAGE II water vapor data, is to calculate and compare monthly zonal means with other published climatologies. In this section we present monthly zonal means for November, 1985 and compare them to two global water vapor compilations, the November 1978 LIMS measurements (5, 6) and the Global Atmospheric Circulation Statistics (GACS), 1958-1973, developed by Oort (4). The LIMS experiment on Nimbus 7 used the 6.9 μ m water vapor band to measure the vertical profile of water vapor from 100 to 1 mb. Near global coverage was obtained (64°S to 84°N) from October 24, 1978 to May 28, 1979. The GACS water vapor climatology has been developed from several data sets composed primarily of rawinsonde observations. Southern hemisphere climatology covers the 1963 to 1973 time period while the northern hemisphere covers an additional 5 years, from 1958 to 1973. Uniform longitudinal coverage is obtained with LIMS in both hemispheres, while most GACS rawinsonde data are taken over land at fixed locations. Altitude coverage of the GACS data ranges from 1000 to 300 mb. Global information covering the intermediate levels from 300 to 100 mb is non-existent to our knowledge.

NOVEMBER 1985

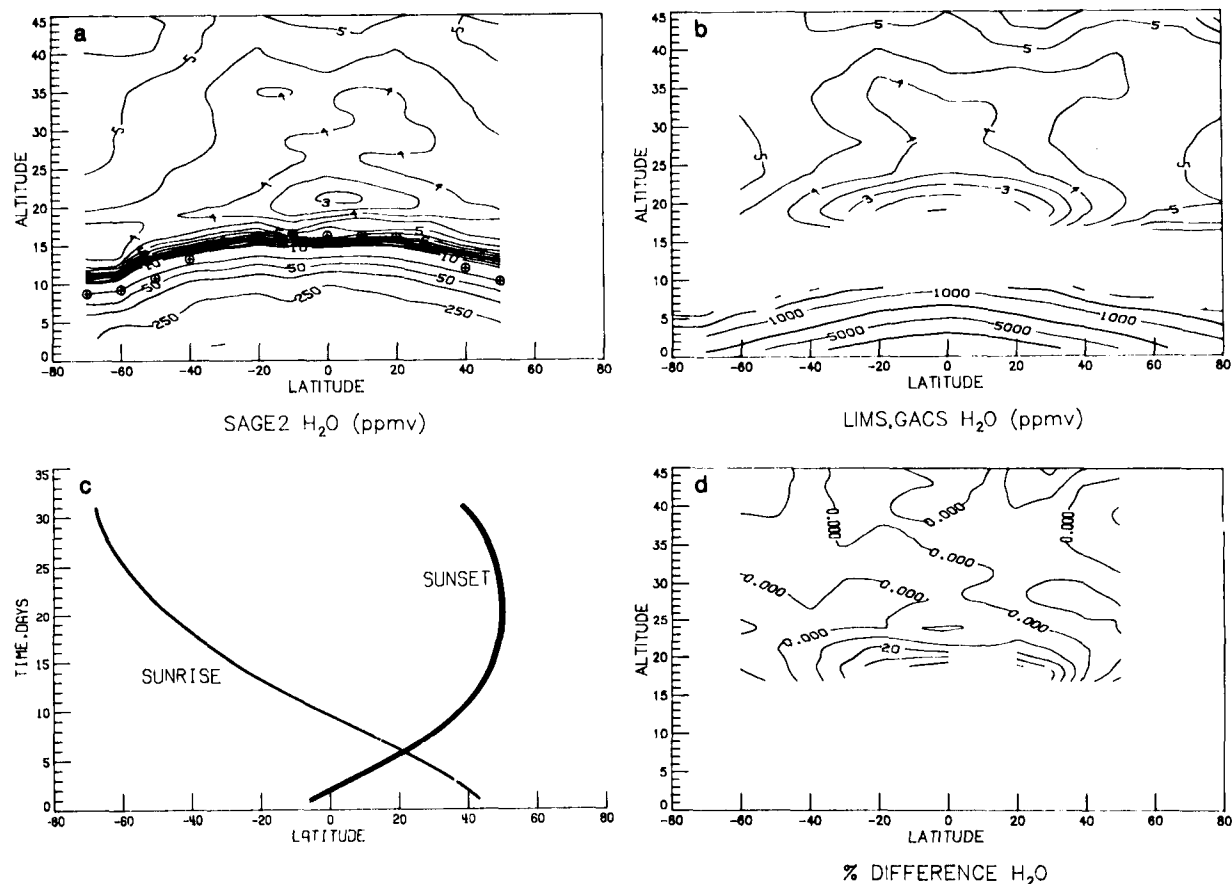


Figure 2. a) SAGE II monthly zonal means for November, 1985. Circles with pluses indicate monthly averaged NMC tropopause altitude. b) Stratospheric LIMS monthly zonal means for November, 1978 and tropospheric GACS monthly zonal means. c) SAGE II latitudinal coverage for November, 1985. d) Percent difference between SAGE II and LIMS monthly zonal means in the stratosphere.

Figure 2a shows the November 1985 monthly zonal means obtained with SAGE II. The SAGE II profiles have been screened for cloud and aerosol contamination as discussed in (8). The screening has the greatest effect in the equatorial lower stratosphere where the most clouds and highest levels of aerosol are found. The screening process tends to bias the data set in the troposphere to cloud free air masses and thus presumably dry conditions.

Mixing ratios of 3 ppmv are found at the hygropause and increase to 5 ppmv at higher altitudes and latitudes. The transition from the stratospheric to tropospheric regime is delineated by the 5 to 10 ppmv contours. At low latitudes this transition region corresponds closely to the average NMC defined tropopause height (circles with pluses) but at high latitudes the water transition region lies above the average tropopause. Figure 2b shows the corresponding November zonal means for the LIMS and GACS water vapor compilations. The SAGE II zonal means were calculated with 10° latitude bins, LIMS with 4° bins and GACS with 5° bins. In the stratosphere, SAGE II and LIMS agree quite well even though the measurements were taken 6 years apart.

The percent difference in mixing ratio, shown in Figure 2d, is better than 20% outside of the hygropause region. Within the hygropause region, the differences reach 40%. Some of this may be due to differences in the instantaneous field-of-view, 3.6 km (FWHM) for LIMS versus 0.5 km for SAGE II, but it may also result from the fact that SAGE II obtains all of its equatorial data in the first third of the month as indicated in Figure 2c, thus the SAGE II monthly zonal mean is more representative of the early part of the month. The SAGE II tropospheric water is considerably lower than the radiosonde GACS water data. This difference may be indicative of the level of bias caused by the cloud screening process.

NOVEMBER 1985

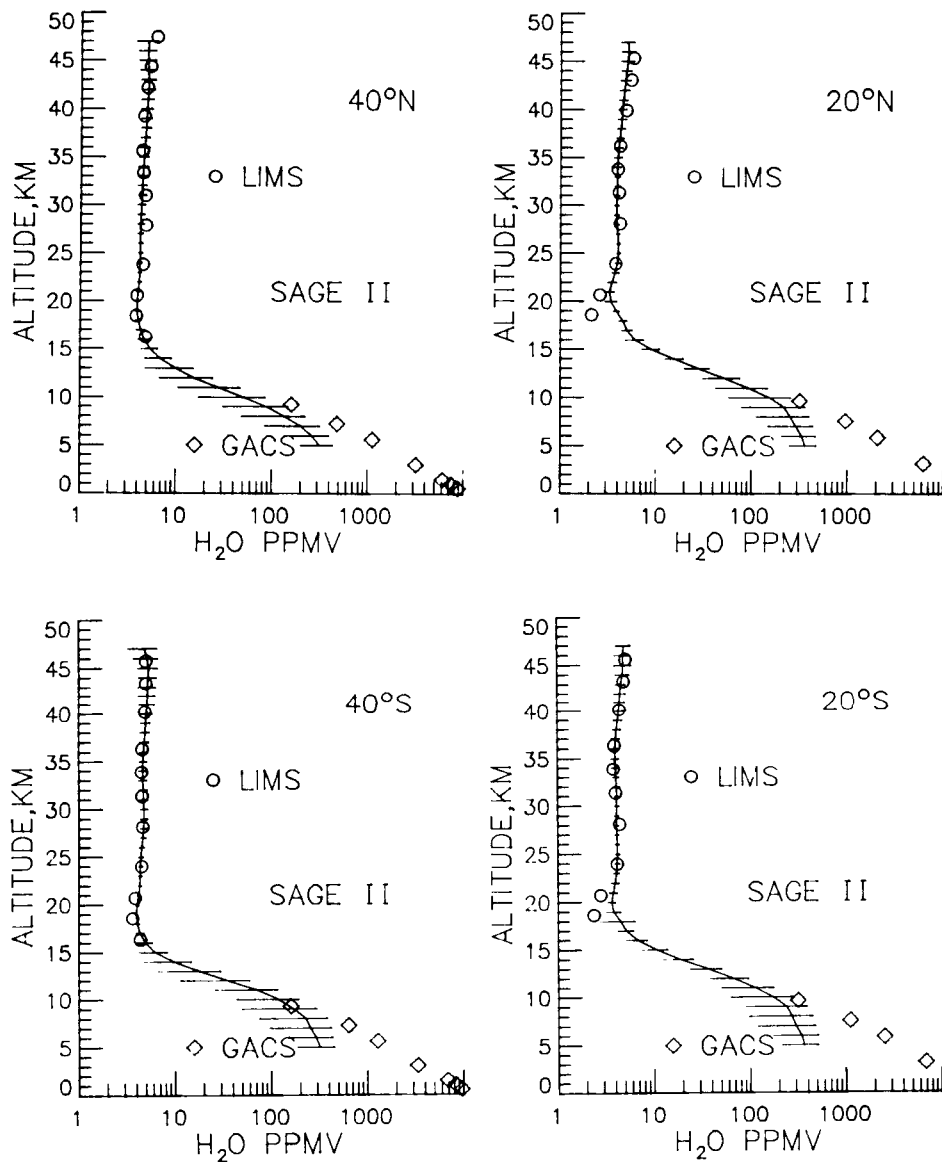


Figure 3. Comparison of selected SAGE II, LIMS and GACS monthly zonal means for November. The SAGE II error bars represent the standard deviation of the mean mixing ratio.

Figure 3 highlights the monthly zonal near vertical profiles for selected latitude bins corresponding to Figure 2. The error bars in this figure represent the standard deviation of the mean SAGE II mixing ratio. The error bars are small in the stratosphere where little variability is expected and large in the troposphere where dynamics determines the distribution to a large extent.

4. Discussion

Given the many differences (measurement techniques, sampling biases and observational periods) between SAGE II, LIMS, and GACS; the agreement between SAGE II and the comparison data sets is quite good. Some of the remaining differences may never be fully explained. The quality of the comparison to LIMS data in the stratosphere shown here for November is representative of that found in other months for which LIMS obtained data. The SAGE II data indicates a smooth transition from the LIMS data at 100 mb to the GACS data at 300 mb. The quality and consistency of the SAGE II water vapor will lead to improved understanding of the global water vapor climatology, aerosol formation mechanisms, and tropospheric/stratospheric exchange processes.

5. Acknowledgements

J. C. Larsen is supported by NASA Contract NAS1-17022. The authors would like to thank S. J. Oltmans for providing the frost-point hygrometer data.

REFERENCES

1. McMaster, L. R. (1986) Sixth Conference on Atmospheric Radiation, Williamsburg, VA, May 13-16, J46-J48.
2. Mauldin, L. E., M. P. McCormick, L. R. McMaster and W. R. Vaughn (1985) SPIE 2nd International Technical Symposium on Optical and Electro-Optical Applied Science and Engineering, Cannes, France, November, Paper No. 589018.
3. Chu, W. P. (1986) Sixth Conference on Atmospheric Radiation, Williamsburg, VA, May 13-16, J49-J51.
4. Oort, A. H. (1983) Global Atmospheric Circulation Statistics, 1958-1973, NOAA Professional Paper 14, U.S. Govt. Printing Office, 1983-404-474.
5. Russell, J. M., J. C. Gille, E. E. Remsberg, L. L. Gordley, P. L. Bailey, H. Fischer, A. Girard, S. R. Drayson, W. F. J. Evans and J. E. Harries, J. Geophys. Res., 89, 5115-5124.
6. Remsberg, E. E. and J. M. Russell III (1986) The Nimbus 7 LIMS Water Vapor Measurements. MECA Workshop on Atmospheric H₂O Observations of Earth and Mars. Lunar and Planetary Institute, Houston, TX, in press.
7. Oltmans, S. J. (1986) Water Vapor Profiles for Washington, DC; Boulder, CO, Palestine, TX; Laramie, WY; and Fairbanks, AK; During the Period 1974 to 1985, NOAA Data Report ERL ARL-7.
8. Larsen, J. C., L. R. McMaster, M. P. McCormick and W. P. Chu (1986) Sixth Conference on Atmospheric Radiation, Williamsburg, VA, May 13-16, J56-J58.

187407

FLUX OF WATER VAPOR IN THE TERRESTRIAL STRATOSPHERE AND IN THE MARTIAN ATMOSPHERE. Conway Leovy, Matthew Hitchman, Dept. of Atmospheric Sciences, University of Washington, Seattle, WA 98195, Daniel McCleese, Jet Propulsion Laboratory, 4800 Oak Grove Dr., Pasadena, CA 91109.

Measurements of terrestrial stratospheric water vapor concentration are reviewed with emphasis on data obtained with the Limb Infrared Monitor of the Stratosphere Experiment on Nimbus 7 (LIMS; Ref. 1). These data clearly show that the equatorial tropopause region is a source of "anti-water" throughout the year. That is, relatively dry air introduced to the stratosphere at the equatorial tropopause is carried upward in the equatorial branch of the zonal mean diabatic circulation to the upper stratosphere. Methane is also introduced at the equatorial tropopause, carried upward in the same stream, and photochemically oxidized in the upper stratosphere to form water vapor which is transported downward into the lower stratosphere in the high latitude branches of the diabatic circulation (Ref. 2). The structure of the important rising branch of this diabatic circuit is controlled and modulated seasonally and interannually by a variety of dynamical processes including Kelvin, and Rossby waves. Details of these controlling mechanisms have also been revealed by LIMS measurements of temperatures and ozone concentrations. LIMS measurements allow diagnosis of the wave structures as well as accurate calculations of the diabatic circulation (Ref. 3). Thus, a single well-focused limb scanning experiment has revealed both the global scale flux of H_2O in the terrestrial stratosphere as well as important features of the natural stratospheric pump driving the flux.

Figs. 1 and 2 illustrate some of these points. A zonal mean water vapor cross section for Jan. 10-15, 1979 shows a dry tongue extending upward from the equatorial tropopause, moister air at high latitudes and evidence for

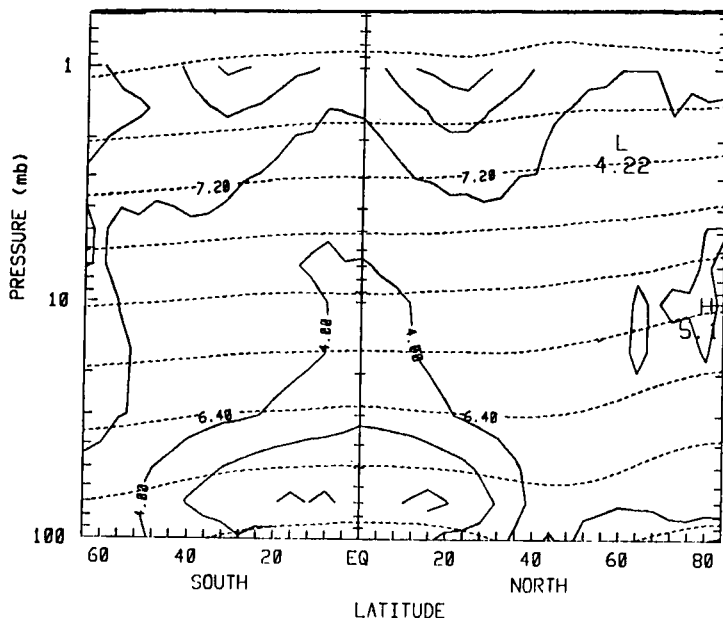


Fig. 1. Zonal mean LIMS water vapor concentration (ppmv) averaged for Jan. 10-15, 1979 superimposed on potential temperature ($\ln(^{\circ}K)$, dashed).

moister, possibly subsiding air, between 1 and 3 mb near 30°N and 30°S (Fig. 1). The zonal mean diabatic circulation averaged over Dec. 12-17, 1979 (Fig. 2) exhibits rising and sinking centers near the equator and 30°N and 30°S between 0.5 and 3.0 mb that may have been responsible for water vapor vertical transport over the intervening 28 day period. This complex vertical velocity pattern at low latitudes is due to the pattern of low latitude wave driving (Ref. 3).

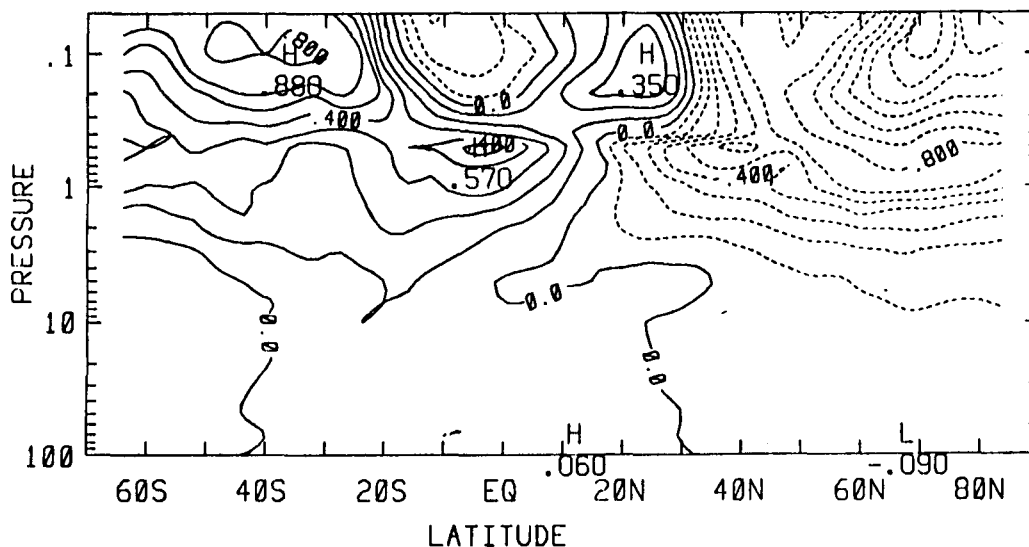


Fig. 2. Zonal mean diabatic circulation deduced from LIMS ($\text{cm}\cdot\text{s}^{-1}$) averaged for Dec. 12-17, 1978.

The Pressure Modulator Infrared Radiometer (PMIRR) which is part of the current Mars Orbiter experiment package will be able to make comparable observations of Mars (Ref. 4). It will measure temperature, dust, and water vapor distributions with $\frac{1}{2}$ scale height vertical resolution. The temperature and dust measurements should make it possible to calculate the zonal mean diabatic circulation, and the high vertical resolution should make it possible to identify and characterize Rossby and Kelvin waves. Thus, there is good reason to expect that PMIRR on the Mars Orbiter will lead to an understanding of the atmospheric branch of Mars' water cycle comparable to that achieved for Earth's stratosphere with the aid of the LIMS data.

REFERENCES

1. Remsberg, E., J. M. Russell III, L. L. Gordley, J. C. Gille, and P. L. Bailey, 1984. Implications of the stratospheric water vapor distribution as determined from the Nimbus 7 LIMS experiment. *J. Atmos. Sci.*, **41**, 2934-2345.
2. Jones, R. L., and J. A. Pyle, 1984. Observations of CH_4 and N_2O by the Nimbus 7 SAMS: a comparison with in situ data and two dimensional model calculations. *J. Geophys. Res.*, **89**, 5263-5279.

3. Hitchman, M., and C. Leovy, 1986. Evolution of the zonal mean state in the equatorial middle atmosphere during October 1978 - May 1979. J. Atmos. Sci., 43, (in press).
4. McCleese, D. J., J. T. Schofield, R. W. Zurek, J. V. Martonchik, R. D. Haskins, D. A. Paige, R. A. West, D. J. Diner, J. R. Locke, M. P. Crisp, W. Willis, C. B. Leovy, and F. W. Taylor, 1986. Remote sensing of the atmosphere of Mars using infrared pressure modulation and filter radiometry. Applied Optics (in press).

577-91

70

AB- 5057

18- 187408

N89-25807

REGELATION AND ICE SEGREGATION; R. D. Miller, Department of Agronomy, Cornell University, Ithaca, NY 14853.

If it turns out that a globally significant quantity of Martian groundwater exists as segregated ice beneath the Martian landscape, how did it get there?

On earth, segregated ice (other than buried surface ice) is most likely to form as a consequence of thermally-induced regelation⁽¹⁾ although locally important amounts can be produced as a consequence of freezing-induced hydraulic fracturing⁽²⁾. Thermally-induced regelation ostensibly accounts for essentially all of the segregated ice that may be formed during seasonal freezing of earth's "active layer" whether it is underlain by unfrozen soil in earth's middle latitudes or by permafrost at higher latitudes. Hydraulic fracturing, induced by centripital freezing of a water-saturated 'talik' in terrestrial permafrost, ostensibly accounts for segregated ice found in the core of a closed-system pingo, for example. Such ice may have been formed over a period of a some scores of years.

For Mars, it seems to be difficult to contrive plausible scenarios that would rationalize thermally-induced regelation as a mechanism for producing globally significant quantities of segregated ice; a much warmer and wetter climate would be necessary. It is less difficult to contrive scenarios for freezing-induced hydraulic fracturing but the quantities would be significant only at the scale at which isolated taliks could be envisioned. These might be at the scale of a natural basin; a somewhat warmer climate or a major episode of local thawing would have been a necessary antecedent. Segregated ice formed in this way should not exceed, say, 5% of the original volume of the talik.

Freezing-induced hydraulic fracturing represents formation of locally significant quantities of high pressure water which could be released as artesian water by an event which ruptured the frozen overburden. Such a discharge might account for some fluvial features that have been observed on the Martian surface.

(1) O'Neill K. and Miller, R. D. (1985) Water Resour. Res., 21, p. 281-296.

(2) Mackay, J. R. (1978) Canadian Jour. Earth Sci., 15, P. 1219-1227.

510-46
N89-25808⁴⁸
187409⁷¹

MEASUREMENTS OF H₂O IN THE TERRESTRIAL MESOSPHERE AND IMPLICATIONS FOR EXTRA-TERRESTRIAL SOURCES; J.J. Olivero, Department of Meteorology, The Pennsylvania State University, University Park, PA 16802

Water vapor is an important minor constituent in the terrestrial mesosphere (approx. 50 km to 85 km or 10⁰ mbar to 10⁻² mbar) and nearly coincident D-region ionosphere (~60 km to 90 km). Its photolysis products control ozone above the ozone mixing ratio peak; they are radiatively active, especially in the infrared; water sublimates to cause polar mesospheric clouds and possibly other suggested aerosol phenomena; the molecules cluster to form massive ions which dominate the chemistry of the lower ionosphere; and, finally, as the principal hydrogen compound below the mesosphere, it controls the global hydrogen budget and H escape rate.

During the last decade several measurement techniques have been employed to observe H₂O at these atmospheric levels; these are presented in Figure 1 with symbols given in Table 1.

Five of these data sets were produced by ground-based microwave radiometry (B1, SC, B2, OL, TS). These results were all contributed by a collaboration between The Pennsylvania State University and the Naval Research Laboratory, joined recently by the Jet Propulsion Laboratory. The observations cover all seasons but are limited to a small range of latitudes - 34N to 24N - over North America.

The second group (AK, GR, OE, RD, SN, WA) involve various aircraft and rocket techniques and were observed over a much wider range of latitudes.

Ground-based microwave measurements at mid-latitudes strongly support a very dry mesopause-lower thermosphere. Other measurements, [6] and [7], can be interpreted as being consistent with a high altitude or external source of H₂O. The latter process was not seriously considered until very recently-- [12], [13] and [14]--however, these new hypotheses have profound implications for the upper atmospheres of all the planets [15].

The remainder of the talk will discuss the apparent qualitative limits that H₂O measurements to date place upon a downward H₂O flux above the mesosphere.

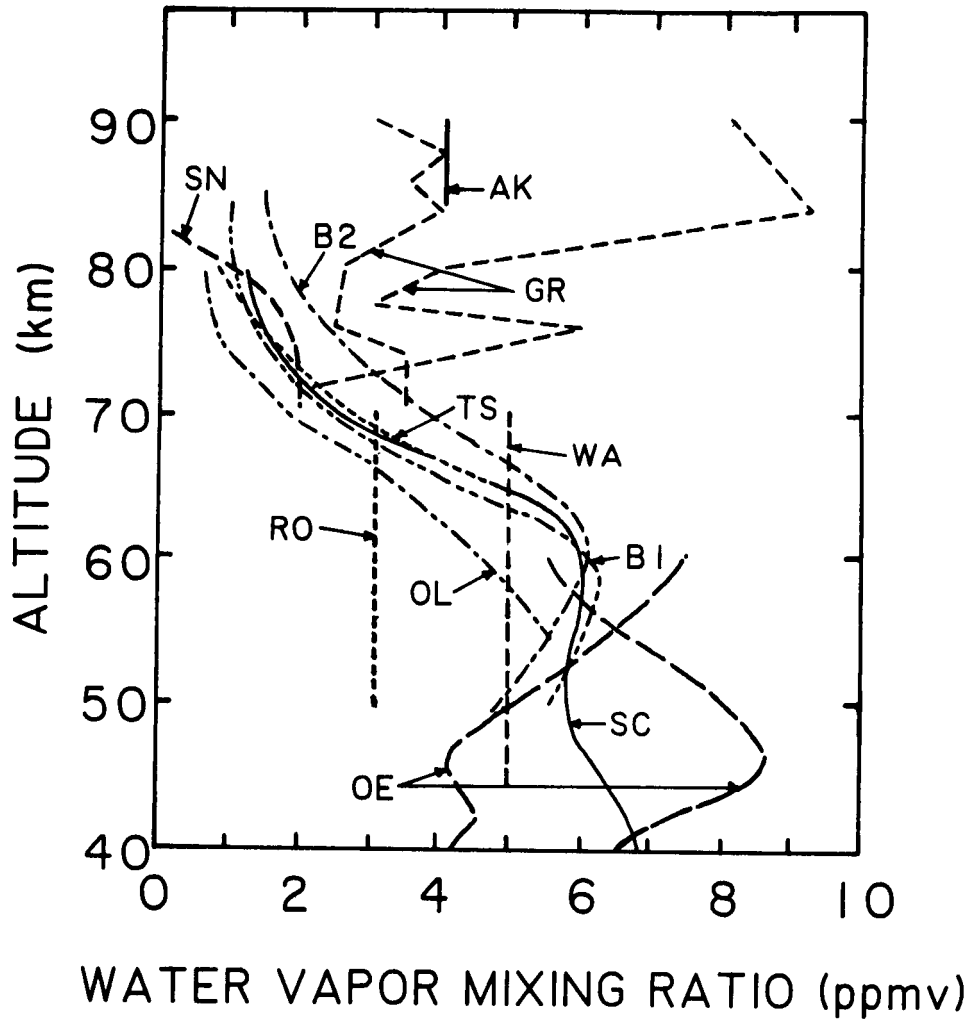


Figure 1. A collection of measurements of mesospheric water vapor from the past decade; symbols referenced in Table 1.

Table 1.

KEY TO SYMBOLS IN FIGURE 1

<u>SYMBOL</u>	<u>REFERENCE</u>	<u>COMMENT</u>
B1	Bevilacqua, et al. (1983)..... [1]	GROUND-BASED
SC	Schwartz, et al. (1983)..... [2]	MICROWAVE
B2	Bevilacqua, et al. (1985)..... [3]	RADIOMETRY
OL	Olivero, et al. (1986)..... [4]	MID-LATITUDES
TS	Tsou (1986)..... [5]	
AK	Arnold and Krankowsky (1979).. [6]	MISCELLANEOUS
GR	Grossmann, et al. (1982)..... [7]	TECHNIQUES
OE	O'Brien and Evans (1981)..... [8]	-
RO	Rogers, et al. (1977)..... [9]	RANGE OF
SN	Swider and Narcisi (1975)..... [10]	NON-POLAR
WA	Waters, et al. (1980)..... [11]	LATITUDES

REFERENCES

1. Bevilacqua, R. M., Olivero, J. J., Schwartz, P. R., Gibbins, C. J., Bologna, J. M. and Thacker, D. L. (1983) J. Geophys. Res., 88, 8523-8534.
2. Schwartz, P. R., Croskey, C. L., Bevilacqua, R. M. and Olivero, J. J. (1983) Nature, 305, 294-205.
3. Bevilacqua, R. M., Wilson, W. J., Ricketts, W. B., Schwartz, P. R. and Howard, R. J. (1985) Geophys. Res. Lett., 12, 397-400.
4. Olivero, J. J., Tsou, J. J., Croskey, C. L., Hale, L. C. and Joiner, R. G. (1986) Geophys. Res. Lett., 13, 197-200.
5. Tsou, J. J. (1986) Microwave Radiometric Measurements of Mesospheric Water Vapor: Ground-Based Observations in Both Solar Absorption and Atmospheric Emission Modes, Ph.D. dissertation in Meteorology, The Pennsylvania State University, University Park, PA, 185 pp.
6. Arnold, F. and Krankowsky, D. (1977) Nature, 268, 218-219.
7. Grossman, K. U., Frings, W., Offerman, D. O., Joos, W., Andre, L. and Kopp, E. (1982) Concentrations of some minor neutral constituents in the mesosphere and lower thermosphere above northern Europe, XXIV COSPAR Asembly, Ottawa.
8. O'Brien, R. S. and Evans, W. F. J. (1981) J. Geophys. Res., 86, 12101-12107.
9. Rogers, J. W., Stair, A. J., Jr., Degges, J. C., Wyatt, C. L. and Baker, D. J. (1977) Geophys. Res. Lett., 4, 366-368.
10. Swider, W. and Narcisi, R. S. (1975) J. Geophys. Res., 80, 655-664.
11. Waters, J. W., Gustincic, J. J., Swanson, P. N. and Kerr, A. R. (1980) Measurements of upper atmospheric H₂O emission at 183 GHz, in Atmospheric Water Vapor, edited by A. Deepak, T. O. Wilkerson, and L. H. Ruhnke, Academic Press, New York, 229-240.
12. Frank, L. A., Sigwarth, J. B. and Craven J. D. (1986) Geophys. Res. Lett., 13, 307-310.

13. Frank, L. A., Sigwarth, J. B. and Craven, J. D. (1986) Geophys. Res. Lett., 13, 307-310.
14. Dubin, M. (1986) Noctilucent clouds-the problems of origin, American Geophysical Union - Spring Meeting, Baltimore.
15. Donahue, T. M. (1986) Geophys. Res. Lett., 13, 555-558.

DIURNAL AND ANNUAL CYCLES OF H₂O IN THE MARTIAN REGOLITH; 187410

J.R. Philip, CSIRO Division of Environmental Mechanics, GPO Box 821, Canberra, ACT 2601, Australia.

1. *Atmospheric Heat Engines on Earth and Mars.* A terrestrial micrometeorologist is constantly aware of the intimate connection between the surface fluxes of H₂O and of sensible heat. This connection is ubiquitous evidence of the Earth's atmospheric heat engine in action. Its character depends, *inter alia*, on the tightness of the linkage between the energy cycle and the cycle of H₂O. H₂O is an important component of the working fluid because the temperature and pressure at the Earth's surface are such that H₂O is always present there in at least one condensed phase as well as vapor; and because the surface air's latent heat content is relatively large compared to its sensible heat capacity, with consequent correlation between energy transport and H₂O transport.

The same micrometeorologist finds however, that the latent heat capacity of surface air on Mars is only about one ten-thousandth that on Earth. H₂O-based latent heat fluxes represent only a trivial fraction of total energy fluxes on Mars: the linkage between H₂O and energy fluxes is extremely weak [1]. Unlike on Earth, H₂O on Mars is an ineffective component of the working fluid. CO₂ is the dominant component.

Can we make these considerations quantitative? Equation [1] defines Θ , which we propose as an index of the relative importance of latent heat transport by a particular component under particular surface conditions:

$$\Theta = \frac{\rho_v L}{\rho c_p} \quad [1]$$

Here ρ is the density and c_p the specific heat at constant pressure of the surface air, ρ_v the surface vapor density of the component, and L its latent heat of phase change (evaporation or sublimation).

The quantity Θ , with the dimensions of temperature, is the excess of surface equivalent temperature (2) for the particular component, over the surface air temperature. We may call it the *equivalent temperature excess*. A tight linkage between energy flux and the mass flux of a component will give large values of Θ under given surface conditions; and conversely.

Figure 1 graphs evaluations of Θ for H₂O on Earth and for H₂O and CO₂ on Mars. On Earth Θ decreases from 93 K for a surface dewpoint of 310 K to 0.1 K for a frostpoint of 225 K. On Mars Θ for H₂O decreases from 6.2 K for a frostpoint of 220 K to 10⁻⁵ K for one of 150 K. Contrast the very large value for CO₂ on Mars, $\Theta = 692$ K. The latitudinal distribution of Θ on the two planets signalizes vividly their different meteorology. Earth's atmospheric heat engine is most effective and active in the tropics and least so at the poles. On the other hand, the Martian heat engine is most effective over the polar CO₂ caps, with Θ there more than 10 times that of tropical Earth; but it is ineffective elsewhere.

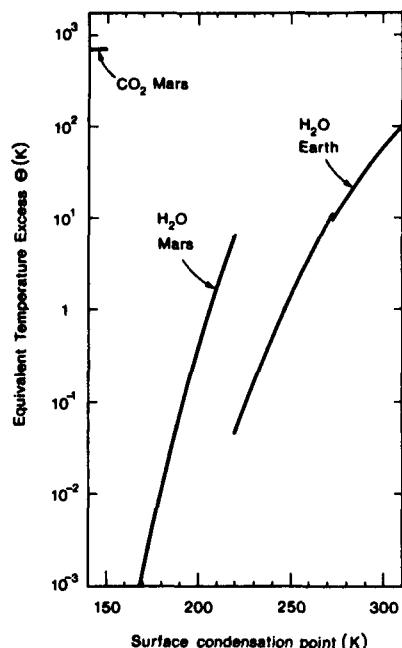


Figure 1.

Variation of Θ with surface condensation point for H_2O on Earth and for CO_2 and H_2O on Mars.

2. *Diurnal and Annual Cycles of H_2O in the Martian Regolith.* The looseness of the atmospheric linkage of energy and H_2O surface fluxes enables analysis of the equilibrium and flux of H_2O in the Martian regolith with the atmosphere entering only through surface boundary conditions on temperature, T , and H_2O vapor density. The regolith is so cold that we need consider only the processes of sublimation, vapor diffusion, and thermal conduction. In such systems ice behaves as a "wetting" capillary substance. Many of the concepts of terrestrial soil-water physics (e.g. 3,4) with appropriate modification, carry over. Details are given in (5,6), where this approach was used to investigate model diurnal and annual H_2O cycles. The vector flux density of H_2O , q , is described by the equation

$$q = -D_\theta \nabla \theta - D_T \nabla T \quad [2]$$

where the coefficients D_θ , D_T are strongly nonlinear functions of both T and of the regolith volumetric ice content θ .

D_T increases very strongly (approximately exponentially) with T , so that an harmonic temperature wave imposed at the surface produces a net downward flux due to the temperature field. For equilibrium over the year this must be balanced by a net upward flux due to θ increasing with depth. These considerations yield the equilibrium ice content profile. In principle, this profile is perturbed by diurnal and annual oscillations in surface boundary layers. These perturbations, in fact, prove to be trivial.

The earlier work produced ice tables (regolith saturated with ice) at depths below the surface which were very sensitive to the surface humidity cycle. In the light of later information, the humidities used then were unrealistically high. The present calculations are for conditions approximating the mid-latitudes. They are: mean surface temperature 200 K with diurnal and annual semi-amplitudes of 30 K; and daytime surface frostpoint (DSF) from 190 to 200 K. The solutions give θ in the range 0.02 - 0.03, with a slow increase with depth down to about 12 m. There the areothermal heat flux becomes important, reversing the gradient of θ . See Table 1.

Table 1. Equilibrium Ice Content Profiles

Daytime Surface Frostpoint (K)	190	195	200
Depth (m)	Ice Content θ		
0	0.02497	0.02569	0.02648
0.1	0.02630	0.02719	0.02819
1	0.02803	0.02924	0.03090
2	0.02883	0.03034	0.03246
6	0.03074	0.03319	0.03994
12	0.03122	0.03455	0.04209

Figure 2 shows the annual cycles of H₂O flux into and from the regolith for DSF's of 190, 195, and 200 K. Figure 3 shows, for a DSF of 195 K, the diurnal H₂O cycles for 12 representative sols. The notable point about these results is the very small value of the H₂O fluxes. Even for the largest DSF, 200 K, the total annual variation of condensed H₂O in the regolith is only 120×10^{-6} m. This corresponds to variations of θ of only $+ 0.00006$ distributed over the top 1 m of the regolith. The largest diurnal change in ice content (DSF = 200 K, sol 167) is 1.2×10^{-6} m, corresponding to a change in θ of only 0.00003 distributed over the top 0.04 m of the regolith.

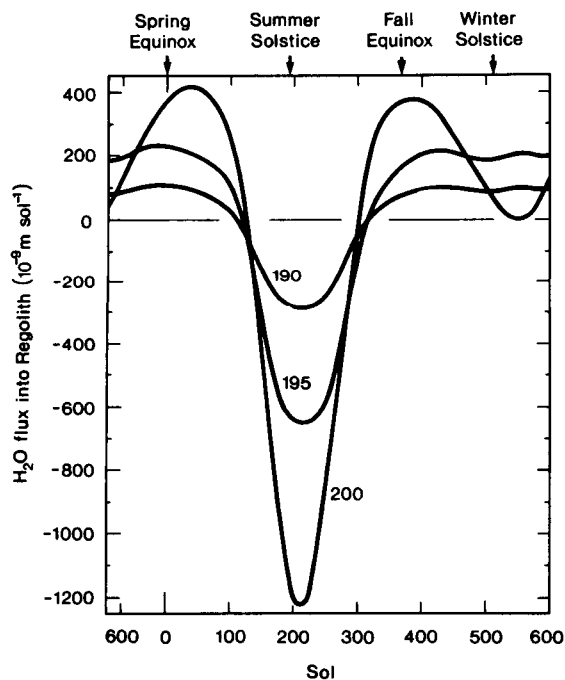


Figure 2.
 Annual cycles of H₂O exchange with the Martian regolith. Illustrative examples with DSF = 190, 195, 200 K.

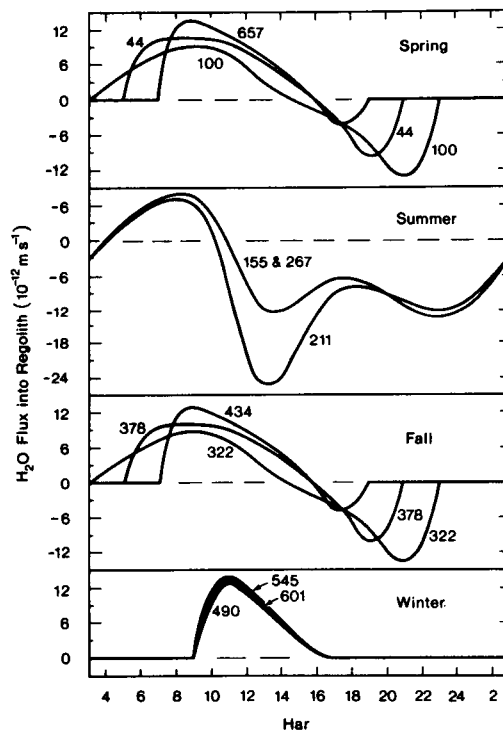


Figure 3.
 Diurnal cycles of H₂O exchange with the Martian regolith. Illustrative example with DSF = 195 K. Note that 24 hars (Martian hours) = 1 sol. Numerals on curves show sol number, with sol 0 at vernal equinox.

3. *Influence of Areothermal Heat Field on Regolith H₂O.* We have already noted that the areothermal heat field interacts with the damped surface temperature waves in the unsaturated regolith leading to a maximum value of θ at about 12 m. Below this θ decreases slowly to negligible values in depth.

Interest attaches to the possibility of liquid water in the regolith at great depths. The depth to the 273 K isotherm,

$$z_{273} = \frac{\bar{\lambda}}{Q} (273 - \bar{T}_0) , \quad [3]$$

with \bar{T}_0 the mean annual surface temperature (at $z = 0$), $\bar{\lambda}$ the mean thermal conductivity in $0 < z < z_{273}$, and Q the areothermal heat flux density. We adopt $Q = 0.025 \text{ W m}^{-2}$ and take $\bar{\lambda} = 0.728 \text{ W m}^{-1} \text{ K}^{-1}$, consistent with the profiles of θ of the examples discussed above. We thus find, for $\bar{T}_0 = 200 \text{ K}$, the value $z_{273} = 2126 \text{ m}$. Typically, the possibility of liquid H₂O in the regolith arises only at depths of the order of kilometers.

If the regolith H₂O is in equilibrium with the present Martian atmosphere, its H₂O content below the 273 K isotherm seems likely to be so small that the H₂O may exist primarily in an adsorbed phase.

Matters would be different, of course, if a mass of fossil ice-saturated regolith were connected to the 273 K isotherm. In the unlikely circumstance where the region below 273 K was undrained, one would then have water-saturated regolith underlying the ice-saturated mass. Underdrainage seems the more likely possibility. In this case the final profile of H₂O beneath the ice-saturated mass would be established by H₂O vapor equilibration in the areothermal heat field.

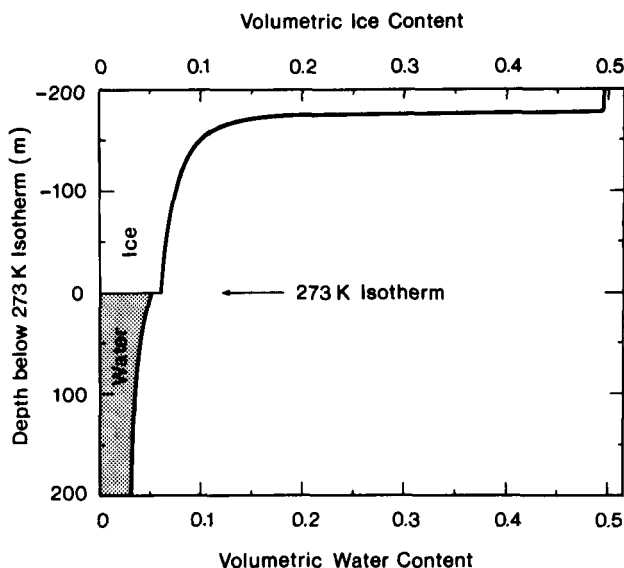


Figure 4.

Case of ice-saturated regolith with ice extending to 273 K isotherm. Volumetric ice and water content profiles above and below isotherm.

Figure 4 shows the profile of ice and water content for an illustrative example. For a regolith with underdrainage, we see that, even granted the existence of fossil ice-saturation above 273 K, liquid H₂O can occur only at a depth of order of kilometers, in minor concentrations.

4. References

- (1) Philip, J.R. (1979). In *Water, Planets, Plants and People*, Aust. Acad. Sci., Canberra, pp. 35-59.
- (2) Iribarne, J.V., and Godson, W.L. (1973). *Atmospheric Thermodynamics*, Reidel, Dordrecht, p.105
- (3) Philip, J.R. (1969). *Adv. Hydrosci.*, 5, 214-296.
- (4) Philip, J.R. (1973). In *Applied Mechanics*, Proc. 13th Int. Congr. IUTAM, Moscow, 1972, pp. 279-294.
- (5) Philip, J.R. (1976). *Proc. Colloq. on Water in Planetary Regoliths*, Hanover NH, pp. 59-63.
- (6) Philip, J.R. (1978). *Proc. Colloq. on Planetary Water and Polar Processes*, Hanover NH, pp. 32-39.

THE NIMBUS 7 LIMS WATER VAPOR MEASUREMENTS; Ellis E. Remsberg and James M. Russell III, Atmospheric Sciences Division, NASA Langley Research Center, Hampton, Virginia 23665-5225

The Limb Infrared Monitor of the Stratosphere (LIMS) experiment on Nimbus 7 used the technique of thermal infrared limb scanning to sound the composition and thermal structure of the Earth's stratosphere (1). One of the LIMS channels was spectrally centered at 6.9 micrometers to measure the vertical profile of water vapor radiance from about 15 to 55 km. Data were obtained from late October 1978 until May 1979 over a latitudinal extent of 64 S. to 84 N. providing near global coverage.

The water vapor radiances were registered against pressure-altitude using temperature versus pressure profiles retrieved concurrently from radiances measured in the 15 micrometer CO₂ band. Water vapor mixing ratio profiles were then retrieved using a fully iterative, nonlinear technique that is independent of the first-guess climatological water vapor profile shape (2). Details of the measurements and their validation are given in (3) along with determinations of their uncertainty. Mixing ratios are in the parts per million by volume (ppmv) range throughout the Earth's stratosphere. Data precision was estimated to be 0.2 to 0.3 ppmv, and the accuracy, based on computer simulations, is 20 to 30 percent. Comparisons with several co-located balloon measurements of water vapor during the LIMS measurement period indicated agreement that was consistent with accuracy estimates. The high precision (5 to 10 percent) of the data yields excellent information on the relative variations of the water vapor fields with time and latitude.

Radiance profiles were obtained every 12 seconds along the orbital tangent path, both day and night, and approximately every fifth profile (spaced about 4° apart in latitude) was retrieved. The vertical resolution of each individual profile is about 5 km, while the horizontal resolution set by the LIMS field-of-view and limb viewing geometry is about 18 km by 300 km. The profile tapes were placed in the archive at the National Space Science Data Center (NSSDC) in 1984.

The synoptic profile data were processed into a zonal mean and six sine and six cosine Fourier coefficients for the synoptic time of 12 GMT by using a Kalman filter algorithm at each 4° of latitude and for 12 pressure levels from 100 mb to 1 mb. These Fourier coefficients were then used to create hemispheric maps of water vapor and to investigate its transport (4). Examples of the fields and their variability will be shown. This coefficient form of the data was archived at NSSDC in the spring of 1985.

The distribution of LIMS water vapor was initially discussed in (3), (5), and (6). The data show that (a) there is a poleward latitudinal gradient with mixing ratios that increase by a factor of 2 from Equator to $\pm 60^\circ$ at 50 mb; (b) that most of the time there is a fairly uniform mixing ratio of 5 ppmv at high latitudes, but more variation exists during winter; (c) a well-developed hygropause or minimum in mixing ratio exists several kilometers above the tropopause at low to mid latitudes; (d) a source region of water vapor exists in the upper stratosphere to lower mesosphere that is consistent with methane oxidation chemistry, at least within the uncertainties of the data [see also reference (7)]; (e) an apparent zonal mean water vapor distribution prevails that is consistent with the circulation proposed by Brewer in 1949; and (f) a zonal mean distribution exists in the lower stratosphere that is consistent with the idea of quasi-isentropic transport transport by eddies in the meridional direction.

REFERENCES

1. Gille, J. C. and Russell, J. M. III, 1984, J. Geophys. Res., 89, 5125-5140.
2. Gordley, L. L. and Russell, J. M. III, 1981, Appl. Opt., 20, 807-813.
3. Russell, J. M. III; Gille, J. C.; Remsberg, E. E.; Gordley, L. L.; Bailey, P. L.; Fischer, H.; Girard, A.; Drayson, S. R.; Evans, W. F. J.; and Harries, J. E., 1984, J. Geophys. Res., 89, 5115-5124.
4. Haggard, K. V.; Marshall, B. T.; Kurzeja, R. J.; Remsberg, E. E.; and Russell, J. M. III, 1986, NASA Technical Report, in preparation.
5. Remsberg, E. E.; Russell, J. M. III; Gordley, L. L.; Gille, J. C.; and Bailey, P. L., 1984, J. Atmos. Sci., 41, 2934-2945.
6. WMO Global Ozone Research and Monitoring Project Report, No. 16, 1986.
7. Jones, R. L.; Pyle, J. A.; Harries, J. A.; Zavody, A. M.; Russell, J. M. III; and Gille, J. C., 1986, Quart. J. Roy. Met. Soc., in press.

521-91

82

107412

MEASUREMENTS OF THE VERTICAL PROFILE OF WATER VAPOR ABUNDANCE IN THE MARTIAN ATMOSPHERE FROM MARS OBSERVER. J. T. Schofield and D. J. McCleese, Jet Propulsion Laboratory, California Institute of Technology, Pasadena, CA 91109.

In October 1991, the Mars Observer spacecraft will be inserted into a nearly circular, 361 km altitude, 92.8° inclination, sun-synchronous mapping orbit around Mars. From this platform, the Pressure Modulator Infrared Radiometer (PMIRR) will employ filter and pressure modulation radiometry using nine spectral channels, in both limb scanning and nadir sounding modes, to obtain daily, global maps of temperature, dust extinction, condensate extinction, and water vapour mixing ratio profiles as a function of pressure to half scale-height or 5 km vertical resolution. Surface thermal properties will also be mapped, and the polar radiative balance will be monitored.¹

The Mars Observer spacecraft has many advantages over previous Mars missions, and compares favorably with terrestrial atmospheric mapping orbiters for measurements of atmospheric constituent profiles by remote sounding. The circular, low orbit and spacecraft 3-axis stabilization, favour high vertical resolution limb sounding. Earth experience has shown that limb sounding is essential for the unambiguous retrieval of high vertical resolution constituent profiles.^{2,3} The high orbit inclination and short orbital period give complete latitudinal coverage and provide the daily, synoptic-scale mapping of atmosphere fields achieved by terrestrial atmospheric sounders. The 2 pm sun synchronous orbit allows mapping at local times representing diurnal extremes and permits diurnal and seasonal effects to be differentiated clearly. Finally the continuous mapping period of one martian year allows the complete seasonal cycle of water to be described in detail.

Measurements of water vapour are made by filter and pressure modulation radiometry in the near wing of the ν_2 band of water vapour at 6.9 μm , and by filter radiometry in the rotation band at 46.5 μm . In its mapping mode, PMIRR uses continuous in-track limb and nadir scanning in a repetitive cycle to obtain coincident water vapour vertical profile and column abundance measurements by day and during the night. Table 1 summarizes the horizontal, vertical and temporal resolution of the individual measurements, and mapped fields. The limiting sensitivity of nadir measurements is approximately 1 pr μm in the column, whereas that of limb measurements is about 50 times better.

The precision of retrieved profiles and column abundances depends on the actual profiles of temperature, dust and water in the Martian atmosphere. Computer simulations have been used to evaluate this precision given model profiles representing a best estimate of expected conditions on Mars. Water, dust, and temperature profiles have been retrieved simultaneously using a non-linear, iterative, relaxation technique.⁴ Figures 1a and b

compare input and retrieved water vapour profiles for a two very different model atmospheres. Figure 1a uses the Viking Lander 1 temperature profile and Figure 1b a profile from the Viking radio-occultation experiment. Both models include uniformly mixed dust with an optical depth in the nadir of 0.4 at visible wavelengths. Precision is in the range 10 - 20% up to 30 km.

Figure 2 shows a retrieved water vapour cross-section corresponding to water and temperature models developed to represent the northern summer hemisphere of Mars. Again, uniformly mixed dust with an optical depth of 0.4 is included at all latitudes. The difference between input and retrieved connections is also shown. Precision is of order 10 - 20% below 20 km. Figure 3 compares input and retrieved water vapour columns in μm derived from the data of Figure 2. Again the precision is of order 10 - 20%.

Retrieval simulations, of which Figures 1-3 represent a subset, show that a precision of 10 - 20% in profiles and column abundances can be expected. However, they also show that above certain limits dust degrades the results. For limb sounding, dust optical depth to the tangent point must not exceed unity in the infrared. For the surface limb path, this limit corresponds to a nadir visible optical depth of 0.4, although this can be raised to 1.5 if relative dust extinction at 6.9 and 45 μm is known. Clearly, profile measurements are not possible near the surface during dust storms, the lower boundary being 15-20 km. Column abundances can be obtained from nadir measurement provided dust nadir optical depth to the surface is less than unity. This corresponds to visible optical depths of less than 7.5, so that column abundance measurements are almost always available.

When the primary water vapour fields outlined in Table 1 are combined with the other simultaneous, co-located PMIRR measurements, further scientific objectives relating to the water cycle on Mars can be addressed. Temperature and condensate profile data allow the atmospheric saturation state to be defined, and derived wind fields make estimates of water vapour transport possible. With water vapour abundance, profile and transport data available, sources and sinks of water vapour such as surface reservoirs and airborne dust can be identified.

References

- 1 McCleese, D. J., Schofield, J. T., Zurek, R. W., Martonchik, J. V., Haskins, R. D., Paige, D. A., West, R. A., Diner, D. J., Locke, J. R., Chrisp, M. P., Willis, W., Leovy, C. B., and Taylor, F. W. 1986. Remote sensing of the atmosphere of Mars using infrared pressure modulation and filter radiometry. Applied Optics, in Press.
- 2 Gille, J. C. and Russell, J. M. III. 1984. The limb infrared monitor of the stratosphere: Experiment description, performance and results. J. Geophys. Res. 89, 5125-5140.
- 3 Barnet, J. J., Corney, M., Murphy, A. K., Jones, R. L., Rodgers, C. D., Taylor, F. W., Williamson, E. J., and Vyas, N. M. 1985. Global and seasonal variability of the temperature and composition of the middle atmosphere. Nature 313, 439-443.
- 4 Susskind, J., Rosenfield, J., Reuter, D., and Chahine, M. T. 1984. Remote sensing of weather and climate parameters from HIRS2/MSU on TIROS-N. J. Geophys. Res. 89, 4677.

TABLE 1.
**PMIRR WATER VAPOR - MEASUREMENT AND
 MAPPED FIELD RESOLUTION NOMINAL LIMB
 SCAN MODE**

MEASUREMENTS					
VIEW	COORDINATE	IN-TRACK (LATITUDE)	CROSS-TRACK (LONGITUDE)	VERTICAL	SAMPLING (LATITUDE)
LIMB		240 km (4°)	25 km	5 km	95 km (2°)
NADIR		6 km	5 km	COLUMN	95 km (2°)
MAPPED FIELDS ⁽¹⁾					
	REPETITION	RATE	1 day	3 days	56 days
VIEW	COORDINATE				
LIMB	LATITUDE		4°	4°	4°
	LONGITUDE		28°	10°	4°
	ALTITUDE		5 km	5 km	5 km
NADIR	LATITUDE		2°	2°	2°
	LONGITUDE		28°	10°	2°
	ALTITUDE		COLUMN	COLUMN	COLUMN

(1) BOTH DAY AND NIGHTSIDE FIELDS OBTAINED AT THIS RESOLUTION AND REPETITION RATE

JPL

FIGURE 1A. **PMIRR
 RETRIEVAL OF VERTICAL PROFILE OF
 WATER VAPOR**

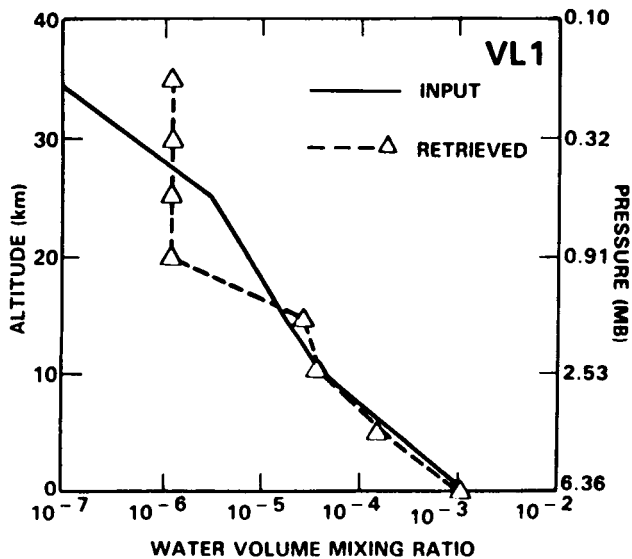


FIGURE 1B. **PMIRR
 RETRIEVAL OF VERTICAL PROFILE
 OF WATER VAPOR**

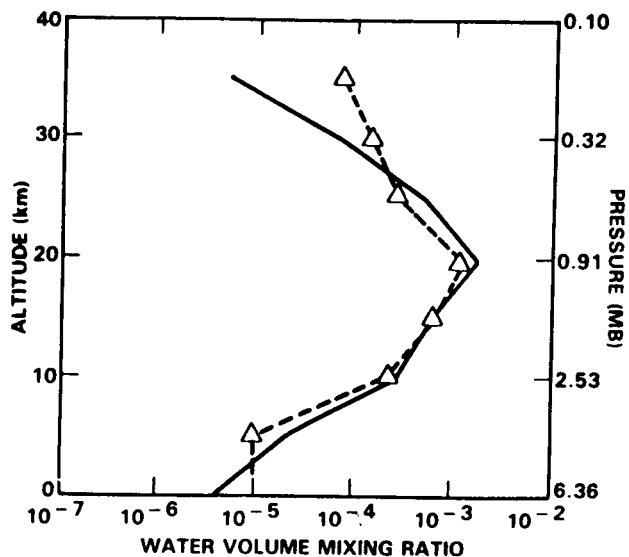


FIGURE 2.
RETRIEVED WATER VAPOR AMOUNT

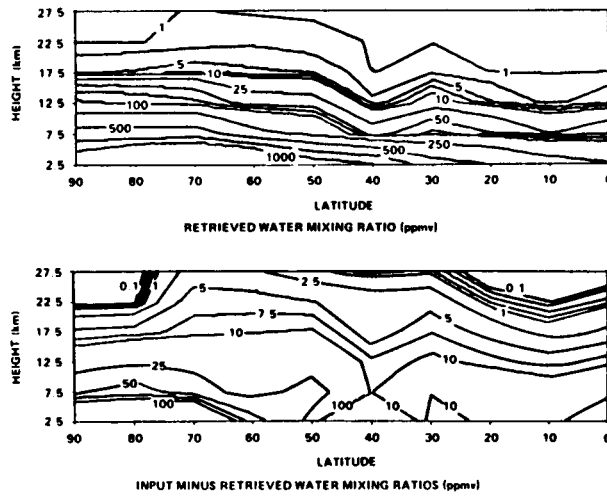
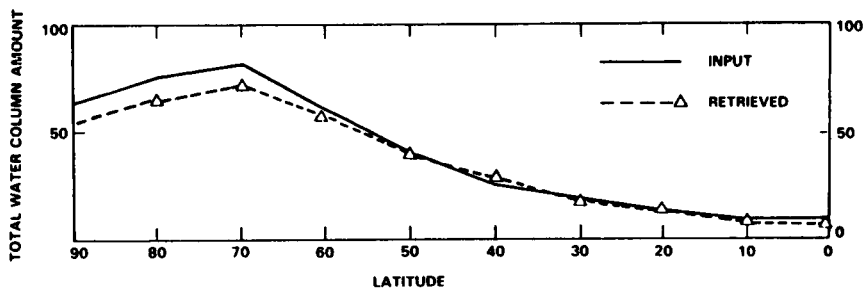


FIGURE 3. PMIRR
RETRIEVAL OF WATER COLUMN AMOUNT



ATMOSPHERIC H₂O AND THE SEARCH FOR MARTIAN BRINES Zent, A. P., F. P. Fanale and S. E. Postawko, Planetary Geosciences Division, Hawaii Institute of Geophysics, University of Hawaii, Honolulu, Hi. 96822

Abundant martian brines would have significant implication for current theories of volatile migration on Mars, since, although the presence of metastable brines is quite plausible, any brine in the reasonably near surface should be completely depleted on a timescale short in relation to the age of Mars. Their presence would strongly imply either large-scale subsurface mass transport, or juvenile outgassing rates significantly in excess of those believed currently possible. Any H₂O transport mechanism with sufficient capacity to maintain a near-surface brine in the martian regolith must be the dominant transport mechanism in the martian subsurface. As such, it is important to determine whether brines exist in the martian subsurface, for our current paradigm for understanding martian volatile regime will require substantial alteration if they are found to exist.

There are no stable brine systems on Mars today. The net annual escape flux of H₂O would be significant at all latitudes where the subsurface temperature exceeds the eutectic of chemically reasonable brines (2). Thus, if any brines do exist, they are constantly losing H₂O molecules to the atmosphere at a rate that depends upon the depth at which the melting occurs, the local thermal regime, and the porosity and mean pore size of the overlying regolith. The loss of H₂O molecules from a regolith source to the atmosphere, which supports only a very low ambient H₂O abundance (controlled by polar temperatures), may provide a means of detecting Martian brines, if they exist. We will discuss, in qualitative terms, some of the factors which would affect the utility of atmospheric H₂O observations as tools for detecting, or refuting the existence of, Martian brines. That is, it is important to understand whether unreasonable near-surface stratigraphy needs to be postulated to prevent the water flux to the atmosphere from any putative brine system from exceeding that allowed by the MAWD data. These factors may be broadly divided into two categories: those peculiar to the brine and its immediate environment, and those that are determined by the position of the system within the global environment.

The Brine. In our initial analysis (1), we found that for most chemically reasonable brines that might undergo annual melting, the annual average mass loss rates are on the order of 10⁻² g H₂O yr⁻¹ down to 10⁻⁴ g H₂O yr⁻¹. This range of net annual escape fluxes applies to a remarkably large percentage of the plausible shallow, seasonally

active brine systems; there are plausible brine systems which are too deeply buried to have any annual cyclicality imposed on them at all. We will return to them briefly below. The escape of H_2O molecules from a melting interface at depth Z falls off as Z^{-1} , approximately in accordance with Fick's Law; the escape flux achieves $\sim 10^{-2} \text{ g H}_2\text{O yr}^{-1}$ at depths of 30cm or less, for a nominal 50% porosity. The porosity of the regolith also plays a significant role in determining the escape rate of H_2O , with the flux increasing almost as the square of the porosity. A brine which releases $10^{-4} \text{ g H}_2\text{O yr}^{-1}$ to the atmosphere through a regolith with 10% porosity, will release an order of magnitude more H_2O per year at a porosity of $\sim 30\%$. The mean pore size of the regolith is not of great importance in determining escape fluxes, unless the mean free path of the H_2O becomes substantially greater than the pore size. Under such conditions, Knudson diffusion is the dominant transport mechanism and the escape flux falls off with pore size. With respect to both of these topics, the natural tendency of groundwater to leach materials from its surroundings and precipitate them on evaporation should not be ignored. Such a process should produce a kind of duricrust, much like those observed by Viking; however, duricrust may also decrease mean pore size and bulk porosity of the regolith. In principle, a duricrust cap could allow metastable brine systems to exist without violating the MAWD data.

Another factor which plays a role in determining the detectability of subsurface H_2O sources is their areal extent. Very concentrated sources, even though they may be supplying H_2O at a prodigious rate, are unlikely to be detected because of resolution problems.

There is a conflicting set of requirements involved in atmospheric H_2O detection of brines, because those systems which are best suited to identification are also the shortest-lived. Loss of H_2O molecules results in recession of the melting interface until the seasonal thermal wave is no longer sufficient to cause melting, unless resupplied from depth. At depths of $\sim 1 \text{ m}$, average mass loss rates of $10^{-3} \text{ g H}_2\text{O cm}^{-2} \text{ yr}^{-1}$, the recession rate of a brine would be on the order of 10^5 yr m^{-1} . Brines below about 2m should be quite well insulated from the annual thermal wave. Such deep brines however cannot be invoked to explain seasonal variability in radar reflectivity measurements.

There are some brines which have eutectics below the annual average temperature at low latitudes. Such brines could conceivably remain liquid throughout the martian year at depths greater than a few meters. These putative brines would remain liquid and would be entirely undetectable, with mass loss rates on the order of a fraction of a perceptible micron per year, and well below the penetration depth of radar

signals.

The composition of the brine system is also critical. Melting begins with a brine of eutectic composition and continues isothermally until the supply of one of the components is exhausted. As long as ice is present in the system, the vapor pressure over the brine will equal the vapor pressure over ice at the temperature of the system. However, once all the ice has melted, the vapor pressure over the brine will be lower than it would be over ice at the same temperature. Therefore incomplete melting of the brine, which results from a bulk composition significantly less saline than the eutectic composition, favors higher escape fluxes and hence detectability.

A brine which has a high evaporative loss to the atmosphere, for whatever reason, will be most detectable. High loss rates may be due to a highly porous overburden, a water-rich brine system, or a shallow melting interface. High salinity brines, capped by a great deal of overburden, or by overburden of low porosity, will hide brines effectively from atmospheric detection.

The Environment Environmental factors are those which are approximately independent of the existence of the brine, such as the local thermal regime, the background column abundance of H₂O and the regional wind velocities.

Atmospheric signatures of escaping brines will have greater absolute magnitude at low latitudes because the warmer melting interface will support a greater equilibrium water vapor abundance. Naturally, escape fluxes become more seasonally dependent as latitude increases, and the annual average escape flux decreases. Higher escape fluxes favor detection, and low latitude brines should be more easily detectable.

Detection is also aided by the escape of H₂O molecules into a low background abundance of water vapor, since it is the difference between the escaping and ambient H₂O that is indicative of a regolith source. Therefore, in general, the likelihood of detecting a brine increases as one moves away from the north pole, although again, seasonal variations in local H₂O abundances will affect the outcome of any search.

H₂O molecules which escape from a seasonal vapor source in the regolith to the atmosphere will be dispersed by the winds. The lower the local wind velocities, the more likely that an excess abundance of H₂O will accumulate in the atmosphere.

The most likely location for brine detection, assuming the same brine exists everywhere on the planet, is one in which the subsurface temperatures are high, while the atmospheric H₂O abundances are low. On Mars, this is most closely approximated during low southern latitudes near perihelion. Temperatures are warmer at that time than in the northern hemisphere summer because perihelion occurs during southern

hemisphere summer. At most locations on the planet though, peak atmospheric H₂O abundances are more closely correlated with peak surface temperatures. Unfortunately, the low southern latitudes also experience their peak annual wind velocities near perihelion.

We conclude that the prospect for detection of a subsurface brine via atmospheric water vapor measurements is marginal, for four reasons. 1) There is an inherent inadequacy in using escape to the atmosphere to detect regolith water sources, since one does not really observe the source at all, but a product of the system's dissipation. Those brines which are best suited for detection are therefore the same ones that are most unstable, and hence have the shortest mean lifetimes. 2) Not only the mass loss itself, but processes which take place concurrently with evaporation also tend to reduce the escape flux; evaporation leads to concentration of salts in the brine which depresses the equilibrium water vapor abundance at the melting interface, and hence the escaping flux. Continued evaporation then leads to deposition of a duricrust-type deposit which may have the effect of decreasing the porosity of the overburden, further decreasing the escape flux. For most reasonable putative brine systems, this process requires no more than about 10⁵ years. 3) Those brines which do not suffer from rapid degradation, and are consequently longest-lived, are also those least detectable since they are either found at great depth, or are capped by a very low porosity overburden. 4) The environmental factors which are most important in determining the detectability of such a system (i.e. temperature and atmospheric water vapor) tend to be correlated in a manner opposite that which is best suited to facilitate brine detection.

REFERENCES

1. Zent, A. P., and Fanale, F. P., (1986). *J. Geophys. Res.*, Vol. 91, D439 - D445.
2. Fanale, F. P., and Clark, R. N., (1983), *Proc. Fourth Int. Conf. on Permafrost*, 289-294, Nat. Acad. Press, Washington, D.C.

N89-25813

52-91

1135 11/27

91

18.

THE INTERANNUAL VARIABILITY OF ATMOSPHERIC WATER VAPOR
ON MARS. Richard W. Zurek, Jet Propulsion Laboratory, California
Institute of Technology, Pasadena, CA 91109.

187414

The acquisition of several north-south scans during the Survey/Completion Mission by the Mars Atmospheric Water Detector (MAWD) onboard Viking Orbiter 1 make it possible to compare water vapor column abundances during northern spring and early summer seasons from three successive Mars years. All three years exhibit very similar seasonal trends. Differences between years tend to be localized, and not regional, with maximum differences between years occurring in the same general areas that the day-to-day variability of water vapor as observed by MAWD is large. These regions are also where clouds frequently occur during these seasons (Christensen et al., 1986, MECA, Houston), and these are thought to account for much of the day-to-day variations in atmospheric water vapor, as observed by MAWD (Jakosky et al., 1986, MECA, Washington, D.C.). This suggests that the observed year-to-year differences are also artifacts of clouds in the MAWD field-of-view and that, in fact, there is remarkably little difference in the water cycle during northern spring and early summer, despite very different dust-storm episodes during the preceding three years.

524.9-187415

N89-25814

92

18. 1/10/54

THE MARTIAN ATMOSPHERIC WATER CYCLE AS VIEWED FROM A TERRESTRIAL PERSPECTIVE. Richard W. Zurek, Jet Propulsion Laboratory, California Institute of Technology, Pasadena, CA 91109.

From a terrestrial perspective, water is important in at least three contexts: it is key to certain biological and many biogeochemical processes, to surface weathering and sediment transport, and to climate. Historically, these are the same contexts in which water on Mars has been studied, with the biological implications having received the greatest attention. With Viking's failure to find evidence of biological activity on the Martian surface and with the discovery by Viking and Mariner 9 of channel networks and layered terrain suggesting significant climatic change, attention has shifted somewhat to the other two contexts for the study of water on Mars. There are, however, important differences between Earth and Mars. First of all, Mars is too cold and its atmosphere too thin at present for water to have a stable liquid phase at its surface or in its atmosphere. This has significant implications for weathering rates, for sediment transport and for the ability of water to close the atmospheric water cycle by flow at or beneath the surface. Secondly, the Martian atmosphere can not hold enough water that phase changes can release sufficient latent heat to alter the atmospheric circulation. In these respects, the state of water vapor in the Martian atmosphere closely resembles that of water vapor in the Earth's stratosphere. Water budget studies for both the terrestrial stratosphere and troposphere indicate that atmospheric water vapor transports can be used to define surface sources and sinks if the divergence of the transports can be computed with sufficient precision (see T-C Chen's and R. M. Haberle's presentations, this issue). Alternatively, the distributions of water vapor themselves can be used qualitatively (see Remsberg et al., this issue) or the concept of the residual-mean or "diabetic" circulations can be used (see Leovy et al., this issue) together with the water vapor distribution to diagnose the Martian water cycle.

List of Workshop Participants

Duwayne M. Anderson

Associate Provost for Research
Texas A & M University
East Bizzell Hall, Room 305
College Station, TX 77843

Edwin Barker

RLM 15-308 Department of Astronomy
University of Texas/McDonald Observatory
Austin, TX 78731

Joseph Chamberlain

Space Physics and Astronomy
Rice University
Houston, TX 77251

T. C. (Michael) Chen

326 Curtiss Hall
Meteorology Program
Iowa State University
Ames, IA 50011

Philip Christensen

Department of Geology
Arizona State University
Tempe, AZ 85287

Stephen Clifford

Lunar and Planetary Institute
3303 NASA Road One
Houston, TX 77058

David Colburn

Mail Code 245-3
NASA Ames Research Center
Moffett Field, CA 94035

Leo J. Donner

National Center for Atmospheric Research
P.O. Box 3000
Boulder, CO 80307

Fraser Fanale

Institute for Planetary Geosciences
Hawaii Institute of Geophysics
University of Hawaii
2525 Correa Road
Honolulu, HI 96822

James L. Gooding

Mail Code SN2
NASA Johnson Space Center
Houston, TX 77058

Robert Haberle

Mail Code 245-3
NASA Ames Research Center
Moffett Field, CA 94035

Helen Hart

Laboratory for Atmospheric and Space Physics
Campus Box 392
University of Colorado
Boulder, CO 80309

Daniel Hillel

11 Stockbridge Hall
University of Massachusetts
Amherst, MA 01003

Bruce Jakosky

Laboratory for Atmospheric and Space Physics
Campus Box 392
University of Colorado
Boulder, CO 80309

Philip James

Physics Department
University of Missouri, St. Louis
St. Louis, MO 63121

Fred Jaquin

Space Sciences Building
Cornell University
Ithaca, NY 14853

Jack Larsen

SASC Technologies, Inc.
17 Research Drive
Hampton, VA 23666

Steven Lee

Laboratory for Atmospheric and Space Physics
Campus Box 392
University of Colorado
Boulder, CO 80309

Conway Leovy

Department of Atmospheric Sciences
AK-40
University of Washington
Seattle, WA 98195

Robert D. Miller

Department of Agronomy
Cornell University
Ithaca, NY 14853

James Murphy

Department of Atmospheric Science
University of Washington
Seattle, WA 98195

John J. Olivero

Department of Meteorology
Penn State University
509 Walker Building
University Park, PA 16802

John Philip

Environmental Mechanics
Commonwealth Science and Industrial Research Organization
P.O. Box 821
Canberra, A.C.T.
2601 Australia

Ellis Remsberg

Mail Stop 401B
NASA Langley Research Center
Hampton, VA 23665

Sara Roberts

*Office of the Associate Provost for Research
Texas A & M University
College Station, TX 77843*

J. T. Schofield

*Mail Stop 183-601
Jet Propulsion Laboratory
4800 Oak Grove Drive
Pasadena, CA 91109*

Carol Stoker

*Mail Code 245-3
NASA Ames Research Center
Moffett Field, CA 94035*

Aaron Zent

*Institute for Planetary Geoscience
Hawaii Institute for Geophysics
University of Hawaii
2525 Correa Road
Honolulu, HI 96822*

James Zimbelman

*Center for Earth and Planetary Studies
National Air and Space Museum
Smithsonian Institution
Washington, DC 20560*

Richard W. Zurek

*Mail Stop 183-601
Jet Propulsion Laboratory
4800 Oak Grove Drive
Pasadena, CA 91109*